Triglyceride Matrices for Controlled Release

Characteristics for Manufacturing and Release
–
Biocompatibility and Erosion Behavior

Dissertation zur Erlangung des Doktorgrades der Naturwissenschaften
(Dr. rer. nat.)
der Fakultät Chemie und Pharmazie
der Universität Regensburg

vorgelegt von
Christian Guse
aus Unterneuhausen bei Landshut
im Mai 2005

Diese Doktorarbeit entstand in der Zeit von Januar 2001 bis Mai 2005 am Lehrstuhl für Pharmazeutische Technologie an der Universität Regensburg.

Die Arbeit wurde von Herrn Prof. Dr. Achim Göpferich angeleitet.

Promotionsgesuch eingereicht am:	04. Mai 2005
Datum der mündlichen Prüfung:	02. Juni 2005
Die Arbeit wurde angeleitet von:	Prof. Dr. Achim Göpferich
Prüfungsausschuss:	Vorsitzender: Prof. Dr. Heilmann Erstgutachter: Prof. Dr. Göpferich Zweitgutachter: Prof. Dr. Siepmann Drittprüfer: Prof. Dr. Buschauer

Meiner Familie und meiner Frau Eva, gewidmet in Liebe und Dankbarkeit.
Im Andenken an meine Großeltern.

« On ne voit bien qu´avec le coeur »

Le petit prince de Antoine de Sait-Exupérie (1946)

Table of Contents

Chapter 1

Introduction
and
Goals of the Thesis

Introduction

Parenteral therapies

In recent decades medicine and pharmacy have had to face many new challenges. Not only the need to treat cancer [1,2] encouraged innovation, but also the need to develop therapies for widespread diseases, such as diabetes mellitus [3] or numerous cardiac diseases [4] have called for enormous progresses. To give an impression of the extent of the issue, the incidences of selected solid tumors in the US, estimated for the year 2000 and 2004 by the American Cancer Society, are depicted representatively in Table 1.

Table 1: Incidences of selected solid tumors in the US in the years 2000 and 2004 (source: American cancer society).

Type of cancer	**Number of new cases**		**Number of deaths**	
	2000	**2004**	**2000**	**2004**
Breast	182,800	217,440	41,200	40,580
Prostate	180,400	230,110	31,900	29,900
Lung	164,100	173,770	156,900	160,440
Colon	93,800	106,370	47,700	56,730
Rectum	36,400	40,570	8,600	N/A
Pancreas	28,300	31,860	28,200	31,270
Ovary	23,100	25,580	14,000	16,090
Brain & other nervous system	N/A	18,400	N/A	12,690

These data show the tremendous increase in the newly occurring cases of cancer and the limited chances for healing lung and brain cancer. But Table 1 also shows that the number of cancer deaths increased less rapidly or in some cases even decreased from the year 2000 until present. In the field of pharmaceutical science, therapies can be approved by the development of new drugs and by increasing the efficacy of treatments with existing drugs. But consequently, with increasing possibilities in the design of new drugs, the requirements for their application have increased tremendously, too. In recent years many sensitive substances, above all proteins and peptides, have gained much importance [5,6]. The investigated triglyceride matrices can contribute to the treatment of various cancer forms such as for example brain cancer [7] and they are one possibility to overcome limitations for the

administration of proteins and peptides [8]. Because although the oral application of a protein like insulin would be desirable, due to advantages such as easy administration and good compliance, this mode of administration would lead to a bioavailability of less than 1-2% [5,9]. This is only one example among a plethora of proteins and peptides, which are rapidly degraded when administered via the oral route. Likewise, many efforts have been undertaken in the field of cancer treatment with various proteins, such as cytokines [10,11], which also undergo rapid degradation and can additionally cause severe side effects when administered orally. Therefore, the parenteral routes of application have been of increasing interest for cancer therapy.

Parenteral, from *para enteron* (Greek), meaning "to avoid the intestines", is generally limited to the direct application of drugs into tissues, tissue spaces, vessels or body compartments [12], for example by injection, infusion or also implantation, whereby the most commonly used routes for the administration of drugs are intravenously (i.v.), intramuscularly (i.m.) or subcutaneously (s.c.), depending on the disease to be treated and the desired effects. Nevertheless, the definition also includes also several other important ways to apply drugs, such as ocularly, nasally and transdermally [12], which represents the exact interpretation of the term, meaning all administration principles for drugs, which do not utilize the alimentary canal for the delivery of a drug to body tissues. The parenteral application of drugs offers several advantages compared to non-parenteral routes. These are, for example, more predictable pharmacokinetics and pharmacology and the possibility to quickly interdict a rapidly progressing lethal process or disease [12]. Generally, we can distinguish between two forms of the treatment. On the one hand, there is the parenteral administration of a drug, for example to fight a cardiac arrest by the injection of adrenalin, and on the other hand a long-term treatment with the goal to treat a disease over an extended period of time. Since the first is more often applied in cases of emergency, the long-term therapy becomes much more interesting and challenging for pharmaceutical and medical scientists.

Progress in the parenteral administration of such long-term treatments has already contributed to positive developments, for example in the abovementioned successes in cancer treatment (Table 1). The triglyceride matrices investigated in this thesis are another possible alternative for the long-term administration of medications.

Necessity of controlled release

Parenteral therapies carried out over an extended time period rapidly lose patient compliance when drugs have to be administered by direct infusion or injection. Subsequently, the cost of these treatments rises tremendously, due to the need of more highly supervised medical care. Therefore, the parenteral controlled release of therapeutic substances over longer time periods ranging from a few weeks up to several years is desirable for the treatment of many diseases, such as several types of cancer [13-15], diabetes [16], cardiac diseases [4], Parkinson's disease or Alzheimer's disease [17]. Concomitantly sustained drug delivery devices can be used for the treatment of glaucoma [18] or other vitreoretinal diseases [19] and for hormonal contraception [20] or hormone substitution [21]. Recent investigations also deal with the use of controlled release forms in the field of gene delivery [22-25] for the treatment of neurodegenerative diseases.

Controlled release delivery systems have several advantages, compared to the intermittent i.v. or oral drug administrations [6,16,26], such as the maintenance of therapeutic levels of a drug and the reduction of negative side effects due to a lower required amount of drug when administered locally. Additionally, the number of dosages can be decreased and the delivery of drugs with short in vivo half-lives can be facilitated. With regard to the limited ability of many drugs, especially proteins, to cross physiological barriers, such as the blood-brain barrier (BBB) [6,17] or the inner and outer blood-retinal barriers [19], another important advantage for the use of local parenteral drug delivery systems, such as the triglyceride matrices investigated for this thesis, becomes obvious.

Drug delivery devices

In recent decades, tremendous efforts have been undertaken in the field of controlled release devices and a plethora of systems have been developed and investigated for their use in parenteral drug delivery. Thus, it would be impossible to give a complete overview of drug delivery devices; therefore only a brief description of the classes of systems used for controlled release and drug delivery follows.

Generally particulate systems, such as nanoparticles [27-30] (including liposomes [31,32]) and microparticles [6,33-35] can be distinguished from macroscopic implantable devices [2,7,36,37] in the field as the most important candidates for the design of controlled release

systems. In addition, a plethora of new strategies for the controlled parenteral delivery of drugs have been investigated, such as in situ gelling systems [38], microchip devices [2,4,39] or stents which are able to control the release of drugs [4,40].

Nanoparticles and liposomes are already used in several areas of drug delivery and cosmetics. They offer the advantage of facilitated specific targeting [41], due to their size, which leads to an uptake into cells via phagocytosis [42,43]. Nanoparticles usually are smaller than 100nm and thus are not excluded from cells. Small molecules, peptides, proteins and nucleic acids can be loaded into nanoparticles that are not recognized by the immune system and that can be targeted to particular tissue types. Nonspecific attachment or uptake can be reduced by the use of poly(ethylene glycol) (PEG) [44]. Hitherto nanoparticles and liposomes have been investigated for their use in cancer therapy [45] or gene delivery [27] and recently research involving the nuclear targeting of these small devices has also been carried out [46].

Microparticles are also a widely investigated device for drug delivery, due to improved abilities for sustained release compared to nanoparticles. Their size can range from one to several hundred micrometers, which allows for a larger drug reservoir and thus facilitates a more prolonged drug release. One major advantage of microparticles is the possibility to suspend and inject them. Microparticles can be administrated to provide localized release of therapeutic agents as controlled release devices in several ways. Drug delivery via subcutaneous as well as intracranial injection for example has been widely investigated [47-49]. An appealing aspect of a microparticle-based delivery system is that stereotactic injection to a specific region of the brain passes the BBB, thereby enabling prolonged delivery directly to the CNS. Efforts have also been undertaken in the fields of inhalative aerosol delivery of drugs into deep lung tissue [50,51] and oral insulin delivery [52] by the use of microparticles. But despite several advantages such as injectability, facilitated preparation procedure and longer drug release periods compared to nanoparticles, the capability of microparticular devices for drug incorporation and thus for controlled prolonged release is still limited.

The third system for parenteral drug delivery, which should be described, is macroscopic implants. They have been investigated for many purposes. In 1999, Evans et al. described their fabrication into structural supports, which can be used to promote nerve regeneration [53], which is also described in other references [54,55]. Their use in the treatment of various cancers has been widely investigated [7,13] and a plethora of scientific papers describe their use as cell carriers in tissue engineering or cell transplantation [56-60]. A disadvantage of three-dimensional macroscopic implants, which can be on the millimeter to centimeter scale,

compared to particulate devices, which can be suspended and injected, is the need for surgery to administer the device. But due to their size, implants can provide a larger depot of the administered drug compared to particulate systems. Their macroscopic size also facilitate the incorporation of larger proteins, which is limited for example in case of nanoparticular systems. Additionally, implantable devices are easier to prepare and allow for a variation in their geometries like size, shape and porosity, which can be tailored to the application.

Thus, implants can be considered to be one of the most important candidates for controlled release drug delivery over an extended period of time like several months.

Non-degradable and bioerodable drug delivery systems

Many materials have been investigated for applications in drug delivery devices. The first controlled release systems were based on non-degradable synthetic polymeric materials, principally silicone elastomers. In 1964, Folkman et al. noticed the penetration of certain dye molecules through the wall of silicone tubing [61,62]. This observation lead to the development of so called reservoir drug delivery systems, which are hollow tubes filled with a drug suspension or compact drug cores surrounded by permeable non-degradable membrane. The device properties, such as thickness and permeability of the tubing or membrane, respectively, control the release rate of the drug [2]. This principle is used for example in the Norplant® contraceptive delivery system and was tested for carmustine delivery from silicone-encased drug reservoirs in cancer treatment [16,63]. Two advantages of such systems are the variability of membrane materials, which allows for exact adjustment of the desired release profile and the possibility to achieve zero order drug release kinetics comparable to i.v. injection. The major disadvantage of the reservoir principle is the danger of the so-called dose dumping when a mechanical defect in the membrane of the system occurs and the whole drug is released rather abruptly. This may cause severe or even lethal side effects.

The second type of non-degradable implantable controlled release device is represented by the matrix system, within which the drug is homogenously dispersed. Thus, these devices are simpler and potentially safer compared to the reservoir type systems. Controlled release from matrix devices occurs by diffusion of the substances throughout the matrix. An example for this kind of release system is the Cypher coronary stent®.

Figure 1 depicts the mechanisms of drug release from reservoir and matrix type of non-degradable drug delivery systems.

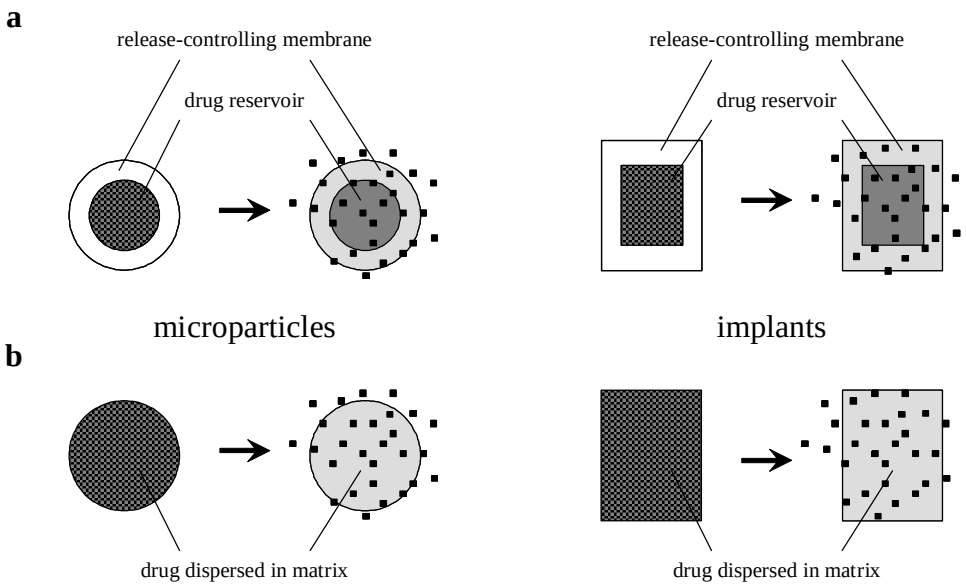

Figure 1: Mechanisms of drug release from non-degradable drug delivery systems
a) diffusion controlled reservoir systems, a core is surrounded by a non-degradable membrane
b) matrix system, drug is embedded homogenously into the matrix material, release can be controlled by diffusion, erosion or both.

Both reservoir and matrix systems require minor surgery to implant as well as to remove the devices. This disadvantage of invasive procedures when administering non-degradable drug delivery systems is less pronounced in veterinary medicine, where the removal of subdural implants is not necessary. Thus implants for the controlled release delivery of estradiol to improve the growth rate and feed uptake in cattle were developed by Lilly research laboratories [64,65].

Another example for non-degradable drug delivery system, which was used in the 1990ies for the treatment of osteomyelitis, is a device containing gentamycin embedded into a matrix of poly(methylmethacrylate) (PMMA, also called “bone cement”) [66-70]. Investigations carried out by Wahling et al. using gentamycin-loaded PMMA beads revealed much higher local antibiotic concentrations than can be safely achieved with the usual parenteral administration techniques [71,72]. Also in 1992 Dash and Suryanarayanan investigated this means of treatment for bone infection by using tobramycin embedded in poly(dimethylsiloxane) (PDMS) [73]. The major advantage of this device is the locally targeted therapy directly at the site of infection. However, the underlying disadvantage of this delivery system is the necessity for surgical removal of the implant after the therapy is completed and thus therapy of the exemplified indication has changed in the recent years.

Degradable macroscopic drug delivery systems

The fact that all non-degradable drug delivery systems have to be removed surgically is obviously the most important limitation these devices. This both reduces patient compliance and also makes therapy more difficult. Thus, in recent decades, biodegradable systems have gained much popularity over non-degradable delivery devices [74,75]. Biodegradability of an administered material means the capability to be degraded and eliminated by the body within a certain time period. The major advantage of biodegradable drug delivery systems is that the inert materials used for the fabrication of the devices are eventually absorbed or excreted by the body. This alleviates the need for surgical removal of the implanted system after the completion of the therapy, thereby increasing patient acceptance and compliance [76]. Biodegradable materials can be used for the preparation nearly every drug delivery system, including for example nanoparticles, liposomes, microparticles, micelles and macroscopic implants. Biodegradable drug delivery devices which are already commercially available are for example Lupron Depot® [77], Decapeptyl® [78] and Zoladex® [79] all used for the treatment of prostate cancer and Nutropin Depot® which is employed in the growth failure therapy [6]. All these devices are based on poly((D,L-lactic-*co*-glycolic acid) (PLGA) in contrast to Gliadel® [80], which is based on poly(bis(p-carboxyphenoxy)propane) - sebacic acid (pCPP-SA), representing a further biodegradable material for the preparation of parenteral drug delivery devices. However, the design of a biodegradable drug delivery system is not easy, due to many factors, which can influence the degradation rate and thus play important roles for the resulting release profile, especially when using polymeric materials. Alterations in pH of body compartments or body temperature as well as changes in the surface area or shape of the device have to be considered in the design of a biodegradable drug delivery system [81]. Another problem that occurs with bioerodable controlled release devices is the slow diffusion of the drug from the matrix [76] which becomes a major challenge to overcome when developing biodegradable systems whose use is intended for extended release applications or situations in which the drug has a narrow therapeutic index [16]. One of the key factors in the design of a biodegradable controlled release drug delivery system seems to be the chosen matrix material.

Materials

Hitherto most investigations on drug delivery have been carried out on polymers and all commercially available controlled release devices for parenteral administration utilize polymers to obtain a sustained liberation of the drugs [2,6,16,20]. Table 2 gives a partial overview of the commercially available sustained release devices and the used materials [6,13,82-84], which are all synthetic polymers and whose biocompatibility is widely accepted.

Table 2: Partial overview of commercially available drug delivery systems and the used materials.

Product name	**Material**	**Drug released**	**Application**
Cypher coronary stent®	Ethylvinylacetate copolymer EVAc + PBMA	sirolimus	coronary artery disease
Decapeptyl®	poly(D,L-lactic-*co*-glycolic acid) PLGA	(D-Trp^6)LH-RH	prostate cancer
Gliadel®	pCPP-SA	carmustine	glioblastoma multiforme
Lupron Depot®	poly(D,L-lactic acid) PLA	leuprorelin acetate	prostate cancer, endometriosis
Jadelle®	dimethylsiloxane/ methylvinylsiloxane	levonorgestrol	contraception
Norplant®	silastic rubber	levonorgestrol	contraception
Nutropin Depot®	poly(D,L-lactic-*co*-glycolic acid) PLGA	human growth hormone	growth failure
Septopal®	poly(methylmethacrylate) PMMA	gentamycin sulfate	osteomyelitis
Taxus coronary stent®	translute[a]	paclitaxel	coronary artery disease
Trelstar Depot®	poly(D,L-lactic-*co*-glycolic acid) PLGA	triptorelin pamoate	prostate cancer
Zoladex®	poly(D,L-lactic-*co*-glycolic acid) PLGA	goserelin acetate	prostate cancer, endometriosis

[a]A Boston Scientific proprietary non-degradable polymer

Since the number of materials investigated for the manufacture of controlled release drug delivery devices is tremendous, only a partial overview of materials is depicted in Table 3. The materials are devided into synthetic and natural polymers, natural hydrogels and lipid materials.

Table 3: Materials investigated for their use in the design of biodegradable controlled release drug delivery systems.

synthetic polymers	**natural polymers**	**hydrogels**	**lipid materials**
ABA triblock copolymers [135]	albumin [106-110]	alginates [120,121]	cholesterol [35,127]
Ethylvinylacetate copolymer (EVAc) [136]	cellulose [83]	collagen[6]	dipalmitoyl-phosphatidyl-choline [126]
hydroxyapatite [137]	chitosan / chitin [113]	fibrin [118,119]	fatty acid anhydrides [142]
poly(ortho esters) [17]	chondroitin sulfate [116,117]	gelatin [82,111]	fatty acids [128,142]
polyamides [138]	hyaluronic acid [114]		Gelucire®, [1] [143]
polyanhydrides [6,38,138]	starch [102-105]		hydrogenated castor oil [144]
poly(ε-caprolactone) [139]			lecithin [145]
polycarbamates [138]			monoglycerides [146]
polycarbonates [138]			triglycerides [34,35,131]
poly(glycolic acid) (PGA) [141]			waxes [129]
poly(D,L-lactic-*co*-glycolic acid) (PLGA) [140]			
poly(lactid acid) (PLA) [63]			
polyphosphazene [138]			
polyurethanes [138]			
silicone [6]			

[1] Gelucire® is a mixture of glycerides and fatty acid esters.

In addition to polymers used in the commercially available drug delivery systems a plethora of polymeric materials and structures are available and numerous groups are currently carrying out experiments on cancer treatments using these materials for the design of controlled release devices. The delivery of hormones [122-124], cytokines [104], and non-protein anticancer drugs, such as 5-Fluorouridine [95], Cisplatin [125,126] or Doxorubicin [127-130] from polymeric systems has been investigated for cancer therapy. Concomitantly, polymeric materials are investigated for their use in the treatment of neurodegenerative diseases, such as Parkinson's and Alzheimer's disease [17] and for future therapy of diabetes mellitus [3] and various cardiovascular diseases [131-134].

For their suitability as material for the preparation of parenteral controlled release drug delivery systems, synthetic polymers display some advantages, such as variable release properties, well-defined degradation pathways [135] and acceptable in vivo biocompatibility [136-138]. However polymeric materials also show several disadvantages, especially as the delivery of proteins proves to be a more challenging task for pharmaceutical scientists. High shear forces, heating, exposure to organic solvents [139], interface formation [140], as well as the chemical microenvironment inside eroding polymers with acidic pH [141], increased osmotic pressure [135] and acylating degradation products [142] often result in irreversible changes in protein structure and activity [139]. Therefore, alternative materials to biodegradable synthetic polymers that avoid these stress factors may become increasingly important for the delivery of protein and peptide drugs in the near future.

For this purpose, several natural materials were investigated. Early examples with natural polymers are controlled release experiments of Mitomycin C, 5-Fluorouracil and 5-Fluorouridine from starch microspheres [110-113] carried out in the eighties and nineties by a few groups. Also albumin [86-90] and gelatine [104,105] microspheres were investigated in the field of controlled release for cancer treatment. Further studies were carried out on chitosan [98,143], hyaluronic acid [108], cellulose [95], ethylcellulose [144] and chondroitin sulfate [102,103], all representing natural biodegradable polymeric materials for the controlled release of drugs. By the use of natural polymers for controlled release, most of the abovementioned disadvantages of the synthetic polymers, especially the stress factors to which the incorporated drugs are exposed, can be alleviated and their biocompatibility is also widely accepted. However, there might be difficulties in the design of the desired release profile or degradation time, due to structural limitations.

A second group of alternative materials to the synthetic polymers for the preparation of parenteral delivery systems, generally also being natural polymers, are natural hydrogel-forming agents. Potential candidates, which are currently investigated are fibrin [99,100], alginates [91,92], carboxymethylcellulose [145-147], gelatine [104,105] or collagen [6,148]. Natural hydrogels have the advantage that they can protect proteins and peptides from degradation [6], which makes them promising candidates for the use as carrier materials in the field of controlled release.

As a third group, lipid materials might be a promising alternative to synthetic polymers for the design of controlled release drug delivery devices, whereby several substances were investigated for their potential in this field. Among these physiologically existing materials, which also include cholesterol [37], phospholipids [96], lecithin [93], fatty acids 106] and waxes [120], all forms of glycerides with fatty acids of variable chain lengths are of great importance [29,36,37,149,150]. Lipid materials show high variability of available structures, and thus allow for the design of many desired release profiles. Concomitantly, the mentioned negative stress factors for polymeric materials can be avoided and, as physiologically occurring substances, these materials should prove to be biocompatible. This makes lipid materials a promising candidate as an alternative material to the synthetic polymers for the design of controlled release parenteral drug delivery systems.

Triglycerides as one representative for the lipid materials showed promising controlled release properties [36,37] and their use for the preparation of microspheres [118] and solid lipid nanoparticles (SLN) [151,152] have shown good results for the incorporation of proteins. Thus with regard to a long-term administration of proteins, developing triglyceride implants that allow for a more prolonged release period [36,37] and higher drug dosages, due to their macroscopic size, may be of great interest for researchers in this field.

Goals of the thesis

Compared to synthetic polymers, the use of triglycerides avoids the abovementioned stress factors for the incorporated drug, such as the microenvironment within eroding polymeric implants with increased pH and osmotic pressure, acylating degradation products, which often irreversibly changes the structure and activity of incorporated proteins or peptides. In addition, triglycerides show structural variability, which facilitates the design of a controlled release system with a desired release profile. As physiologically occurring material, the biocompatibility of triglycerides is likely.

The general goal of this thesis was the investigation of triglycerides as materials for the preparation of parenteral controlled release matrices. The main intentions were to characterise the material to facilitate the design and preparation of controlled release matrices and to ensured the in vivo safety of the material.

Due to their promising properties, triglycerides are currently being investigated for their use as carrier material for proteins and peptides [36,37,153,154]. To facilitate investigations on the stability of proteins and peptides within the matrix, an extraction method for the recovery of the incorporated drugs was the first aim of this thesis (**chapter 3**). Insulin and somatostatin served as model drugs for the development, optimization and evaluation of the procedure.

Many basic factors concerning the preparation procedure for triglyceride matrices and their release properties as well as the biocompatibility and in vivo erosion of the triglyceride matrices are of great importance for the design of cylindrical triglyceride matrices, necessitating the mechanistic studies that were carried out and described in this thesis.

The investigations presented in **chapter 4** served to evaluate the preparation of the cylindrical triglyceride matrices, to identify crucial parameters during the manufacturing procedure and to quantify their influence on the resulting release profiles. Concomitantly, basic release properties of the triglycerides were characterized and release mechanisms from the material identified. To this end, fluorescence dyes were used as model drugs.

After the preparation procedure for cylindrical triglyceride matrices was evaluated and basic release properties of the material were investigated, in **chapter 5** the in vivo biocompatibility of triglycerides, which is the most essential prerequisite for a biomaterial to prove suitability for the preparation of drug delivery systems for the parenteral administration, was examined. Additionally, in vivo erosion and stability of lipid matrices was of special

interest in this part of the thesis, representing another important requirement for controlled release of drugs in vivo.

Subsequent to the determination of long term in vivo stability of triglyceride matrices in **chapter 5**, possibilities to accelerate triglyceride erosion is described in **chapters 6** and **7**. First, the use of several excipients as modifiers in the erosion of triglyceride matrices was examined in vitro in **chapter 6**. The goal of this study was to decrease the matrix stability and thus accelerate the erosion but to maintain the prolonged release properties of the triglyceride material. The influence of the excipients on the release from triglyceride matrices was characterized and their suitability for prolonged in vitro release over several weeks was investigated. Consequently, the hypothesis for the use of hydrophilic erosion modifiers and the dependence of the in vivo erosion on the triglyceride particle size was then investigated in **chapter 7**.

As one possible application for lipid implants as controlled release drug delivery systems, programmable implants containing a drug-loaded triglyceride core embedded into a drug-free bulk-eroding polymer mantle were also investigated (**chapter 8**). These devices were first described by Vogelhuber et al. [39], but only allowed for pulsatile release, because of a polyanhydride core. It was thus important to demonstrate the viability of prolonged drug liberation from programmable implants having a triglyceride core. Last, but not least, convolution theory was investigated for its suitability to predict release profiles from programmable implants showing the controlled release of the drug from the core material.

Chapter 2

Materials and Methods

1 Materials

1.1 Matrix materials

The triglycerides for matrix preparation were purchased from Sasol GmbH, Witten, Germany. Materials included glyceroltrilaurate (Dynasan® 112), glyceroltrimyristate (Dynasan® 114), glyceroltripalmitate (Dynasan® 116) and glyceroltristearate (Dynasan® 118). Cholesterol and gelatin, which served as further matrix materials were obtained from Sigma-Aldrich (Deisenhofen, Germany). Polymeric matrices were made from polylactic-glycolic acid (PLGA) and polylactic acid (PLA) of varying molecular weights. The PLGAs Resomer® RG502H (50/50, M_w = 10,500, ***PLGA$_{10}$***) and Resomer® RG502 (50/50, M_w = 17,000, ***PLGA$_{17}$***) as well as the PLA Resomer® R503 (M_w = 30,000, ***PLA$_{30}$***) were kindly provided by Boehringer Ingelheim (Ingelheim, Germany).

1.2 Excipients for the matrix manufacture

Experiments on the biocompatibility and erosion behavior of the lipid materials were carried out using the phospholipids dimyristyl-phosphatidyl-choline (DMPC), dipalmitoyl-phosphatidyl-choline (DPPC) and distearoyl-phosphatidyl-choline (DSPC). All phospholipids were kindly provided by Lipoid GmbH (Friedrichshafen, Germany). Sucrose (Südzucker, Regensburg, Germany) and agarose (Fluka/Sigma-Aldrich, Deisenhofen, Germany) were used as further excipients for the matrix preparation.

1.3 Model drugs

Bovine insulin used for extraction analysis was a gift from Hoechst (Frankfurt, Germany) and somatostatin was kindly provided by Dr. Wilmar Schwabe Pharmaceuticals (Karlsruhe, Germany). For release experiments, the fluorescent dyes pyranine, fluorescein-di-sodium salt and nile red (all Sigma-Aldrich, Deisenhofen, Germany) served as model drugs.

1.4 Chemicals

All reagents used were analytical grade or better. Water used for the experiments was double-distilled and filtered through a 0.2µm cellulose nitrate filter (Sartorius, Göttingen, Germany) prior to use. Tetrahydrofuran (THF), methylene chloride, chloroform and ethanol were obtained from Merck (Darmstadt, Germany) and acetonitrile was purchased from Mallinckrodt Baker B. V. (Deventer, Netherlands). Trifluoroacetic acid (TFA) was obtained from Sigma-Aldrich (Deisenhofen, Germany). Silicon oil was purchased from Carl Roth GmbH & Co. (Karlsruhe, Germany). Tissue Tek for cryo-sectioning was obtained from Sakura Finetek (Torrane, CA, USA). Sodium azide, which was purchased from Sigma-Aldrich (Deisenhofen, Germany), was added to release buffers as a preservative.

1.5 Animals

All in vivo studies were carried out with female immunocompetent NMRI-mice, which were purchased from Charles River Deutschland GmbH (Sulzfeld, Germany).

1.6 Instruments

Used substances were weighed on a Mettler Toledo AT261 analytical scale (Mettler Toledo, Giessen, Germany) or an electronic Sartorius 4401 micro-balance (Sartorius, Göttingen, Germany). Matrix preparation was carried out using a self-made manual compression tool made of hardened steel (machine shop, University of Regensburg, Germany) and a hydraulic press (Perkin Elmer, Rodgau-Jügesheim, Germany). For thermographic analysis a DSC 2920 differential scanning calorimeter (TA Instruments, Alzenau, Germany) was used.

2 Methods

2.1 HPLC-Analysis of Insulin and somatostatin

HPLC analysis was performed for insulin and somatostatin using a system with a Degasser (Knauer, Berlin, Germany), LC-10AT pump, FCV-10AT$_{VP}$ gradient mixer, SIL-10AD$_{VP}$ autosampler, CTO-6A column oven, SPD-10AV UV-detector, RF-551 fluorescence detector and SCL-10A$_{VP}$ controller (all Shimadzu, Duisburg, Germany). For somatostatin, a linear gradient from 26% to 39% acetonitrile in water, with 0.1% trifluoroacetic acid (TFA), as mobile phase was applied over 15 minutes at a flow rate of 1.0ml/min. 100µl of the samples were separated at a temperature of 40°C using a combination of a C18-reversed phase pre-column (LC318, 4.6mm x 5.0mm) and an C18-reversed phase analytical column from Supelco (Deisenhofen, Germany). Chromatograms were detected at 210nm and 274nm, respectively by UV detection and at wavelengths of 274nm / 308nm (excitation/emission) for the fluorescence detector.

The procedure for insulin differed from that for somatostatin only in the duration of the linear gradient. Here the concentration of acetonitrile in water (+0.1% TFA) was constantly increased from 26% to 39% over a period of 24 minutes. Again 100µl-samples were separated at 40°C using the above-mentioned combination of pre-column and analytical column. Chromatograms were detected by UV and fluorescence detection as described above. Both analytical methods were linear and reproducible in concentration ranges from 4µg/ml to 150µg/ml.

2.2 Stability test of somatostatin and insulin in release medium

To investigate whether the release of the model drugs from triglyceride devices could be determined directly from the release medium, investigations into the stability of insulin and somatostatin were carried out in isotonic phosphate buffer at pH 7.4. To this end, the substances were dissolved in 1.0ml HPLC-vials to a concentration of 150µg/ml. Afterwards the solutions were incubated at 37°C in a Memmert U40 drying oven (Memmert, Schwabach, Germany). Drawn samples were immediately frozen at -80°C and quantitatively analyzed together per HPLC after the incubation time of 5 weeks was completed.

2.3 LC/MS-Analysis of insulin and somatostatin

To clarify the degradation pathways of the model drugs during the incubation in release medium, insulin and somatostatin samples from the stability experiments underwent LC/MS-analysis, which was performed to identify the separated substances. The chromatographic conditions were transferred to a Hewlett-Packard HPLC-system with series 1100 degasser, binary pump, autosampler, column oven and diode array detector (all Hewlett-Packard, Waldbronn, Germany), coupled with a TSQ7000 electro-spray-mass spectrometer (ThermoQuest, San José, CA, USA) with AP12-source (capillary temperature: 350°C, spray voltage: 4.5kV). Substances were detected in total ion chromatograms of the mass spectrometer and characterized by analysis of their individual mass spectra.

2.4 Preparation of insulin- and somatostatin-loaded matrices

For evaluation of the extraction method, which facilitates the recovery of the incorporated model drugs from the triglyceride matrix and further investigations on drug stability within the matrix, insulin and somatostatin were incorporated into glyceroltripalmitate matrices by mixing the two powders. The respective model drug and the triglyceride were both sieved to isolate particles 106µm or smaller prior to the mixing step. The mixture was subsequently compressed for 10 seconds with a compression force of approximately 250N, using the manual compression tool, which is shown in Figure 2, and the described hydraulic press. The resulting cylinders had a diameter of two millimeters and a weight of 6.0 ±0.5mg.

Figure 2: Left: Manual press for matrix manufacture
right: Schematic of the compression molding.

2.5 Extraction methods for insulin and somatostatin

An extraction method previously described by Lucke et al. [141] was applied and afterwards optimized for insulin and somatostatin. In the original method, the sample was weighed into a 1.5ml micro test tube (Eppendorf, Hamburg, Germany) and dissolved in 600µl of chloroform. For somatostatin, 600µl of an acetonitrile/water/TFA-mixture (67.35/32.65/0.1) were added, whereas in the case of insulin either 600µl of 0.01N HCL or of an acetonitrile/water/TFA-mixture (29.85/70.15/0.1) were added. The solvent mixtures in both cases corresponded to the mobile phase at the elution time point during HPLC-analysis, which assured the best solubility of the respective drug. After mixing at 2,200rpm on a Reax Control (Heidolph, Schwabach, Germany), the dispersion was allowed to settle at room temperature for 10 minutes before the chloroform-phase was finally separated from the mixture by centrifugation at 13,200rpm for 5 minutes (Centrifuge 5415 R, Eppendorf, Hamburg, Germany). The upper fraction was then used for further analysis.

To optimize the extraction of the model drugs from glyceroltripalmitate matrices, cyclohexane, tetrahydrofuran (THF), toluene and xylene were tested. First, one rod was weighed exactly into a 1.5ml micro test tube. Afterwards, 500µl of the respective solvent were added and, when needed, was warmed at 35°C in a water bath until the lipid was dissolved. The mixture was then centrifuged at 13,200rpm to achieve sedimentation of the respective model drug and 450µl of the upper fraction were withdrawn. Subsequently, two washing and centrifugation steps with 450µl THF were performed to dissolve and remove the lipid completely. After the third withdrawal of 450µl of the washing solution, the samples were dried over night under vacuum using a RV5 two-stage oil pump from Edwards (Crawley, Sussex, UK). The remaining drug was then dissolved in 1000µl of the aforementioned, acetonitrile/water/TFA-mixture to determine its content via HPLC-analysis.

2.6 Preparation of pyranine-loaded triglyceride matrices

For the investigation of preparation parameters that influence the release from the resulting pyranine-loaded triglyceride matrices, cylinders containing the hydrophilic fluorescent dye as a model drug were prepared under varying conditions. To this end, the respective amount of glyceroltripalmitate was dissolved in tetrahydrofuran and mixed with a solution of the needed

amount of the dye in water. The ratios of triglyceride and pyranine used varied with the drug loading, whereby a total 200.0mg of dye-loaded triglyceride was dissolved. The resulting mixture with a THF/water-ratio of 9:1 was frozen in liquid nitrogen and subsequently freeze-dried, using the two-stage oil pump mentioned above (see section 2.5). Afterwards, the obtained powder was ground and mixed in a mortar and then compressed to cylindrical matrices of 1mm or 2mm diameter, as described in section 2.4.

Drug loading was varied from 1% over 10% up to 33% pyranine. These matrices were compressed with a force of 250N. Additionally, matrices containing 10% pyranine were prepared by applying a compression force of 50N and 500N. Cylindrical matrices with a dye content of 10%, diameters of 1mm and 2mm and heights of 2mm, 4mm and 6mm were compressed by applying a force of 250N. In addition, glyceroltripalmitate was sieved to fractions of particle sizes below 106µm and 106µm-250µm and subsequently mixed with the dye to a total pyranine content of 10%. Afterwards, this powder mixture was compressed to cylinders of 2mm diameter as described above.

For experiments on the effects of drug hydrophilicity, fluorescein-di-sodium salt and nile red served as model drugs in cylinders of 2mm diameter and a dye loading of 10%. Matrix manufacture with fluorescein was performed using the above-described procedure for pyranine. For the incorporation of nile red into the matrices, both the dye and the triglyceride were dissolved in THF and afterwards this solution also underwent the above-mentioned process for manufacture of matrices.

10% fluorescein-di-sodium salt containing matrices for the investigation of involvement of osmosis in release mechanisms from triglyceride cylinders were prepared as described above.

For the investigation of the water uptake into triglyceride matrices, glyceroltripalmitate was sieved to fractions of particle sizes below 106µm and 106µm-250µm and subsequently compressed to cylinders of 2mm diameter as described above.

2.7 Solubility of nile red in release medium

To be able to draw conclusions from release experiments performed with the highly lipophilic florescent dye nile red, which was used as model drug for the investigation of the influence of drug characteristics on the resulting release profile from a triglyceride matrix, the solubility of the dye in the release medium was determined. To this end, 0.2mg nile red were weighed into 20ml of phosphate buffer pH 7.4 and subsequently incubated for 2 days at 37°C

in the aforementioned heating oven. After centrifugation of the mixture, 5.0ml of the upper fraction were taken for the following procedure. Solubility data were obtained by measuring fluorescence of the samples after freeze-drying and re-dissolution of the remaining solid phase in ethanol. A RF-1501 fluorescence spectrophotometer (Shimadzu, Duisburg, Germany, $\lambda_{ex}/\lambda_{em}$: 567nm/629nm) was used for the measurements.

2.8 In vitro release set-ups

2.8.1 Release of pyranine

To investigate the influence of preparation parameters on the release from triglyceride matrices, experiments were carried out using pyranine as model drug. For investigation of the in vitro release of pyranine-loaded matrices, the samples were incubated at 37°C in 50ml 0.1M phosphate buffer solution (pH 7.4) while subjected to gentle shaking in a GFL 1086 horizontal shaking water bath (GFL, Burgwedel, Germany). To suppress the growth of bacteria and fungi, 0.05% sodium azide were added. The withdrawn volume of the samples was replaced by fresh buffer solution and the pyranine content of the samples was measured using the aforementioned fluorescence spectrophotometer (λ_{ex}: 403nm, λ_{em}: 503nm).

2.8.2 Release of fluorescein and nile red

To examine the influence of dye hydrophilicity, fluorescein and nile red were used as model drugs. Fluorescein properties were varied by incubation in buffers having pH values of 2.8, 5.5, and 9.0, respectively. Again a temperature of 37°C was chosen and 0.05% sodium azide was added as a preservative. Fluorescein release from the matrices was investigated by measuring fluorescence in phosphate buffer with pH 9.0 using excitation/emission wavelengths of 491nm/505nm; samples were collected as described in section 2.8.1 for pyranine. Concomitantly, matrices containing the highly lipophilic fluorescent dye nile red were incubated as mentioned in section 2.8.1 for pyranine. Release data from nile red-loaded lipid cylinders were obtained by measuring fluorescence after freeze-drying of the completely exchanged release medium at the specific time points and re-dissolution of the remaining solid phase in ethanol ($\lambda_{ex}/\lambda_{em}$: 567nm/629nm).

2.8.3 Investigation of release mechanisms

To investigate by an in vitro release experiment whether osmosis is involved in release mechanisms from triglyceride matrices, 10% fluorescein-di-sodium salt loaded glyceroltripalmitate cylinders were incubated in phosphate buffer solutions (pH 9.0) having three different osmotic pressures. Sodium chloride was added to the phosphate buffer to achieve osmotic pressures of 293, 7850 and 9500mosmol, respectively. Release data were obtained by measuring fluorescence of the dye as described in section 2.8.2.

2.9 In vitro investigation of water uptake into triglyceride matrices

To further investigate the release mechanisms from triglyceride matrices, their water uptake was examined as follows. For the investigation of the water uptake into glyceroltripalmitate cylinders, the blank rods were incubated for up to 14 days in phosphate buffer containing 30mg/ml fluorescein-di-sodium salt at a pH of 9.0 and a temperature of 37°C. After the withdrawal of the matrices, they were washed with 3.0ml of double distilled water. The dye was subsequently extracted according to the method described by Lucke et al. [141] (see section 2.5) using 1.0ml of chloroform and of the mentioned phosphate buffer as solvents. Afterwards the fluorescein content was measured as described above and the relative amount of water taken up by the cylinder was calculated.

2.10 Cryo-sectioning of matrices

After incubation of the blank cylinders in phosphate buffer containing fluorescein-di-sodium salt, additionally the distribution of the dye solution within the matrices was investigated. To this end, a cross-section of the triglyceride cylinders was made using a HM 550 OMP cryotome from Microm International (Walldorf/Baden, Germany). A chamber temperature of -10°C and a sample temperature of 5°C were applied. Afterwards, approximately one half of the matrices were cut away in slices of 20µm each. To this end the cylinders were embedded on cryo-stubs (Microm International, Walldorf/Baden, Germany) in tissue tek within a ring having a diameter of approximately 1.5cm and a height of approximately 0.75cm. Tissue tek was removed before microscopic investigation of the remaining half of the matrix by using a soft paper tissue.

2.11 Confocal Laser Scanning Microscopy

Subsequent to the cross-sectioning of the matrices, they were investigated by fluorescence microscopy using an Axiovert 200M confocal laser-scanning microscope with LSM510 laser module (both Carl Zeiss, Jena, Germany). For the detection of fluorescein-di-sodium salt ($\lambda_{ex}/\lambda_{em}$: 491nm/505nm) the laser with an excitation wavelength of 488nm was chosen and emission was detected at wavelengths above 505nm. No further filters were used.

2.12 Preparation of sterile matrix materials for in vivo studies

After the in vitro characterization, the triglyceride matrices were tested for their in vivo biocompatibility and erosion. To evaluate tissue reactions, sterile materials had to be used in order to avoid reactions not related to the material. The phospholipid distearoyl-phosphatidyl-choline (DSPC) was produced under aseptic conditions by the manufacturer and therefore underwent no additional sterilization procedure.

2.12.1 Sterilization of glyceroltripalmitate

Glyceroltripalmitate was sterilized for 2h at 160°C in a Memmert U40 drying oven (Memmert, Schwabach, Germany) and afterwards tempered at 55°C for three days to obtain the stable β-modification [8].

2.12.2 Sterilization of gelatin and poly(D,L-lactic-co-glycolic acid) ($PLGA_{17}$)

Gelatin was dissolved in double-distilled water to a concentration of 0.1% and subsequently filtered through a PES membrane filter with 0.2µm pore size (Corning, New York, USA). Afterwards the solution was freeze-dried using the aforementioned two-stage oil pump and subsequent to the drying step the resulting powder was ground in a porcelain mortar (Rosenthal, Selb, Germany) under liquid nitrogen. Then the gelatin as well as the untreated $PLGA_{17}$ (M_w: 17,000) was sterilized by UV irradiation for two hours [155].

2.12.3 Sterilization of cholesterol

Cholesterol used for the matrix preparation for in vivo experiments was first dissolved in diethyl ether. Subsequently, the solution was filtered through a PES membrane filter with 0.2µm pore size (Corning, New York, USA) and then dried under vacuum at room temperature in a vacuum desiccator, which was sterilized before for 2h at 160°C in the aforementioned heating oven.

2.13 Preparation of sterile matrices for in vivo studies

For the in vivo studies, cylindrical matrices were compressed from the obtained sterile powders. All matrices were manufactured under laminar air flow (UVF 6.12 S, BDK Luft- und Reinraumtechnik GmbH, Sonnenbuehl-Gengkingen, Germany) to avoid bacterial contamination using the manual press, which is shown in Figure 2 (see section 2.4) and which had undergone a heat sterilization process at 160°C for 2 hours. The resulting matrices had a diameter of two millimeters and a weight of 6.0 ±0.5mg. A compression force of approximately 250N was applied. The sterility of the obtained matrices was tested, according to the Ph. Eur., and confirmed in the institute of microbiology at the medical center of the University of Regensburg.

2.14 In vivo studies with matrices

For the investigation of the in vivo biocompatibility and erosion of the lipid materials, two in vivo studies were carried out with female NMRI mice (8 weeks old at the beginning of the experiment, Charles River Deutschland GmbH (Sulzfeld, Germany)), which were both authorized throughout an accepted petition for animal studies. In the first study, two control groups of mice received matrices made of gelatin and the aforementioned $PLGA_{17}$, which are accepted to be biocompatible. The two test groups received matrices made of pure glyceroltripalmitate and of glyceroltripalmitate containing 1% gelatin (see Table 4). After anesthetization with a combination of 100mg/kg ketamine and 4-6mg/kg xylazine, the animals underwent subcutaneous implantation of one sterile matrix in each flank (both of the same material). Afterwards, the wound was closed with sterile Michel suture surgical clips (7.5 mm x 1.75 mm, Fine Science Tools, Heidelberg, Germany). Then the animals were returned to the housing facility where they were kept under a 12h/12h light/dark cycle at 20°C

and 50% relative humidity and had free access to food (ssniff R/M-H, Lage, Germany) and water.

In the first study, mice were sacrificed 2, 4, 8, 30 and 60 days post-operation (Table 4) by cervical dislocation and the matrices were excised. One cylinder served to evaluate tissue reactions by histological examination, while the other was used to investigate the swelling and microstructure of the matrix. In the second study, the equal procedure for sample collection was performed. The study designs with a detailed time schedule are shown in Tables 4 and 5. Early time points served for the evaluation of acute reactions, whereas later excision points were chosen for the investigation of chronic tissue reactions.

Table 4: Time schedule for biocompatibility study of glyceroltripalmitate.

group	material	n	excision
test group 1	100% Glyceroltripalmitate	4	d2, d4, d8, d30, d60
test group 2	99% Glyceroltripalmitate 1% Gelatin	4	d2, d4, d8, d30, d60
control group 1	100% Gelatin	4	d2, d4, d8, d30, d60
control group 2	100% $PLGA_{17}$	4	d2, d4, d8, d30, d60

Table 5: Study design of erosion behavior investigations.

group	material	n	excision
control group 1	100% Glyceroltripalmitate	4	d10, d20, d35
test group 1	90% Glyceroltripalmitate 10% DSPC	4	d7, d14, d21, d25, d35
test group 2	50% Glyceroltripalmitate 50% DSPC	4	d2, d6, d10, d15, d28
control group 2	100% Cholesterol	4	d3, d7, d14, d24, d35
test group 3	50% Glyceroltripalmitate 50% Cholesterol	4	d3, d7, d14, d24, d35
test group 4	10% Glyceroltripalmitate 90% Cholesterol	4	d3, d7, d14, d24, d35

One tissue sample from each mouse was fixed in Bouin´s solution, and processed for routine paraffin histology. Afterwards 6µm sections were stained according to the method detailed by Masson & Goldner and examined with an Olympus BH-2 light microscope (Olympus, Hamburg, Germany). The other matrix was detached from the surrounding tissue and then weighed on the above-described Mettler Toledo analytical scale to investigate its

swelling before being examined by light microscopy as described in section 2.16. After a freeze-drying step (see section 2.15), the matrices were weighed again to quantify erosion and subsequently re-examined by light microscopy. Swelling and erosion of the matrices were determined as relative change in mass compared to values before the implantation. Afterwards the freeze-dried matrices were manually broken into two parts and both the surface and cross-section were imaged using scanning electron microscopy, as described in section 2.16.

2.15 Freeze drying of matrices

To determine the extent of erosion of the matrix material, the dry-weight after implantation was investigated. For the drying procedure of the matrices a Christ Beta 2-16 freeze drier (Martin Christ Gefriertrocknungsanlagen GmbH, Osterode am Harz, Germany) was used. The matrices were frozen to –40 °C over 3 hours before starting the main drying step, which was carried out for 24 hours at 8 °C and 0.05 mbar. For the final drying step, the samples were treated at room temperature and 0.005 mbar for two hours.

2.16 Scanning electron microscopy (SEM) and light microscopy investigations

Another important part of the in vivo investigations was the optical examination of the matrices after explantation. The samples were investigated by light microscopy with a M75 zoom-stereomicroscope (Wild, Heerbrugg, Switzerland) and the microstructure of the matrices was examined by scanning electron microscopy (SEM). Samples were glued to aluminium sample holders (machine shop, University of Regensburg, Germany) using a conductive adhesive film (Leit Tabs, Ted Pella Inc., Redding, CA, USA) and gold sputtered for 4 minutes under argon atmosphere using a Polaron Automatic Sputter Coater E 5200 from Polaron Equipment Ltd. (Watford, UK). The coated samples were finally analyzed using a DSM 950 Scanning Microscope from Carl Zeiss (Jena, Germany).

2.17 Incorporaion of erosion modifiers and in vitro release set-up

To be able to modify the in vivo erosion of triglyceride matrices, several excipients were first tested in vitro for their influence on the release of pyranine from cylindrical glyceroltripalmitate matrices. Agarose was used in ratios of 5%, 10% and 15%, respectively, the phospholipids DMPC, DPPC and DSPC were chosen in concentrations from 5% to 50% (see Table 6) and sucrose was used in ratios of 5%, 10%, 25% and 50%. Before incorporation, the sucrose was sieved to four fractions of 25µm-45µm, 150µm-180µm, 250µm-355µm and 560µm-710µm using analytical sieves (Retsch, Haan, Germany).

For these experiments, two preparation methods were developed. The first was an emulsion method that has been previously described [37] and was only performed for the three phospholipids. Using this method, pyranine was dissolved in 200µl water and dispersed in a solution of the lipid and the respective amount of the phospholipid in 5 ml methylene chloride under vigorous vortex mixing (speed 8 vortex genie 2, Scientific Industries, Bohemia, USA). The resulting mixture was then sonicated for 30 seconds at a frequency of 20 kHz and an intensity of 120 Watts using a B12 sonicator made by Branson (Sonic Power Company, Danbury, Connecticut, USA). Afterwards, water and solvent were removed from the resulting W/O emulsion by vacuum drying using the aforementioned two-stage oil pump until a final pressure of 0.5 Pa was reached. After drying, the mixture was ground in a mortar to obtain a free flowing powder with a particle size of less than 106µm.

In the second preparation procedure, 135.0mg glyceroltripalmitate were loaded with 15.0mg pyranine as described in section 2.6 and afterwards the predefined amount of the respective excipient was added in a second step. The resulting powder mixture was subsequently manually shaken in a 2.0ml micro test tube (Eppendorf, Hamburg, Germany) for one hour. Mixing in a mortar was not applied with regard to the defined particle size of the sucrose and consequently for the other materials to maintain the comparability of the results.

The obtained powders from both procedures were subsequently compressed to matrices as described in sections 2.4 and 2.6, respectively, and processed for in vitro release as mentioned in section 2.8.1. Table 6 gives an overview of the investigated ratios and applied preparation procedures for glyceroltripalmitate cylinders containing the three phospholipids as a modifying component.

Table 6: Investigated ratios and preparation procedures for phospholipid containing glyceroltripalmitate matrices. The emulsion method was not performed for DMPC at ratios of 25% and 50%. The two step method was not used for DSPC and DMPC in the ratio of 50%.

preparation method	**DMPC**	**DPPC**	**DSPC**
emulsion method	5%, 10%	5%, 10%, 25%, 50%	5%, 10%, 25%, 50%
two step method	5%, 10%, 25%	5%, 10%, 25%, 50%	-/-

2.18 Particle size determination of lipid microparticles and powders before in vivo study

After the in vitro experiments on various erosion modifiers, the hypothesis of a dependence of the in vivo erosion on the triglyceride particle size was investigated by using glyceroltripalmitate microparticles and powders. To perform particle size analysis of the triglyceride, the samples were investigated using a Mastersizer 2000 laser diffractometer (Malvern Instruments, Worcestershire, UK) as follows: approximately 100µg of the lipid sample were directly added to the dispersion unit (Hydro 2000S), which was filled with an ethanol / water mixture (68.2% (v/v), density 0.9). The particles were dispersed by stirring at 3000rpm for 5min, no sonication was applied. The volume-based particle size distribution was calculated using the Fraunhofer approximation (Malvern Software V5.1).

2.19 X-Ray diffraction analysis

To investigate the degree of crystallinity of the glyceroltripalmitate microparticles and powders, which might also influence the in vivo erosion of the material, wide-angle X-ray scattering (WAXS) was performed for all samples by using a STOE STADIP X-ray diffractometer (Darmstadt, Germany) equipped with a copper anode (Cu $K\alpha_1$ radiation, Germanium monochromator). Experiments were conducted at a scan rate of 2 theta = 0.05° in a 5° to 56° range and obtained data were analyzed using a Winxpow 1.08 software.

2.20 In vivo erosion study

The third in vivo study investigated a dependence of the in vivo erosion on the triglyceride particle size using glyceroltripalmitate microparticles and two glyceroltripalmitate powders, one with a high and one with a low degree of crystallinity. Preparation of the microparticles by spray congealing was conducted as previously described [153]. The resulting lipid microparticles were sterilized by Beta-Gamma-Service (BGS, Saal a.d. Donau, Germany) using β-irradiation of 10MeV. The applied dose of radiation was 25kGy.

To obtain the triglyceride powders for the in vivo experiments, two different sterilization processes were applied. In the first method, which led to a high degree of crystallinity, glyceroltripalmitate was heated for 2h to 160°C and afterwards tempered for 3 days at 55°C in the drying oven to obtain the stable β-modification [8]. Subsequently, the triglyceride was ground in a mortar and sieved to a particle size of 106µm to 250µm. These steps were performed under laminar airflow using a sterilized mortar and sieve, respectively. For the second sterilization method, the triglyceride was dissolved in chloroform and afterwards filtered through a PTFE sterile filter (Corning, New York, USA). Subsequently, the obtained solution was freeze dried in a sterilized desiccator, as mentioned in section 2.12, and the resulting powder was sieved as described above for the first sterilization method.

From the sieved lipid microparticles and powders, 7.5mg portions were prepared in sterile micro test tubes (Eppendorf, Hamburg, Germany) for each mouse, to be implanted subcutaneously into the left flank with a sterilized pipette tip (Corning, New York, USA). Prior to this procedure, the mice were anaesthetized as described in section 2.14. The three groups were investigated in vivo for 8 weeks, using female immunocompetent NMRI-mice, which underwent subcutaneous implantation of the triglyceride into the left flank. Housing conditions were equal to former in vivo studies (see section 2.14). Samples were collected at days 7, 17, 28, 42 and 56. At these time points, the mice were sacrificed by cervical dislocation. Subsequently, the region of implantation was excised from the mice, samples containing the lipid microparticles or powders were fixed in 5% formaldehyde solution, and processed for routine paraffin histology as described in section 2.14.

2.21 Size determination for glyceroltripalmitate microparticles after in vivo study on erosion behavior of lipid microparticles and powders

To investigate the erosion of the glyceroltripalmitate samples, the particle size and its alteration was observed throughout the course of the study. Particle size determination was carried out from histological sections using the described camera and software package with measurement module. Holes stemming from the microparticles and the triglyceride powder were measured by light microscopy using a Leica DFC 320 camera and the IM1000 software package with measurement module (Leica, Heidelberg, Germany). To estimate the real diameter of the spherical particles in the respective histological section, two diameters (d_1=smallest diameter, d_2=largest diameter) were measured as shown in Figure 3, from which the mean was calculated.

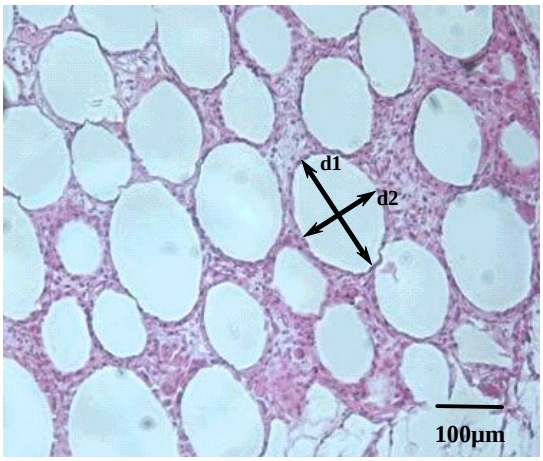

Figure 3: Light microscopy image of a histological section of lipid microparticles 7 days after implantation (HE stained, 100x). Mean diameter was calculated as (d1+d2)/2.

But as Figure 4 illustrates, a significant statistical error would result if only the mean value of all measured diameters of the microparticles is calculated, since the observed diameter depends on the distance of the section from the central plane. Thus, in the depicted example cutting one particle in three different plane sections would result in three different diameters. Consequently, simply taking the mean value of all determined particle sizes within the in vivo study would result in diameters that differ from the real value. This is known and described in literature [156-158] as the so-called “Wicksell-corpuscle-problem”.

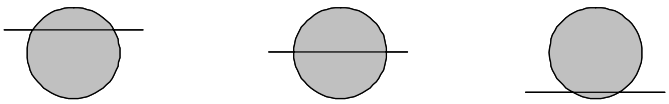

Figure 4: Scheme of the so called “Wicksell-corpuscle- problem”, which occurs, when making plane sections of a sphere.

Stoyan, Kendall and Mecke described in literature [158] an estimator for the real diameter (shown in equation 1), which can be used for the analysis of the particle size of the lipid microparticle group.

$$\hat{d}_V = \frac{\pi n}{2}\left[\sum_{i=1}^{n}\frac{1}{x_i}\right]^{-1} \qquad (1)$$

$\hat{d}_v$ estimated mean diameter of all measured particles
n number of particles which were measured
x_i measured diameter of the respective particle.

But since this estimator is valid only for spherical particles and the two lipid powders were irregularly shaped, it was only possible to obtain qualitative results for the lipid microspheres in our in vivo experiment.

2.22 Manufacture of programmable implants and in vitro release study

Since triglycerides were determined to be suitable for controlled prolonged release and the programmable implants developed by Vogelhuber et al. [39] were only capable of pulsatile release due to the used polyanhydride core matrix, investigations on programmable implants were carried out with glyceroltrilaurate, glyceroltrimyristate, glyceroltripalmitate, glyceroltristearate and cholesterol as core materials. The polymers described in section 1.1 ($PLGA_{10}$, $PLGA_{17}$ and PLA_{30}) were used as mantle materials. Table 7 gives an overview of the core and mantle materials used for the manufacture of programmable implants.

Table 7: Used materials for the preparation of programmable implants.

core materials	**mantle materials**
cholesterol	$PLGA_{10}$
glyceroltrilaurate (C12)	$PLGA_{17}$
glyceroltrimyristate (C14)	PLA_{30}
glyceroltripalmitate (C16)	
glyceroltristearate (C18)	

For the preparation of the matrices, first the respective core material was loaded with pyranine, as described in section 2.6. Afterwards, the cylindrical cores of 1mg weight and 1mm diameter (Figure 5a) were compressed. The different matrix materials all contained 10% of the model drug. Schematics of the manual compression tools are shown in Figure 5.

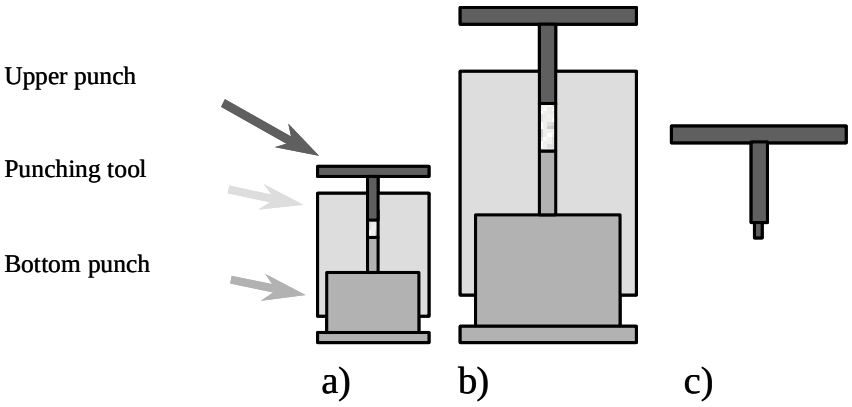

Figure 5: a) manual press with 1mm diameter for manufacture of the core
b) manual press with 2mm diameter and upper punch with plane shape
c) upper punch with staggered shape.

The powder was loaded into the appropriate manual compression tools and placed in the aforementioned hydraulic press; a compression force of 250N was applied and maintained for 10 seconds. In the following step, the bottom of the mantle was prepared with 5.0mg of polymeric mantle material using the manual compression tool with a diameter of 2mm and the upper punch with the staggered shape (Figure 5b, c). Again a compression force of 250N was applied for 10 seconds. Afterwards the core was placed in the resulting cavity of the bottom part and the implant was compressed with another 1.5mg of the polymer as upper part for 10 seconds with 250N using the plane upper punch (Figure 5b). The last step of the implant manufacture was the closure of the pores in the mantle, which could otherwise lead to a preliminary release [39], at a temperature above the glass transition point of the polymer. Two different methods to heat up the polymer mantle were tested and the results were compared. In the first method, the implants underwent a heat treatment in silicon oil (Rotitherm® H250) at 110°C for 3 seconds, whereas in the second method the press was heated in a drying oven and the implant was compressed subsequently with approximately 25N for 10 seconds. Applied temperatures were 48 °C for $PLGA_{17}$ and $PLGA_{10}$ and 50 °C for PLA_{30}. Figure 6 shows a schematic of the preparation procedure with the second compression step at higher temperatures.

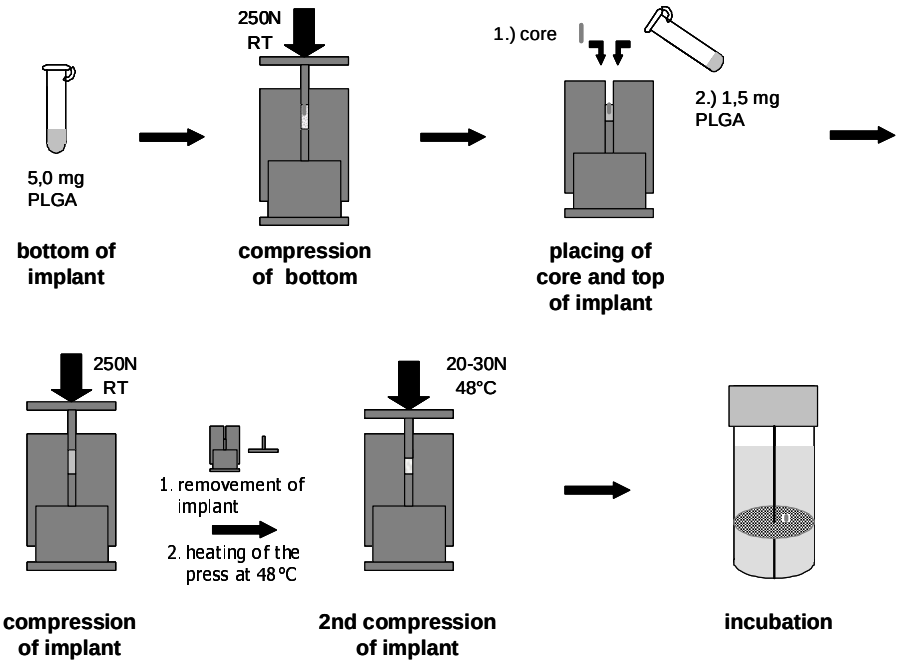

Figure 6: Schematic of the preparation procedure for programmable implants; closure of pores within the mantle occurred through a second compression step at higher temperatures (here 48°C for $PLGA_{10}$ and $PLGA_{17}$).

Drug release was investigated from programmable implants as well as from the cores without mantle as described in section 2.6. Statistical calculations for the investigation of the onset of release was carried out by using one-way analysis of variance (ANOVA) in conjunction with Tukey´s studentized range test.

2.23 Modelling of release profiles for preprogrammable implants

In this study, the method of convolution, which has already been described [159-162], was utilized to predict release profiles from programmable implants and the results of the mathematical modeling were compared to experimentally obtained release profiles. Convolution and deconvolution are parts of the so-called system theory. Following the rules for this theory, the mantle of the programmable implants was handled as a "black box", which reacts on an input function $I(t)$ (e.g. the release of a model drug from a core matrix) with a specific response function $R(t)$ (e.g. the release from embedded core). With the input function being a defined kinetic process (e.g. a bolus release from a core matrix), the system can be characterized by a system function, $F(t)$ (filter function, impulse response). One impulse function is the so-called Dirac´s delta-impulse $\delta(t)$, which is a narrow rectangular impulse having the breadth T and the amplitude $1/T$, which results in the value 1 for the area of the

delta-impulse. Mathematically, the relationship between the functions is described by the following equation:

$$R(t) = F(t) * I(t) \qquad (2).$$

The star indicates that the response function results from a convolution operation on filter- and input functions. The deconvolution can be expressed as follows:

$$I(t) = R(t) // F(t) \qquad (3)$$

$$F(t) = R(t) // I(t) \qquad (4).$$

Consequently, an input function being the impulse $\delta(t)$, results in the following response function:

$$\delta(t) * F(t) = F(t) \qquad (5).$$

With an amplitude having, for example, the value A, which differs from $1/T$, the area of the impulse results in $A \cdot T$. Such an impulse can generally be treated in the same manner as a Dirac-impulse, whose input- and response functions are described as $A \cdot T\delta(t)$ and $A \cdot T \cdot F(t)$, respectively, which results in equation (6).

$$A \cdot T\delta(t) * F(t) = A \cdot T \cdot F(t) \qquad (6)$$

An integratable function $I(t)$ can be divided into pieces having the form $A \cdot T\delta(t)$, whereby the amplitude-value A is replaced by the value of the function $I(iT)$ (Figure 7).

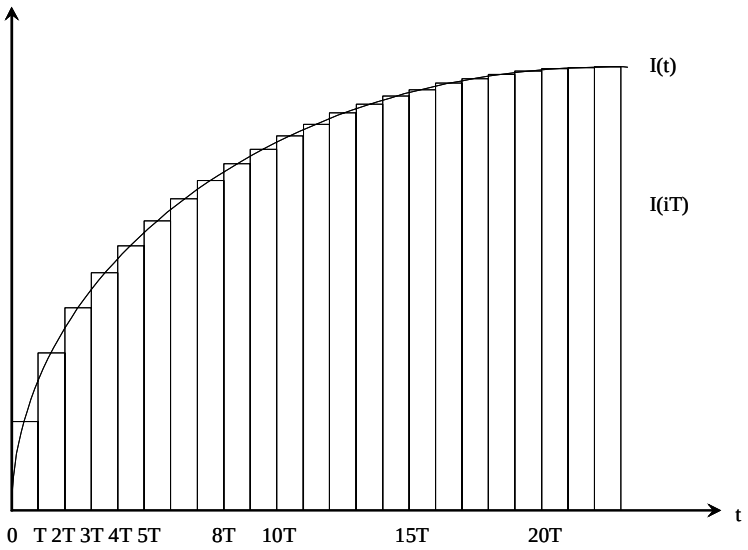

Figure 7: Dissection of the input function $I(t)$ into rectangular impulses (adapted from [162]).

Considering the time-related shifting of the respective impulse, each of them becomes $I(iT) \cdot T\delta(t\text{-}iT)$, which results in equation (7).

$$I(iT) \cdot T\delta(t\text{-}iT) * F(t) = I(iT) \cdot T{\cdot}F(t\text{-}iT) \qquad (7)$$

The response function $R(t)$ now results from the overlapping of each single input function. Since $F(t)$ is generally not as short as the delta-impulse and can be maintained for longer time periods, the previous intervals have to be taken into account. Considering an overlapping of all parameters results in:

$$R(nT) = T\sum_{i=0}^{n} I(iT)F(t-iT) \qquad (8).$$

With the intervals being very small, an integral can be formulated and the discrete time values iT can be replaced by the variable τ:

$$R(t) = \int_{0}^{t} I(\tau)F(t-\tau)d\tau \qquad (9).$$

This integral is called convolution integral. A schematic of the relationship between input function, filter function and response function is depicted in Figure 8.

Figure 8: a) Schematic for a linear system, on which a convolution operation can be applied. For a known filter function, one special response function can be calculated for each known input function. (adapted from [162])
b) Visualization of the transfer of convolution theory to programmable implants.

Generally, for such systems it is valid that when two of the depicted functions are known, the third function can be calculated from the others. For the mathematical modeling in the investigations of programmable implants, the numerical solution of the convolution integral was applied. Thereby the input function or the filter function is considered to be constant within the respective time interval $0 \leq T \leq t$. Starting with equation (8) for the numerical convolution, $F(t)$ becomes the value $F(nT)$ of the function. Thus it can be formulated that: $I(iT) = I_i$, $F(nT\text{-}iT) = F_{n\text{-}i}$, which leads from equation (8) to:

$$R_n = T\sum_{i=1}^{n} I_i F_{n-i} \qquad (10).$$

Thus the numerical algorithm, which is depicted in equations (11-14), can be formulated as a solution of the convolution integral. This algorithm replaces the integration by multiplication and addition of numbers.

$$R_0 = (I_0 \cdot F_0) \cdot T \quad (11)$$

$$R_1 = (I_0 \cdot F_1 + I_1 \cdot F_0) \cdot T \quad (12)$$

$$R_2 = (I_0 \cdot F_2 + I_1 \cdot F_1 + I_2 \cdot F_0) \cdot T \quad (13)$$

$$R_n = (I_0 \cdot F_n + I_1 \cdot F_{n-1} + ... + I_{n-1} \cdot F_1 + I_n \cdot F_0) \cdot T \quad (14)$$

Applying this algorithm, constant values for the input function and the filter function within the respective time intervals were considered. Thus, the values change at the transition to the next time interval (staircase algorithm). When $I(t)$ should be calculated from the integral, a numerical solution is yielded from the inversion of the convolution, the so-called deconvolution. An algorithm can be formulated from equations (11-14). Thereby first I_0 was calculated from equation (11), then the value was inserted into equation (12) and I_1 was calculated. Knowing I_1, I_2 was obtained from equation (13) etc, leading to equations (15-18).

$$I_0 = \frac{R_0}{T \cdot F_0} \quad (15)$$

$$I_1 = \frac{R_1}{T \cdot F_0} - \frac{I_0 \cdot F_1}{F_0} \quad (16)$$

$$I_2 = \frac{R_2}{T \cdot F_0} - \frac{1}{F_0} \cdot (I_0 \cdot F_2 + I_1 \cdot F_1) \quad (17)$$

$$I_n = \frac{R_0}{T \cdot F_0} - \frac{1}{F_0} \sum_{i=0}^{n-1} I_i F_{n-i} \quad (18)$$

Values for the filter function were then calculated as follows:

$$F_0 = \frac{R_0}{T \cdot I_0} \quad (19)$$

$$F_1 = \frac{R_1}{T \cdot I_0} - \frac{I_1 \cdot F_0}{I_0} \quad (20)$$

$$F_2 = \frac{R_2}{T \cdot I_0} - \frac{I_1 \cdot F_1}{I_0} - \frac{I_2 \cdot F_0}{I_0} \quad (21)$$

$$F_n = \frac{R_n}{T \cdot I_0} - \frac{1}{I_0} \cdot \sum_{i=1}^{n} I_i \cdot F_{n-i} \quad (22).$$

Transferred to the programmable implants, convolution means the mathematical modeling of expected theoretical release profiles (=response function), when a core with known release properties (=input function) is embedded into a polymeric mantle (=filter function). Hence the effect of the respective polymeric mantle material was calculated by the use of data gained from core matrices made of cholesterol and embedded cholesterol cores, which showed pulsatile release. For PLA_{30}, the calculation of the filter function was carried out using release data elaborated with a fast releasing polyanhydride by Vogelhuber in [39]. Time intervals of T = 1 day were chosen for the calculations.

Since this mathematical method can only be applied for linear systems, the beginning of the mathematical modeling was fitted to the onset day of release. During the delay time, erosion of the polymeric mantle occurred and thus the filter would not have been linear. Changes within the mantle, taking place after the onset of release, were considered to be negligible in comparison to that occurring during the delay period. Due to this fact, the first value for the input function (I_0 in equations 11-14) had to be the summarized release of the model drug until the day of the onset of release. Time-invariance, which is a second prerequisite, was taken for granted.

Chapter 3

Triglyceride Materials as Carrier for Proteins and Peptides

–

Extraction Methods for the Recovery and Determination of Residue Content

Introduction

Lipid materials are widely investigated for their potential as an alternative to polymeric carrier materials for proteins and peptides. Their properties for controlled release are investigated by several groups [37,150] which obtained their data by simply measuring the concentration of the released model drug directly from the release medium, which was possible since non proteinic model drugs were used. But since there are several degradation pathways, that can affect proteins and peptides in solution during release, their stability in release buffer is of great importance to decide whether a long term release could be investigated directly from the release medium or if the incorporated drugs have to be extracted from the matrices, to determine the residue content for a subsequent calculation of the release data. Thus in these investigations firstly a stability study for insulin and somatostatin, which served as model drugs, was carried out.

But in addition to occurring degradation processes in the release medium, the stability of proteins and peptides inside triglyceride matrices is of great interest. Since instability of this group of drugs was shown when incorporated into polymers [141], the triglycerides might be a promising alternative material. Insulin and somatostatin were incorporated as model drugs into lipid microparticles and release was investigated [118,153]. Thus an extraction of these two model drugs from the triglyceride matrix without the occurrence of degrading processes should become possible to enable the investigation of their stability within the triglyceride. Therefore, the extraction method developed by Lucke et al. [141] was tested and optimized using somatostatin and insulin as model drugs. Additionally a new procedure, to extract insulin and somatostatin from the glyceroltripalmitate matrices was developed. This new extraction method should protect the proteins and peptides from degradation, which can be caused by liquid phase separation during the procedure described in [141].

Results and discussion

Stability test and LC/MS-Analysis

To investigate the stability of Insulin and somatostatin, the model drugs were incubated in phosphate buffer solution of pH 7.4 at 37°C, as described in section 2.2 Insulin showed good stability over two weeks, but after 5 weeks the fraction of unaffected protein decreased to approx. 66% (Figure 9). As Figure 10 shows, somatostatin was degraded continuously and even faster. Thus, at the final time point of the experiment less than 45% of the peptide had maintained its structure.

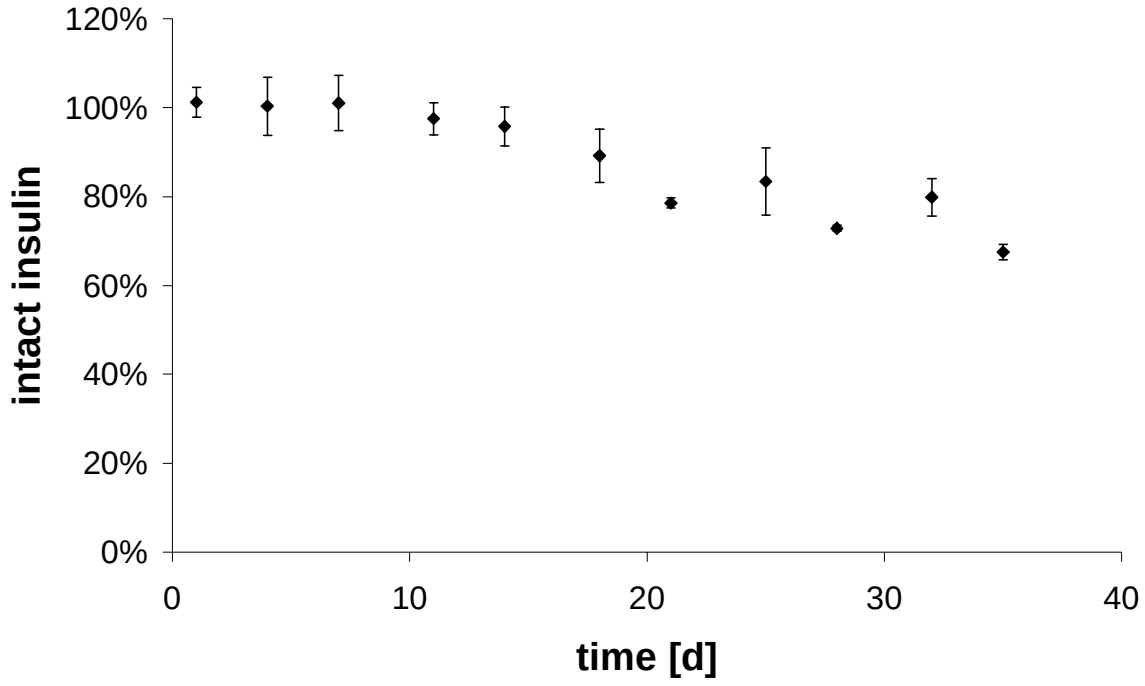

Figure 9: Degradation kinetics of insulin in phosphate buffer solution at 37°C over 35 days, data is shown as mean ± standard deviation, n=3.

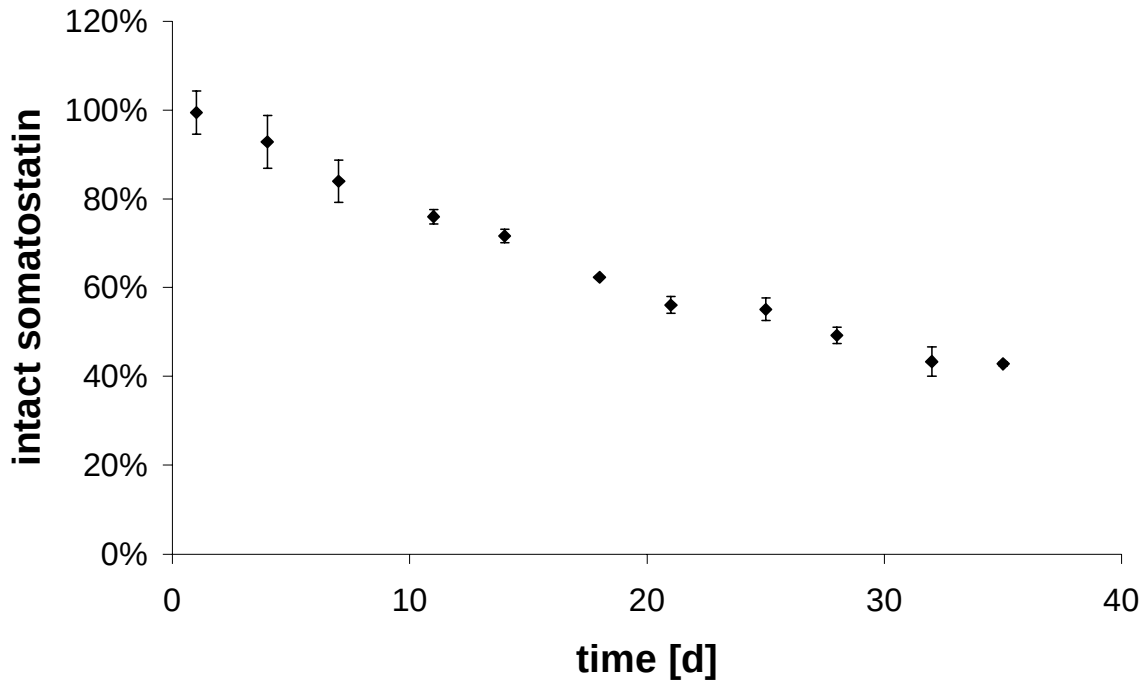

Figure 10: Degradation kinetics of somatostatin in phosphate buffer solution at 37°C over 35 days, data is shown as mean ± standard deviation, n=3.

In the case of somatostatin, the degradation product was identified via LC/MS-analysis as a deamidation product (Figure 11). The exchange of an amido-group (NH_2) into a hydroxyl-group (OH) led to an increase in the molecular mass of the somatostatin of 1Da, which was detected via the LC/MS-analysis.

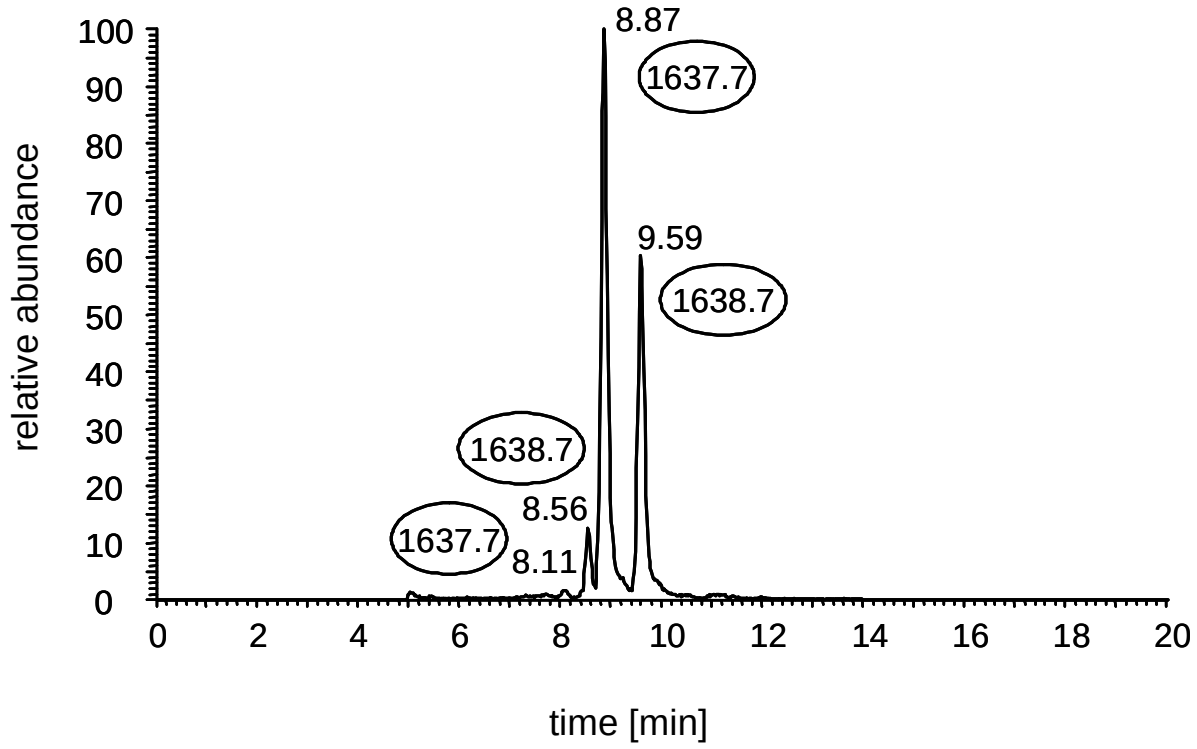

Figure 11: HPLC-chromatogram of somatostatin with retention times and detected mass data from LC/MS (mass of somatostatin: 1637.7, mass of the deamidation product: 1638.7), small peaks at earlier retention times due to somatostatin and its deamitation product containing iso-aspartate.

LC/MS-analysis of insulin showed no differences in the mass of insulin and the degradation product (data not shown). By carrying out GFC-analysis a second peak with earlier retention time, and thus a higher molecular mass was observed (see Figure 12). ESI-MS, which was used for this analysis has a cut-off of 2000Da and detects masses above this cut-off as mass per charge (m/z). Thus, a molecule that is exactly twice as large as the insulin would be hidden in the same peak as insulin in ESI-MS. This lead to the conclusion that the observed degradation product was the non-covalent dimer of insulin.

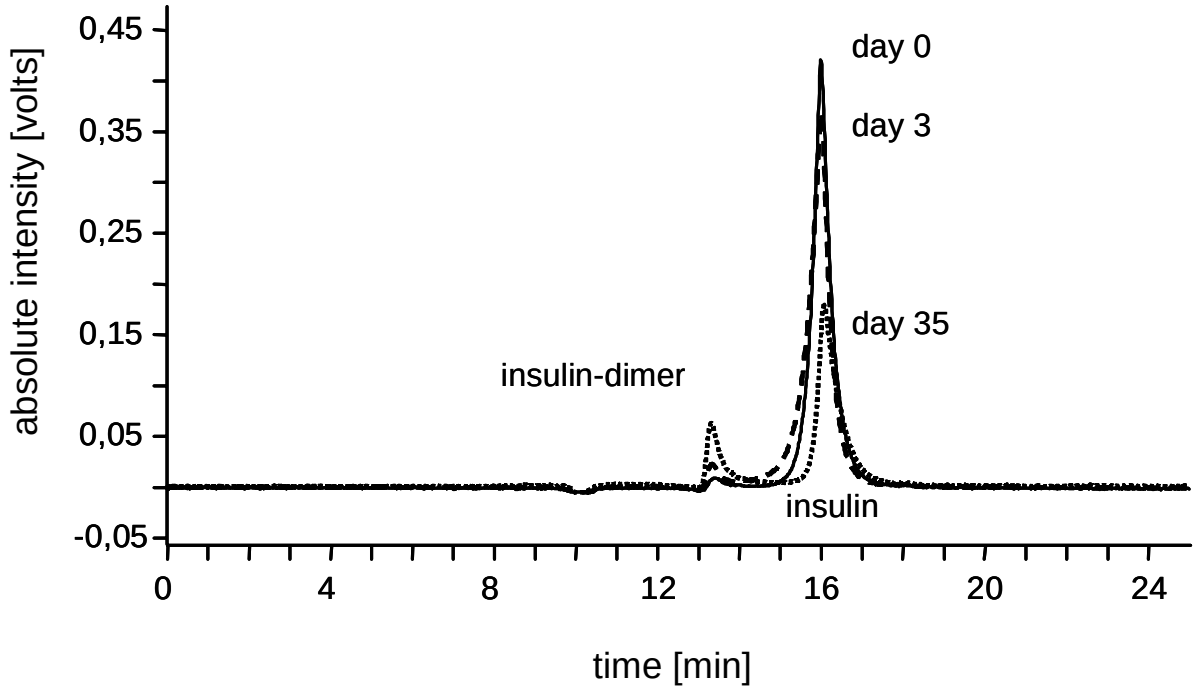

Figure 12: GFC-chromatogram of insulin samples drawn at days 0 (—), 3 (- -), and 35 (▪▪), respectively.

These results made visible, that the determination of protein and peptide release from triglyceride matrices cannot be performed directly from the release medium, due to stability problems. Thus, an extraction method for the two model drugs from the triglyceride, in which they should be incorporated, was necessary for the investigation of a long-term release. Otherwise the number of errors would increase and thus detection of sensible values for the in vitro release would be impossible.

Development of the new extraction method

For the evaluation of the extraction method, insulin and somatostatin were first incorporated into glyceroltripalmitate matrices and afterwards extracted as described in section 2.5. First results using the extraction method described by Lucke et al. [141] revealed impossibly high extraction yields of above 100%, due to the higher amount of acetonitrile in the mixture and a subsequent dissolution of the solvent in the chloroform-phase. This led to a smaller volume of the water-phase and thus higher concentrations of the model drugs were detected. Therefore, in the case of insulin 0.01N HCl, which is a known good solvent for this protein was tested instead of the original solvent mixture. Additionally, a method without liquid phase separation was developed for both model drugs, since it has been stated in the

literature [140] that proteins and peptides may be degraded or denatured at liquid/liquid (l/l) interfaces.

For insulin both methods produced good extraction yields with acceptable reproducibility. Somatostatin was also extracted to a good extent with very small deviations. For both the protein and the peptide the optimized solid/liquid extraction method using THF as solvent showed best results, compared to the other investigated solvents. Extraction yields of 94.5% for somatostatin with a standard deviation of 0.80% could be achieved. For insulin, extraction yields of 91.31% +/-5.11% and 96.33% +/-3.03% were achieved with the solid/liquid and the liquid/liquid extraction methods, respectively.

Not only were good extraction yields observed, but also the stability of the model drugs during the extraction process was investigated within these experiments. Figures 13 and 14 show HPLC-results for insulin (Figure 13) and somatostatin (Figure 14) standards in comparison with the two model drugs after the extraction from a triglyceride matrix. In both cases, no additional peaks were observed and no degradation products could be detected. This shows the suitability of the newly developed method for the investigation of the stability of these model drugs within a triglyceride matrix, such as lipid microparticles.

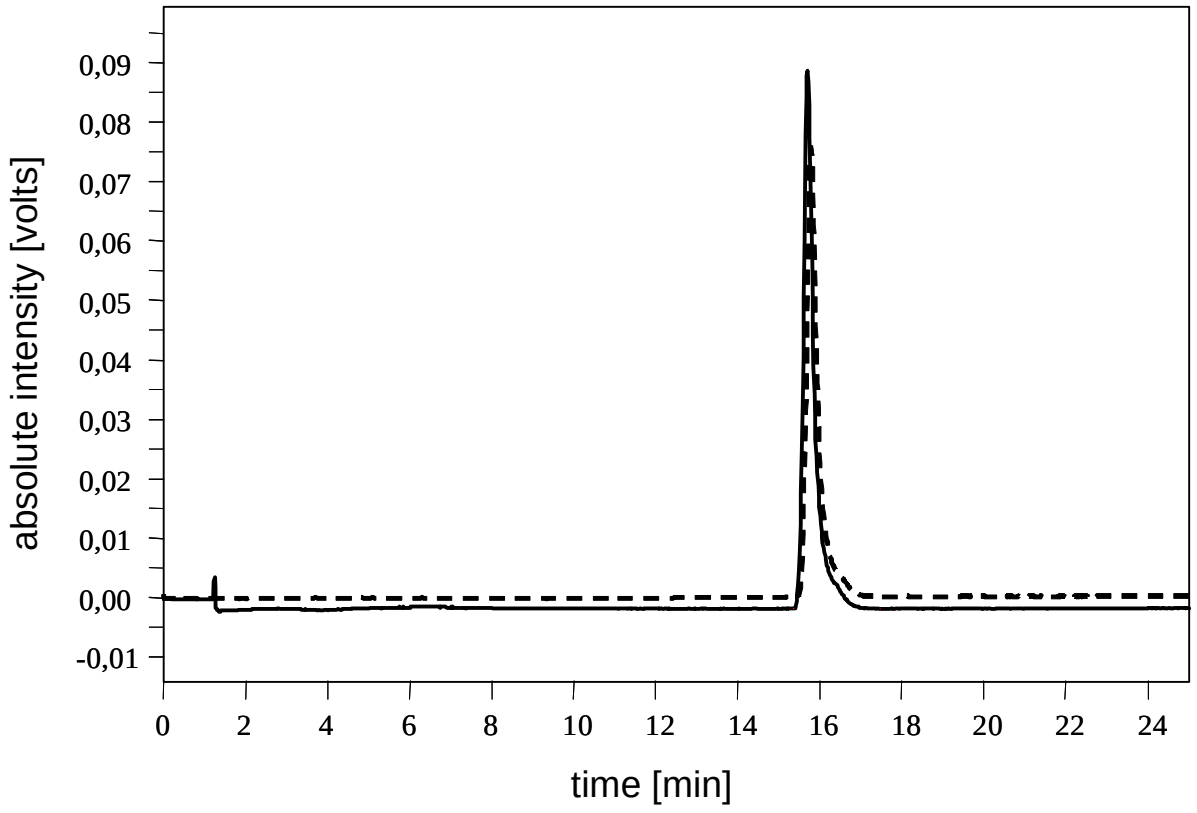

Figure 13: HPLC-chromatograms of an insulin standard solution (—, 50µm/ml) and insulin after the extraction from a glyceroltripalmitate matrix (- -).

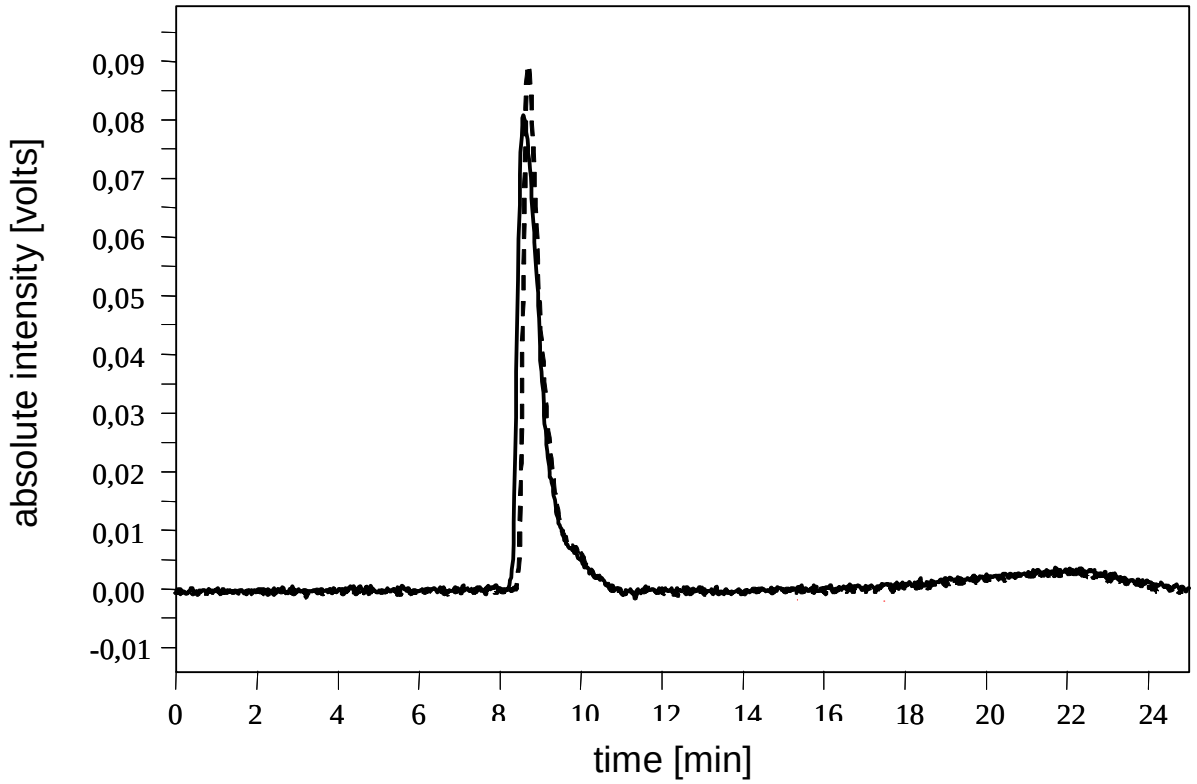

Figure 14: HPLC-chromatograms of a somatostatin standard solution (—, 50µm/ml) and somatostatin after the extraction from a glyceroltripalmitate matrix (- -).

Summary

This study served to investigate how release profiles of the two model drugs insulin and somatostatin from triglyceride matrices can be determined. Due to the instability of insulin and somatostatin over 35 days within the release medium, no direct measurement of the released amount of the model drugs is possible. Thus, the necessity of their extraction from triglyceride matrices for the performance of controlled release studies was proven. A new method for the extraction of proteins and peptides from triglyceride matrices with good extraction yields was developed. This extraction method can be used for the determination the residue content with subsequent calculation of release profiles. Additionally the investigation of protein and peptide stability within the triglyceride matrices was facilitated, due to the avoidance of liquid phase separations during the extraction. This new extraction method could be of great use for the investigation of degradation processes of the drugs within the matrix, since the used peptide and protein were shown to be not affected during the extraction procedure.

Since the investigations carried out with proteins revealed stability problems and the need of drug extraction when release experiments are performed, fluorescent dyes, which were used successfully by Vogelhuber et al. [37], were chosen for future experiments. They can easily be incorporated into the triglyceride matrices. Concomitantly their quantification by fluorescence spectroscopy is very simple and sensitive and can additionally be performed directly from the release medium. Since the further release investigations served to investigate release mechanisms and influence factors, no proteins or peptides were needed as model drugs and thus we were able to facilitate investigations by the choice of the fluorescent dyes as new model drugs.

Chapter 4

Factors Influencing Drug Release From Triglyceride Matrices

Introduction

Information about expected release profiles will aid in the design of an implant for controlled release parenteral drug delivery. Thus, the manufacturing procedure, characteristics of the incorporated drug, and the release mechanisms from the matrix material were identified as central influencing factors in the liberation of drugs from triglyceride matrices. Therefore, investigations were carried out to identify crucial parameters during the manufacturing procedure, such as the compression force, the drug loading, and the drug distribution within the matrix or the implant surface. In the next step, their effects on the resulting release profiles were quantified. Concomitantly, the first results on the release mechanisms from glyceroltripalmitate were elaborated, whereby a special focus was placed on diffusion and osmosis. Additionally, the influence of the hydrophobicity of the model drug on its release from triglyceride cylinders was investigated by the use of fluorescein, which shows a pH-dependent hydrophilicity and the lipophilic fluorescent dye nile red. Thereby it was investigated, whether release occurs slower with increasing lipophilic characteristics of the model drugs. Finally the uptake of water into the matrices was investigated qualitatively and quantitatively over a period of 14 days.

Results and discussion

Crucial factors for the design of triglyceride matrices for controlled release

1. Compression force

For the investigation of the preparation procedure with respect to the influence of several parameters on the resulting release profiles, matrices containing pyranine, a highly water soluble fluorescent dye as model drug, were manufactured under various conditions. The investigated parameters were drug loading, compression force, surface area and drug distribution within the matrices. Lipid cylinders, which contained 10% pyranine and which were compressed with 250N, released the dye within 17 weeks (Figure 15). While an increased compression force of 500N led to similar results, the lower force of 50N accelerated the release significantly. In that case, the complete liberation of the dye after one week (Figure 15) was observed. This indicated the existence of a threshold for the applied force in the compression step during the manufacturing procedure. Below this threshold, a change of

the compression force leads to significant changes in the release properties of the manufactured matrix, but above 250N the compression force seemed to effect the resulting release profile from the glyceroltripalmitate cylinder only negligibly.

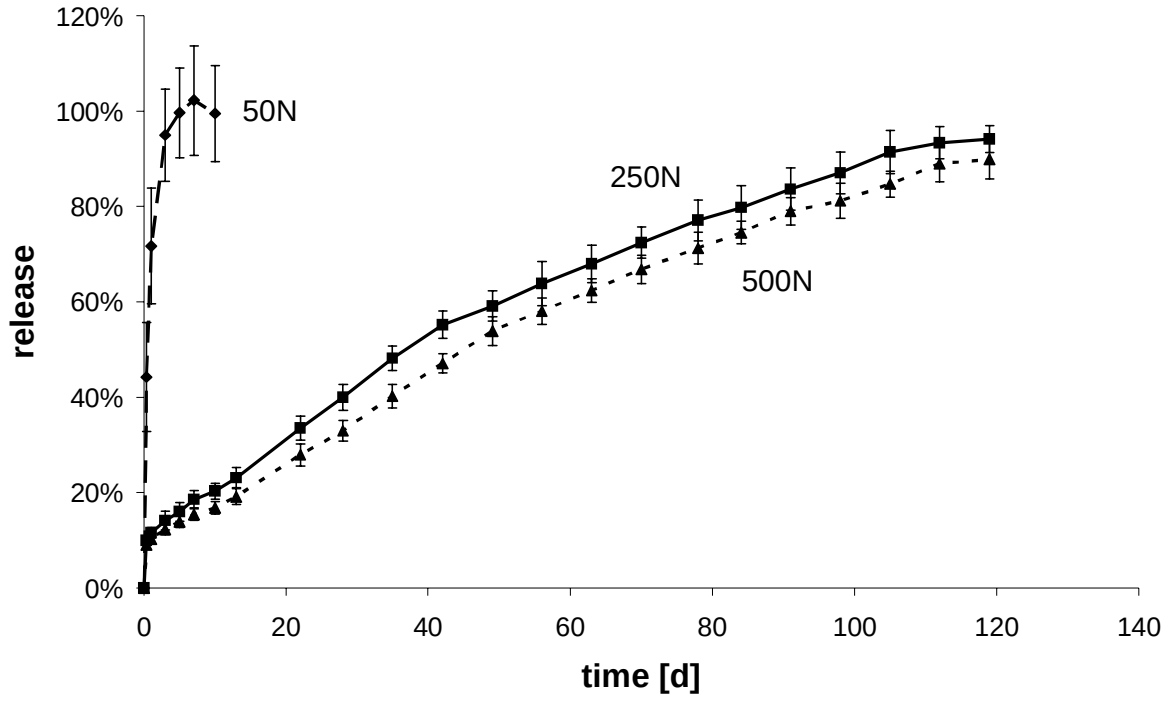

Figure 15: Release profiles from 10% pyranine containing glyceroltripalmitate matrices prepared with compression forces of 50N (- -), 250N (—) and 500N (▪▪), respectively. The diameter and height of the matrices were 2mm and 4mm, respectively; dye incorporation occurred via co-lyophilization method, values represent mean ± standard deviation (n=5).

2. Drug-loading

Different dye loadings were shown to have a tremendous effect on the release properties of the triglyceride matrices (Figure 16). For this comparison, all of the cylinders were compressed with a force of 250N. As mentioned above, the matrices containing 10% pyranine released the dye over 17 weeks; however, an increase of drug loading up to 33% led to a complete release within the first day. When the dye content within the matrices was decreased to 1%, release was not completed and less than 13% of the incorporated pyranine was liberated over the investigated period of 19 weeks. Release of the 1% loaded cylinders was not finished after this time period, but continued slowly. These results confirmed the fact that drug loading is an important factor for lipid matrix manufacture, too.

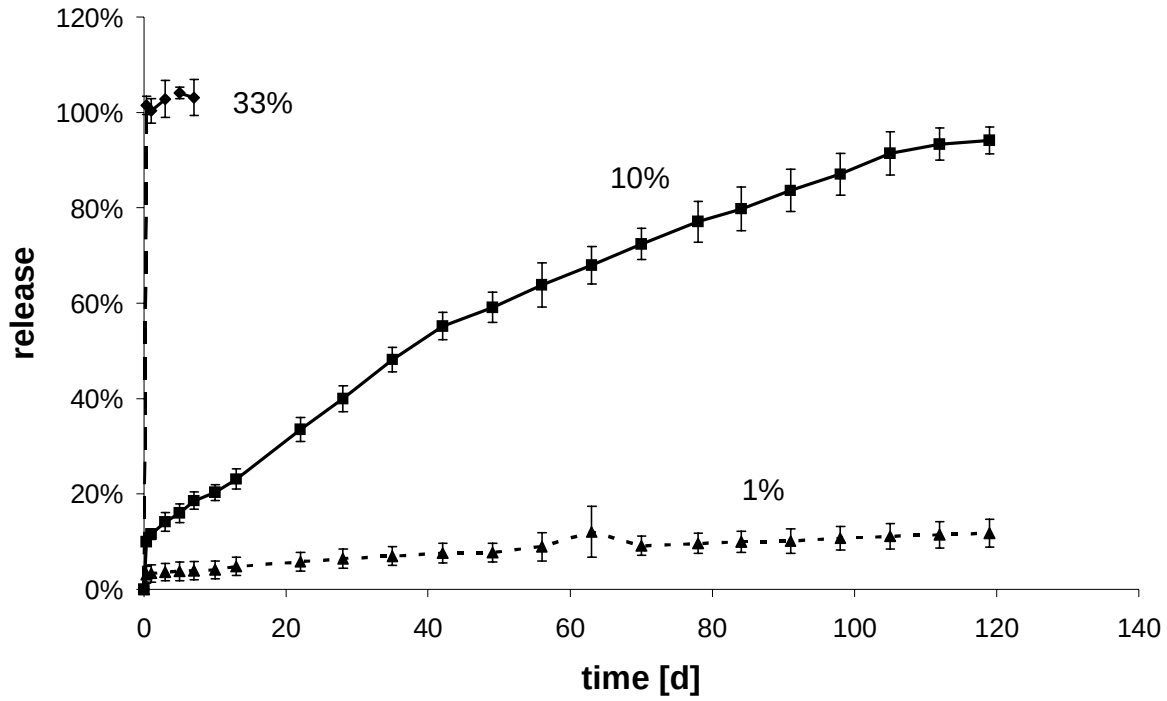

Figure 16: Release profiles from glyceroltripalmitate matrices with a diameter of 2mm and 4mm in height containing 1% (▪▪), 10% (—) and 33% (- -) pyranine, prepared by co-lyophilization. A compression force of 250N was applied; data is expressed as mean ± SD (n=5).

It was observed that long-term release can be achieved with drug loadings of up to 10%. Referring to percolation theory [163,164], it is likely that there is a threshold for the drug loading as well, above which very fast and pulsatile release from the triglyceride matrices occurs. The theory generally deals with clusters of randomly occupied sites in a lattice [165]. It describes crystal structures as well as, for example, the formation of a network when a substance is incorporated into a matrix. Transferred to controlled release devices, the percolation theory can be used to describe the influence of drug-loading on its release from a matrix system. Requirements for, and characteristics of the formation of a network within such matrices [166,167] are discussed as well.

3. Drug distribution within the matrices

Another important parameter for the release of a drug from the glyceroltripalmitate matrices could be the distribution of the drug within the cylinder. When mixing a powder with a small amount of another powder, the homogeneity of the mixture decreases with the increasing particle size of one of the compounds [164]. Thus, this parameter was varied via the particle size of the triglyceride. A decrease in the lipid particle size was considered to lead to a better distribution of the drug within the matrix and vice versa. In these experiments the effect of the dye distribution within the matrices on the release properties was investigated. Again a dye load of 10% was used and 250N were applied for the compression step during the preparation procedure. Dispersity of the model drug increases with decreasing size of the triglyceride. Thus, the distribution of the pyranine was considered to be best for the matrices prepared using the co-lyophilization method (see section 2.6), which was usually performed for the incorporation of the model drug, compared to that within matrices prepared by mixing lipid and dye powders and compressing the mixtures to cylinders. This was confirmed by the in vitro release results. Consequently, release accelerated significantly when lipid particle sizes increased (Figure 17). Using triglyceride particle sizes from 106µm to 250µm, the whole dye content was released after just one week (Figure 17). Reduction in the size of glyceroltripalmitate particles for the preparation of the matrices below 106µm led to a much slower release. Drug liberation was finished after 4 weeks of incubation (Figure 17). Decreasing the particle sizes, which resulted in molecular dispersity of the dye within the matrices, the mentioned controlled release over 17 weeks was achieved. This again confirmed the tremendous influence of the drug distribution on the release properties of the glyceroltripalmitate matrices. These investigations revealed the incorporation by freeze-drying both the lipid and the model drug in one solution as most successful for prolonged, controlled release.

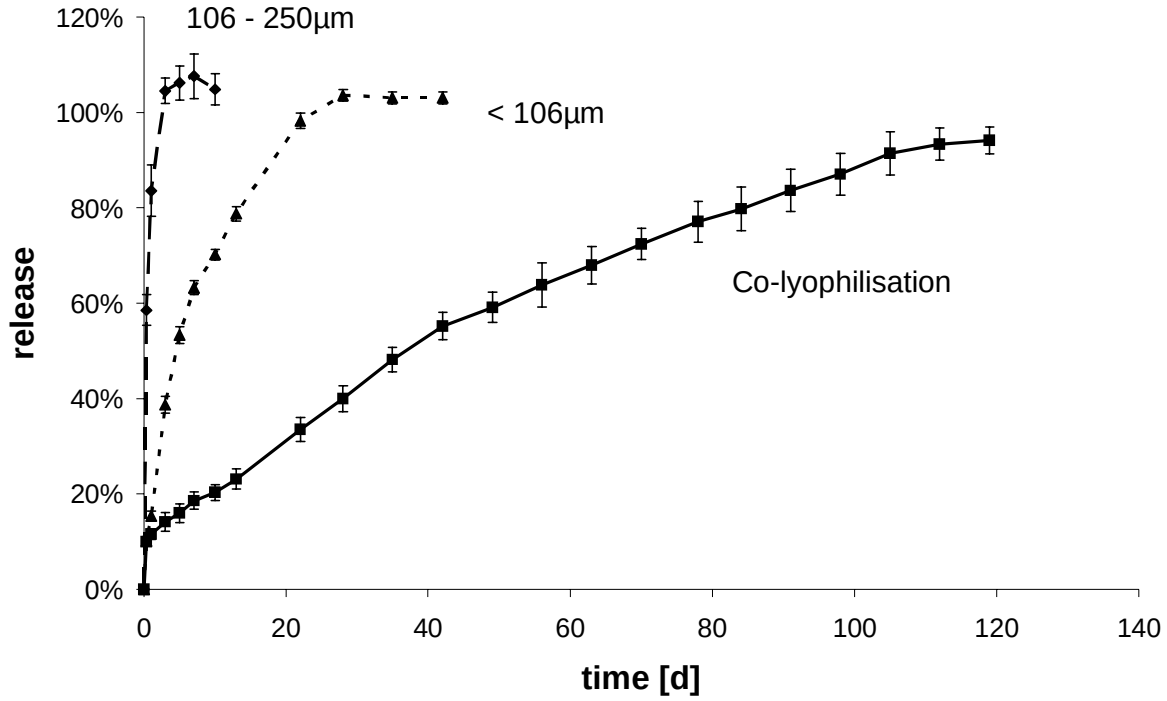

Figure 17: Release profiles from 10% pyranine containing glyceroltripalmitate matrices prepared from triglyceride of differing particle sizes. A compression force of 250N was applied, the diameter and height of the matrices were 2mm and 4mm, respectively; values represent mean ± SD (n=5).

4. Surface/volume ration of the matrices

To investigate the influence of the surface/volume ratio of the matrix on the resulting release profiles, cylinders with varying diameter and height were produced. In the release profiles it was seen that the height of matrices had no significant effect on the release properties of the triglyceride cylinders (Figure 18). Release profiles showed similar shapes comparing cylinders with heights of 2mm, 4mm and 6mm and liberation of the dye from the matrices occurred over the same time period of approximately 17 weeks.

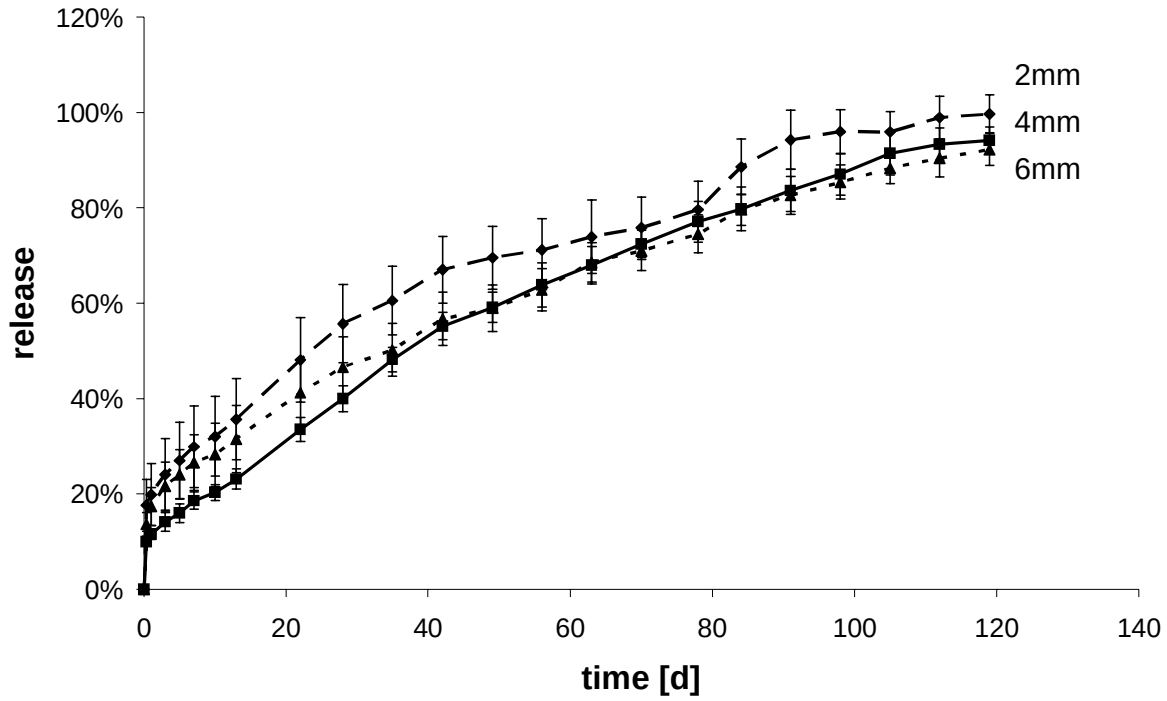

Figure 18: Release profiles from 10% pyranine containing glyceroltripalmitate matrices of 2mm diameter and varying cylinder height. Cylinders were prepared with co-lyophilization method, a compression force of 250N was applied; data is shown as mean ± standard deviation (n=5).

Since these results revealed no significant effect of little variations in the surface areas of the matrices on the release profiles from the glyceroltripalmitate cylinders of 2mm diameter, smaller matrices with a diameter of 1mm and a height of 2mm were produced to achieve larger variations in the surface/volume ratio and to compare the release profiles. Table 8 shows the variation of the cylinder surface in correlation with the diameter and the surface/volume ratio.

Table 8: Geometry data of matrices with varying height and diameter.

diameter	height	surface area	surface/volume ratio
2mm	2mm	18,85mm^2	3 [1/mm]
2mm	4mm	31,42mm^2	2,5 [1/mm]
2mm	6mm	43,98mm^2	2,33 [1/mm]
1mm	2mm	6,91mm^2	7,33 [1/mm]

Investigation of matrices with higher value for the surface/volume ratio demonstrated, in contrast to first release results, an acceleration of the release with increasing surface/volume ratio (Figure 19). Release profiles resulting from matrices with 1mm diameter and 2mm height showed that the reduction in the diameter led to complete release after 8 weeks, in comparison to 17 weeks of release from cylinders with a diameter of 2mm and a height of 4mm.

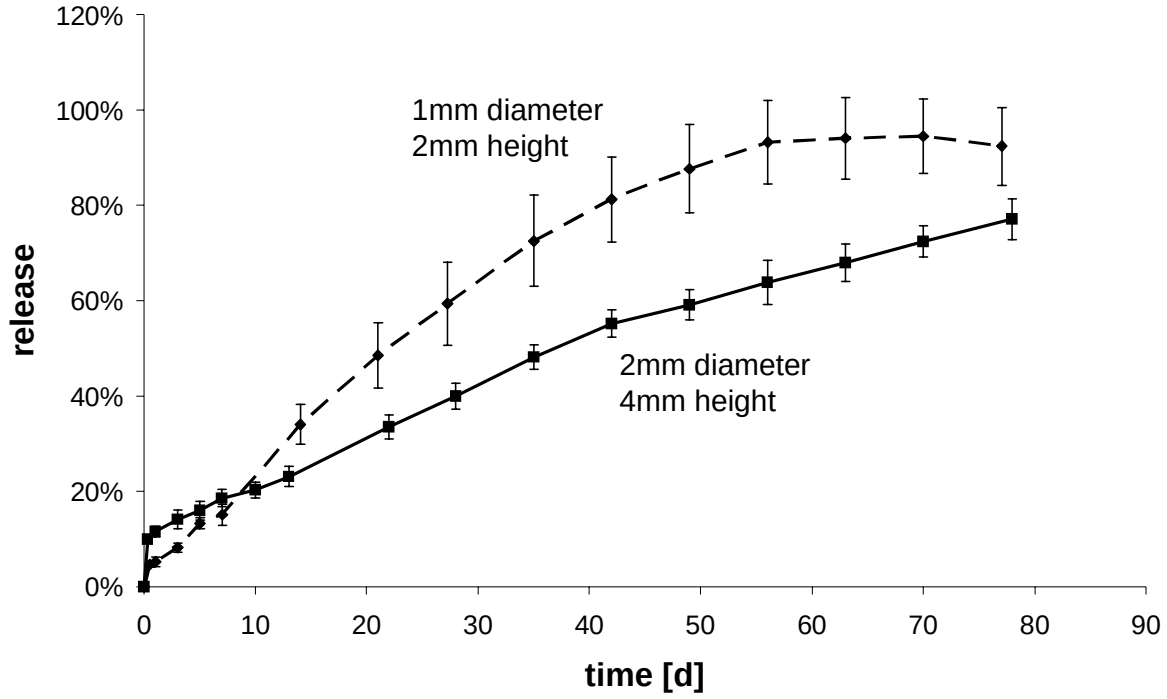

Figure 19: Release profiles from 10% pyranine containing glyceroltripalmitate matrices of 1mm diameter, 2mm height (- -) and 2mm diameter, 4mm height (—).
Matrices were prepared with co-lyophilization method, a compression force of 250N was applied; values are expressed as mean ± SD (n=5).

These results revealed the diameter of the cylinders, but not the height of matrices as an important factor for the design of controlled release devices made of glyceroltripalmitate. Thus height of the matrices can be a very useful tool for the adjustment of the drug dose, which is desired to be applied, because its variation would not lead to an alteration of the resulting release profile.

5. Drug characteristics

These results revealed that the diameter of the cylinders, but not the height of matrices, is an important factor for the design of controlled release devices made of glyceroltripalmitate. Thus height of the matrices can be a very useful tool for the adjustment of the drug dose to be applied, because its variation would not lead to an alteration of the resulting release profile.

In addition to the investigated parameters concerning the manufacturing procedure and the characteristics of the matrix itself, the incorporated drug also affects its release from lipid matrices. Thus in the following experiments the hydrophilicity of incorporated model drugs was investigated for its influence on the resulting release profiles.

Fluorescein-di-sodium salt, a highly water-soluble fluorescent dye, which has different hydrophilicity at different pH-values, was chosen as model drug. Due to its two acidic groups (Figure 20) with pk_a-values of 4.65 and 6.98, at pH 2.8 fluorescein is neutral, whereas at pH 5.5 one and at pH 9.0 both acidic groups are deprotonated and thus the mono- and di-anion forms occur, respectively. Concomitantly, the release of nile red, a highly lipophilic fluorescent dye, was investigated. A solubility of nile red in phosphate buffer (pH 7.4) of 0.7ng/ml was determined as described in section 2.7.

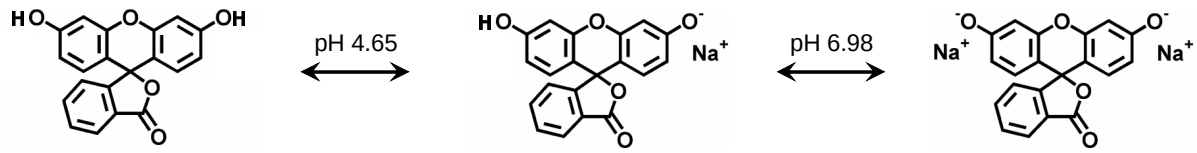

Figure 20: Structures and charges of fluorescein and its ionic forms at different pH-values.

Figure 21 shows distinct correlations between the degree of ionization of fluorescein and release profiles. The liberation of the di-anion occurred most quickly, followed by the release of the mono-anion, whereby the difference between release results for the two ionic forms of fluorescein was only slight. However, liberation of the protonated and thus neutral fluorescein molecule from glyceroltripalmitate matrices at a pH value of 2.8 occurred much slower. In Figure 21 it can also be seen that release of the two ionic forms of fluorescein is completed after 23 days, whereas cylinders incubated at pH 2.8 released only approximately 21% of the dye within 80 days. Liberation from these implants was still ongoing at a low level. Concerning the release of nile red, the lipophilic model dye, no release was observed during the investigated period of 4 weeks (Figure 21).

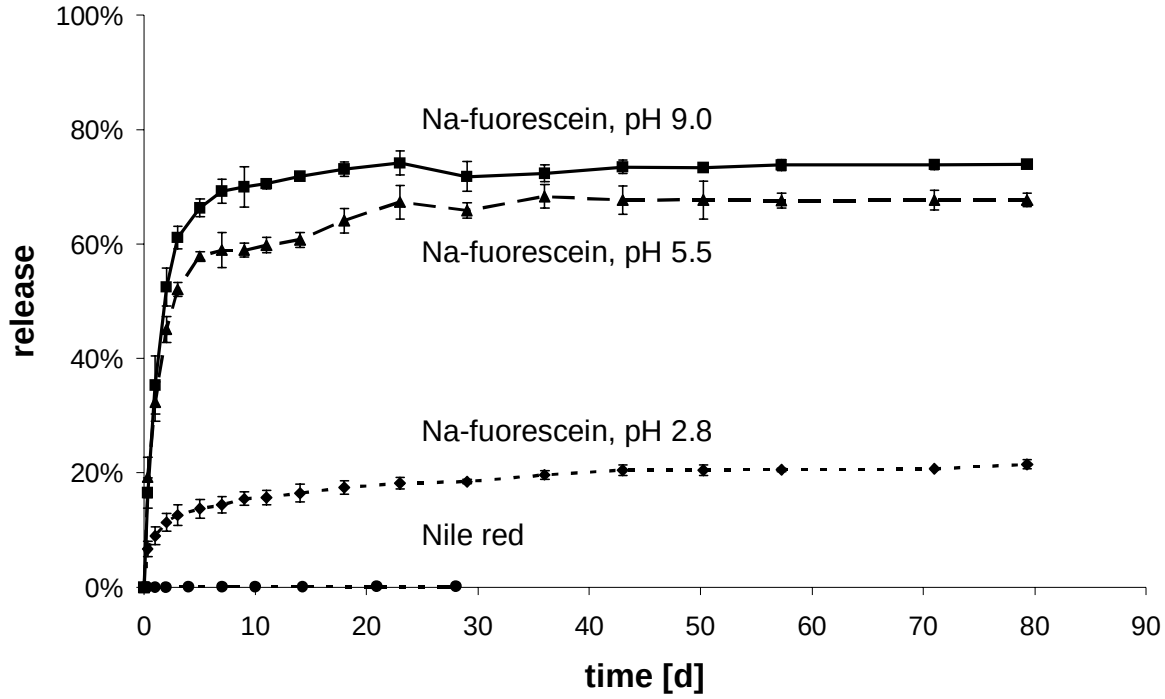

Figure 21: Release profiles from glyceroltripalmitate matrices with a diameter of 2mm containing 10% fluorescein-di-sodium salt and 10% nile red. Fluorescein matrices were incubated in phosphate buffers of different pH values; data represent mean ± SD (n=5).

Release Mechanisms

1. Osmotic effects

While several crucial parameters for the design of lipid implants as controlled release devices have been identified and characterized, the release mechanisms from triglyceride matrices are not yet clear. Thus further investigations were carried out to gather information on processes that occur during the release of drugs from triglyceride matrices [168]. Therefore, in one experiment, glyceroltripalmitate cylinders with a diameter of 2mm containing 10% fluorescein-di-sodium salt were prepared and incubated in phosphate buffers of varying osmotic pressures. Release data obtained from these investigations should elucidate whether osmosis is involved in release processes of the model drug from the matrices. Release results are shown in Figure 22. Distinct effects on release profiles were observed when the osmotic pressure of the release medium was increased from 290mosmol to either 7850mosmol or 9500mosmol.

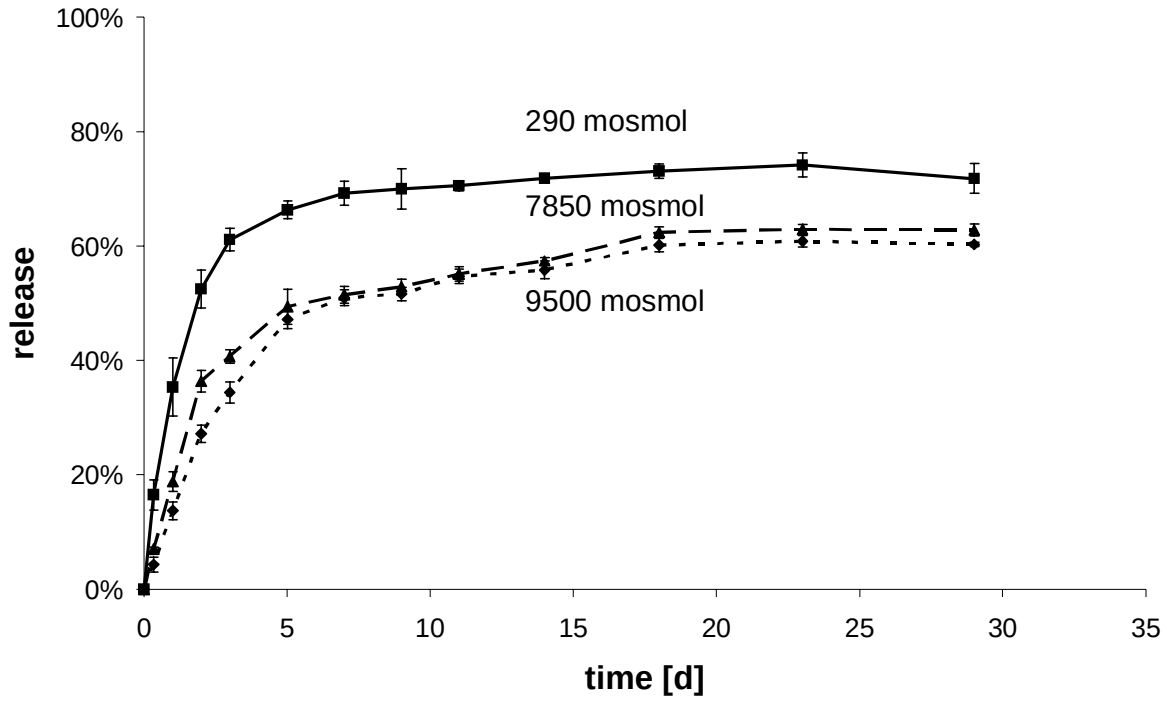

Figure 22: Release profiles from 2mm diameter glyceroltripalmitate matrices containing 10% fluorescein-di-sodium salt, incubated in phosphate buffers of different osmotic pressures (adjusted by NaCl-addition) at ph 9.0; data is shown as mean ± standard deviation (n=5).

Comparing osmolarities of 7850mosmol and 9500mosmol, release profiles differed only during the first period, whereas after 5 days no major differences were observed. An increase in osmotic pressure of the release buffer led to slower release during the first 2 days, resulting in release rates of 53%, 36% and 27% for media with osmolarities of 290mosmol, 7850mosmol and 9500mosmol, respectively. Additionally, the higher osmotic pressure resulted in a lower amount of totally released dye (Figure 22). This indicated the occurrence of “osmotic pumps” during release, which lost effectiveness with decreasing amounts of dye within the matrix.

Figure 23 shows a schematic of the function of “osmotic pumps”, which can be involved in release mechanisms from triglyceride matrices. Osmotic effects can occur when the solvent reaches the model drug within the matrix though pores or by diffusion through the matrix material and dissolves it. At the interface of the drug particles, their dissolution results in a saturated solution and thus in a very high osmotic pressure. Along this osmotic gradient, the model drug can be pumped out of the matrix and thus osmosis can be one important factor for the release of any drug from triglyceride matrices. Even though sink conditions were generated during the release study, a decreased solubility of the model drug within the release

pathways of the matrix at higher osmotic pressures may also play a role in the resulting release profile.

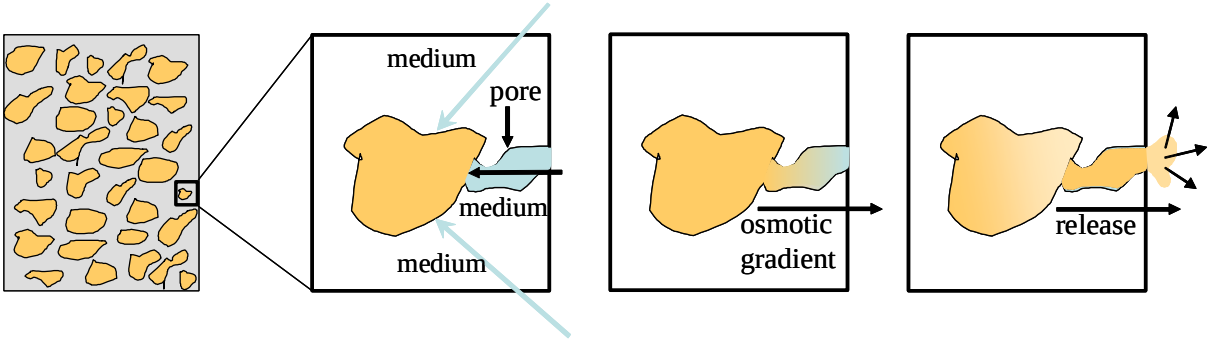

Figure 23: Schematic of an osmotic pump occurring during release from triglyceride matrices. Particles within the cylinder represent the model drug, which is dissolved and released along an osmotic gradient into the release medium. Uptake of the medium into the matrix was not classified, but may occur by diffusion through the matrix material or through pores.

2. Water uptake and pore formation

In the second experiment for the investigation of release mechanisms from lipid matrices, cylinders without any drug loading were manufactured from glyceroltripalmitate of different particle sizes, according to the experiments described above. Matrices prepared of lyophilized triglyceride, lipid powder with particles below 106µm and 106µm-250µm of size, were incubated for 14 days in fluorescein-di-sodium salt containing phosphate buffer. Fluorescence within the matrices was examined at specific time points to obtain information on the water uptake into the matrices and to investigate the occurrence and extent of pore formation processes. The aspect investigated in these experiments into the release mechanisms from triglyceride matrices, was the water uptake into cylinders prepared from glyceroltripalmitate, which gives information on the occurrence of pore formation processes. In the first step, water uptake was quantified, not to obtain exact results on the amount of water within the matrices, but to investigate whether differences in pore formation can be observed when using triglyceride powders of varying particle sizes.

In Figure 24 the relative amount of water taken up by the lipid cylinders, and thus the variance in the extension of pore network, is shown. Even though water uptake was low and thus standard deviations foiled significance, a tendency could be observed. These results elucidated a correlation between the porosity of the glyceroltripalmitate matrices and particle size of the triglyceride powder.

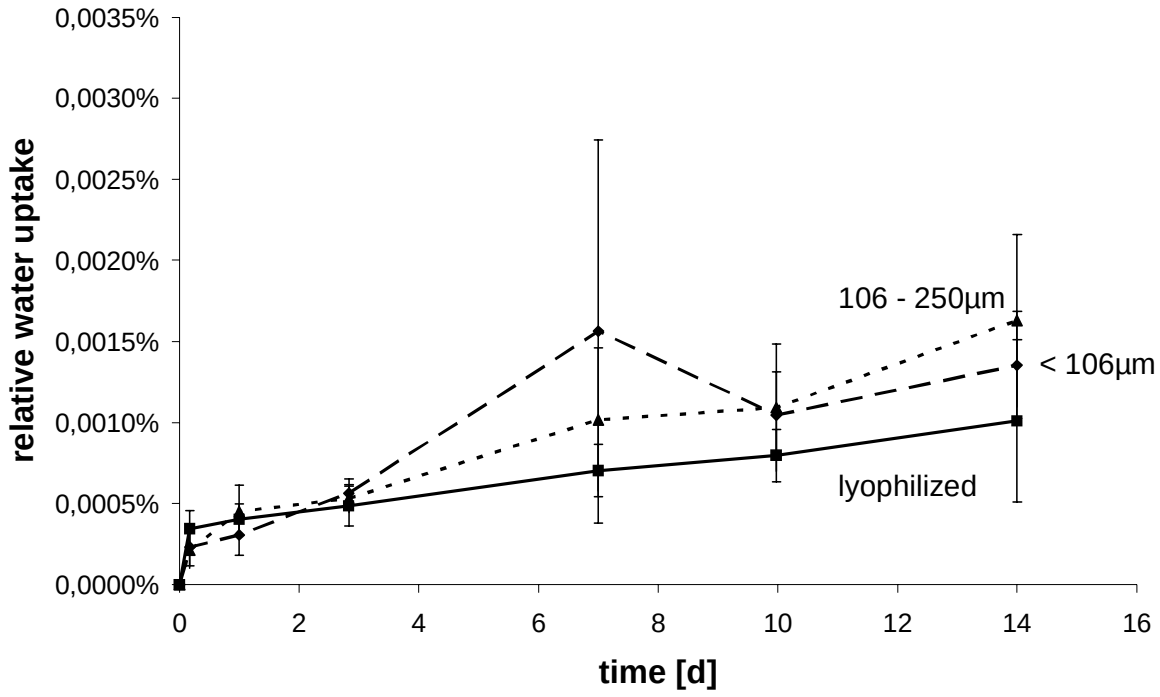

Figure 24: Comparison of water uptake into lipid matrices prepared of glyceroltripalmitate of varying particle size; values are expressed as mean ± SD (n=5).

In the second step, blank triglyceride matrices were incubated in phosphate buffer containing fluorescein-di-sodium salt at pH 9.0 for 14 days. Afterwards the cylinders were freeze dried, cross-sectioned (see section 2.10) and investigated by confocal laser scanning microscopy. In this way, the existence of pores was visualized through the imbibed fluorescence of the dye. In Figure 25 confocal laser scanning microscopy pictures of matrices compressed from lyophilized glyceroltripalmitate and triglyceride powder with particle sizes below 106µm, respectively, are shown. Matrices prepared from the ground and sieved powder displayed fluorescence in outer regions after 4 hours, which spread regularly over the whole matrix during the first day (Figure 25a,b). Cylinders compressed from larger triglyceride powder particles showed similar results, whereas in case of matrices compressed from the lyophilized triglyceride, fluorescence was only detected at the edges of the cylinders and no diffusion into central regions was observed during the investigated period of 14 days (Figure 25c).

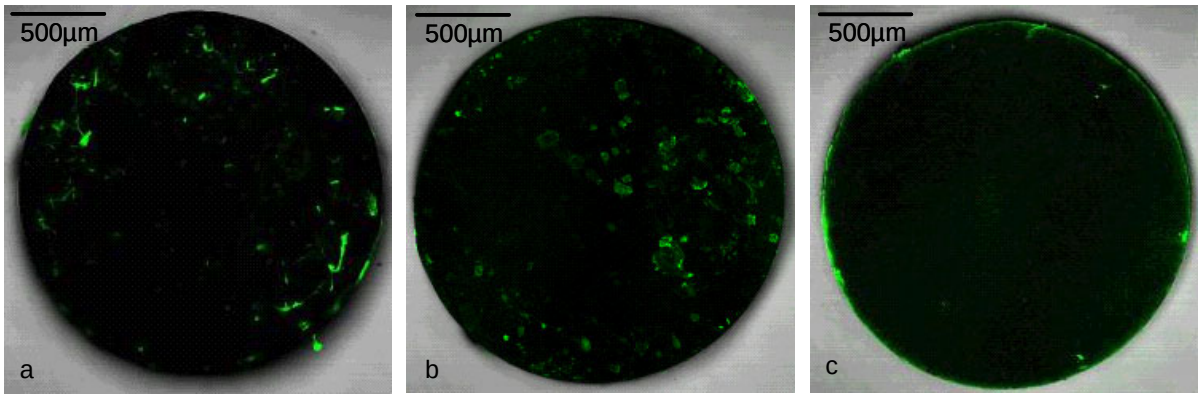

Figure 25: Confocal laser scanning microscopy image of cross sections of glyceroltripalmitate matrices after incubation in buffer containing fluorescein-di-sodium salt, a) lipid powder <160µm, after 4 hours; b) lipid powder <160µm, after 1day; c) lyophilized glyceroltripalmitate, after 14 days.

These results indicated that a more distinct pore network formed when triglyceride matrices are compressed from powders with bigger particle sizes, which agrees with the above-described results of the water uptake and with release data obtained from pyranine loaded lipid matrices.

Summary

In these investigations, the crucial parameters for the lipid matrix manufacture were identified and their influence on the resulting release profiles was quantified with the intent to evaluate the preparation procedure for cylindrical glyceroltripalmitate matrices for controlled release drug delivery. Drug loading, as well as compression force, drug distribution and the surface/volume ratio of the release system, were identified as crucial parameters for the design of triglyceride matrices as controlled release devices and for their preparation procedure. Concerning drug loading, the existence of a threshold higher than 10% was shown, below which controlled release over several months was achieved. For the compression force, a threshold was observed, too. Above 250N the influence of the compression force on the resulting release profile was negligible. Concomitantly, these investigations revealed that better drug distribution leads to longer release periods and thus should be maximized for prolonged release. The surface/volume ratio was revealed as an important and useful tool to vary the release profile of the developed matrix. It can easily be adjusted over the diameter of the cylindrical matrices and consequently the release period of an incorporated drug can be prolonged by increasing the matrix diameter. However the height of the cylinder was demonstrated to be a less important factor. This facilitates the variation of the applied dose,

which can thus be adjusted by changing the weight of the matrix, whereby the expected and desired release profile can be maintained.

The investigations also pointed out the severe influence of the characteristics of the incorporated drug on the release profile. An indirect dependence of the release period on the drug hydrophilicity was observed, leading to slower release of more lipophilic substances from a triglyceride matrix. In addition to the time within which controlled release occurred, the degree of totally released model dye was also shown to be directly dependent on the drug hydrophilicity. Thus the highly lipophilic model drug nile red was retained within the triglyceride cylinder.

Considering the release mechanisms from triglyceride matrices, the occurrence of osmotic processes during drug release and their involvement in the transport of the incorporated drug within the triglyceride cylinder was clearly elucidated. Release of the model drug from the matrices was slower at increased osmotic pressures of the release medium. Thus, when incorporating any drug into a triglyceride matrix, the osmotic pressure resulting from its saturated solution has to be taken into account, due to its influence on the resulting release profile.

Concomitantly, it was shown that pore formation within triglyceride matrices directly depended on the lipid particle size used for the preparation of the cylinders. Pore formation was more distinct in matrices compressed from ground and sieved lipid powder compared to matrices prepared from lyophilized glyceroltripalmitate. The extension of pore formation within the triglyceride matrices is of great importance for controlled release, because pores allow for faster diffusion within the matrix and thus accelerate drug release.

Chapter 5

Biocompatibility and Erosion Behavior of Triglycerides and Blends with Cholesterol and Phospholipids

Inroduction

In the treatment of many diseases, such as brain tumors, acromegaly, or diabetes mellitus, the controlled release of a medication over weeks or months is desirable to facilitate therapy and increase patient compliance [169,170]. Consequently, a plethora of controlled release forms have been investigated, such as nano- and microparticles and implants. Currently, commercially available implantable delivery systems are frequently made of biodegradable polymers. They possess many positive characteristics, such as good biocompatibility [136-138], a chemical structure that results in diverse release properties, biodegradability, and well-defined degradation pathways. However, some of these materials expose drugs to a changing microenvironment inside the eroding implants with acidic pH [139], increased osmotic pressure [139], or degradation products that can affect the stability of incorporated compounds, especially proteins and peptides [141]. Therefore, alternative materials, such as hydrogel materials, have been investigated [171,172] and recently much attention has been given to lipophilic substances such as cholesterol, phospholipids, mono-, di- and triglycerides or mixtures of these materials [173,174]. Cholesterol and triglycerides have been successfully used for controlled drug release over several weeks [8,36]. However, their biocompatibility has not yet been investigated. Therefore, we decided to examine the tissue reactions of mice to subcutaneously implanted lipid matrices. Although microparticles have a small size, round shape and smooth surface, and thus reduce mechanical irritation, we decided to use cylindrical macroscopic implants for in vivo experiments to facilitate recovery of the implant. We chose glyceroltripalmitate for our investigation into triglyceride biocompatibility and compared it to PLGA and gelatin, which are considered to be well tolerated. Furthermore, the in vivo erosion behavior of the triglyceride and the effects of incorporated erosion-modifying components were investigated. Due to their promising release characteristics [36,175], cholesterol and distearoyl-phosphatidyl-choline (DSPC), a phospholipid with two stearic acid side chains, were chosen to serve as erosion modifiers in this study.

In vivo biocompatibility study

We first investigated the in vivo behavior and tolerance of pure triglyceride implants. Time points for the explantation were days 2, 4 and 8 for the investigation of acute reactions and day 30 and 60 to detect chronic tissue reactions. Gelatin and PLGA were chosen as controls with known good biocompatibility. In a second test group, the triglyceride implants were supplemented with 1% gelatin, which can serve as a hydrogel-forming carrier for highly potent substances like growth factors [176]. The time schedule for this biocompatibility study is given in Table 4 (see section 2.14). Although implants made of pure gelatin were already eroded at day 2, the defined outlines of the implants were visible until day 4 and good biocompatibility was observed in all histological sections. One cell layer of connective tissue formed around the implant, but no increase in inflammatory cells was observed (data not shown). Recovery of the PLGA implants was possible up to day 30, whereas after 60 days the material was completely eroded and no implant residues could be found in the subcutaneous tissue. Histological investigations of the polymer implant also revealed good tolerance, evidenced by the minimal encapsulation by connective tissue (1 to 5 cell layers) and no adverse reaction, such as an increase in inflammatory cells (data not shown). Because the T_g of $PLGA_{17}$ (T_g = 46 °C) is near the body temperature of the mice (36,5-38°C, [177]), the implants underwent deformation and lost their cylindrical shape (Figure 26), which led to less mechanical irritation and thus to a reduction of foreign body reaction [178].

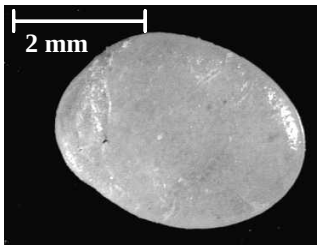

Figure 26: Light microscopy image of a PLGA implant excised at d2.

The implants of the two test groups remained stable over 60 days and maintained their cylindrical shape. Implants prepared with and without gelatin showed similar results concerning the tissue reactions; therefore, only histological pictures of pure glyceroltripalmitate implants are shown (Figure 27). Encapsulation in connective tissue by abundant fibroblasts was observed in both groups and became more apparent with time. A histological section of the typical tissue response to a glyceroltripalmitate implant 4 and 30 days after implantation is shown in Figure 27. At days 30 and 60 the thickness of the capsule amounted to 5 to 10 cell layers compared to 1 to 5 layers at the earlier time points. The

intensity of the encapsulation into connective tissue was comparable to that of the PLGA implants. In a few histological sections at early excision points of the two test groups, isolated foreign body giant cells or macrophages were seen, but for the most part no increase of inflammatory cells was observed. This rarely occurring mild foreign body reaction, which was restricted to the interface and regions very close to the implant surface, may not necessarily be related to the material, but rather be induced by mechanical irritation of the subcutaneous tissue due to the rough edges of the cylindrical implants [178]. Apart from collagenous encapsulation 30 and 60 days after implantation, no further reaction of the organism to the implants (e. g. increase in mononuclear cells) was observed in either the subcutaneous tissue adjacent to the implants or in other sites in the animals.

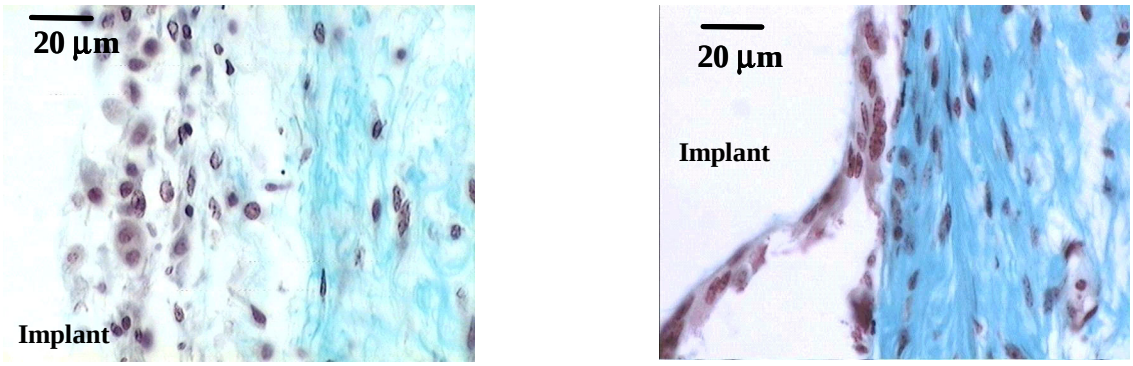

Figure 27: Light microscopy images of a typical tissue response to glyceroltripalmitate implant at day 4 (left) and at day 30 (right), Masson & Goldner stained, both 400x, region of the implant marked at the left side.

When the stability of the implants was examined, it was seen that the triglyceride matrices showed no significant swelling and only a slight increase in dry weight 2, 4, and 8 days after implantation (Figure 28). This may be due to the adhesion of connective tissue that could not be completely removed before drying and weighing of the implants. At days 30 and 60, when the implants were completely encapsulated by connective tissue, a more distinct rise in the dry weight of the matrices was observed (Figure 28), which demonstrates the stability of the implants over the entire time period and their suitability for a long-term release.

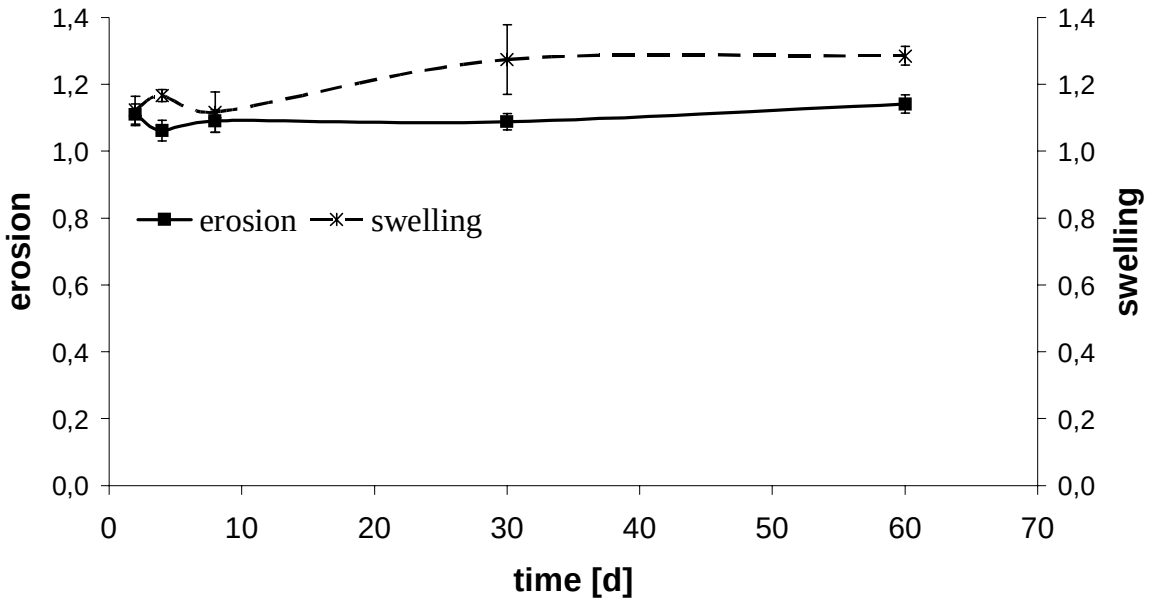

Figure 28: In vivo erosion and swelling of glyceroltripalmitate matrices, normalized to the pre-implantation weight, data is shown as mean ± standard deviation, n=4.

SEM pictures showed that the surface of the pure triglyceride matrices became absolutely smooth (Figures 29,30), adhered particles were no longer seen and grooves, caused by the steel compression tool, disappeared over the 30-day implantation period. Few remnants of connective tissue that could not be removed were seen, due to the encapsulation of the implants in the subcutaneous tissue in mice. Cross-sections of implants made of pure glyceroltripalmitate (Figures 29,30) showed no alteration in the microstructure. Neither signs of degradation, such as pore formation, nor changes in the crystal structure were observed. Implants containing 1% gelatin, however, showed slight signs of erosion, due to the degradation of the water-soluble compound (Figures 31,32). This was apparent in the formation of pores and cavities, which also led to disruptions in the lipid implants. This again demonstrated the stability of the implants, but also showed that the erosion of the triglyceride implants can be influenced by incorporation of a water-soluble compound into the matrix.

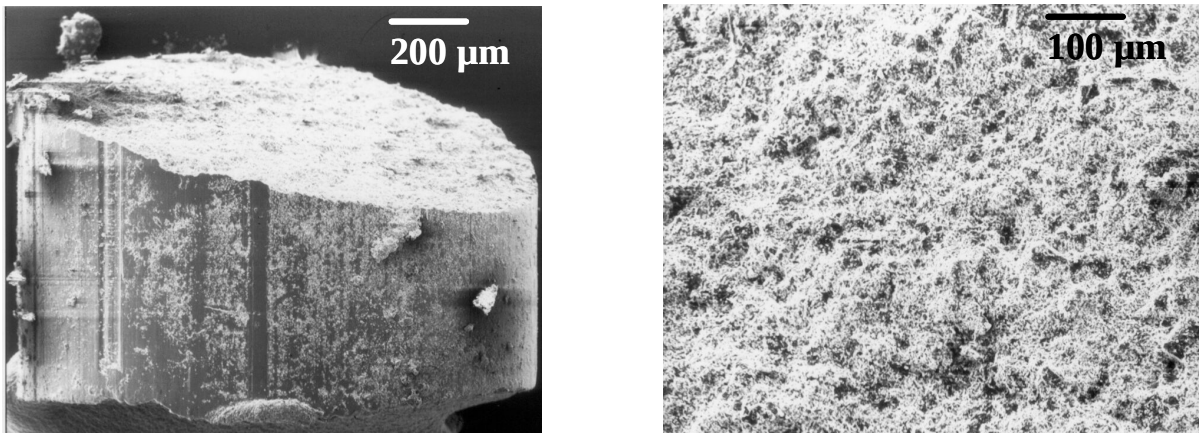

Figure 29: Top view (left, 45x) and cross-section (right, 100x) of glyceroltripalmitate matrix before implantation.

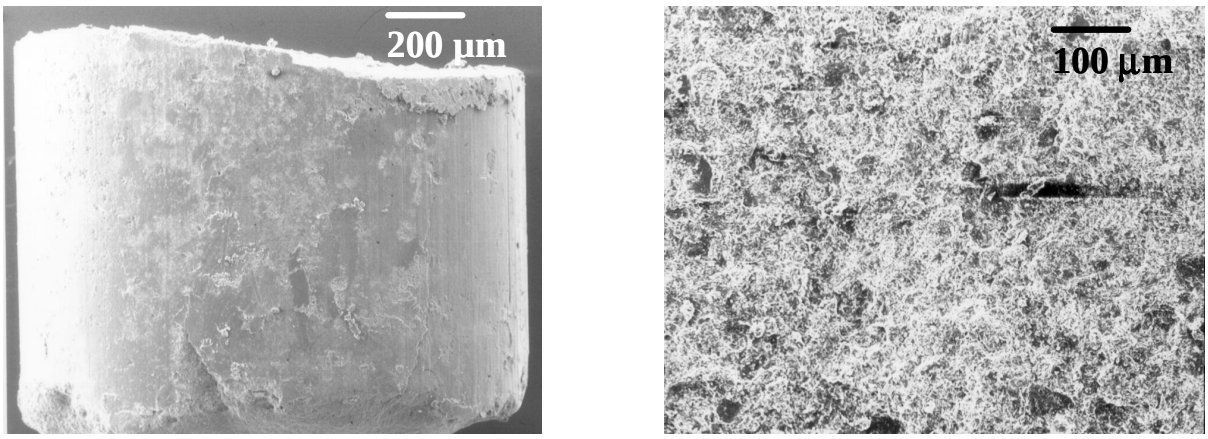

Figure 30: Top view (left, 45x) and cross-section (right, 100x) of glyceroltripalmitate matrix excised at day 30.

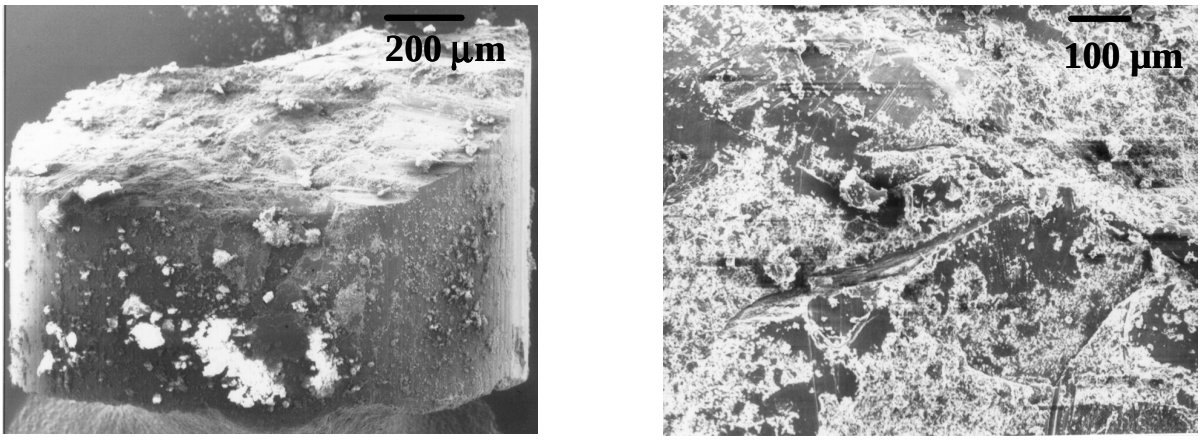

Figure 31: Top view (left, 45x) and cross-section (right, 100x) of glyceroltripalmitate implant containing 1% gelatin before implantation.

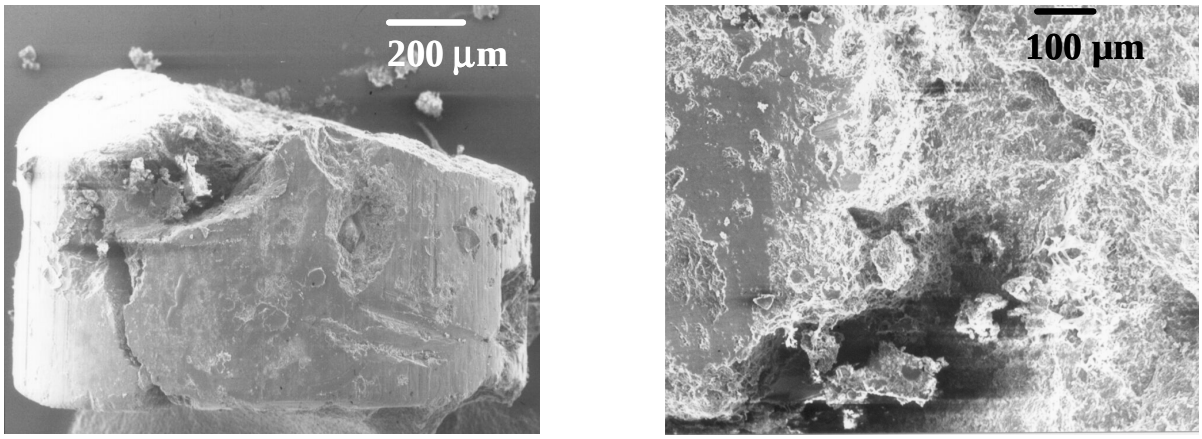

Figure 32: Top view (left, 45x) and cross-section (right, 100x) of glyceroltripalmitate implant containing 1% gelatin excised at d30.

In vivo erosion study

Even though the observed in vivo stability of glyceroltripalmitate is a positive result, because the material is suitable for long-term release applications, the erosion of the material would eventually have to be accelerated to generate an applicable biodegradable device and to obtain a greater variability. With regard to the in vitro release characteristics [36,175], cholesterol and DSPC were chosen to investigate their influence on the erosion behavior of glyceroltripalmitate. To examine the in vivo effects of the phospholipid, two different ratios of glyceroltripalmitate and DSPC were investigated. Implants were manufactured that contained 10% and 50% (w/w) of the phospholipid. As a second non-polymeric material with slightly amphiphilic characteristics and known good properties for controlled release [36], cholesterol was mixed with glyceroltripalmitate in ratios of 1:1 and 9:1 and the resulting mixtures were investigated for their in vivo erosion behavior. The duration of the study was up to 35 days and again time points in the early stage were chosen in addition to that at the end of the study to obtain data for acute tissue response. A detailed time schedule of the study is depicted in Table 5 (see section 2.14).

In this experiment, the addition of cholesterol did not lead to any change in the erosion of glyceroltripalmitate. All implants of the cholesterol groups remained stable, maintained their cylindrical shape, and displayed no evidence of significant erosion. SEM photographs showed similar behavior in these implants as was described above for the glyceroltripalmitate implants. There was no observable change in the microstructure or pore formation (Figure 33).

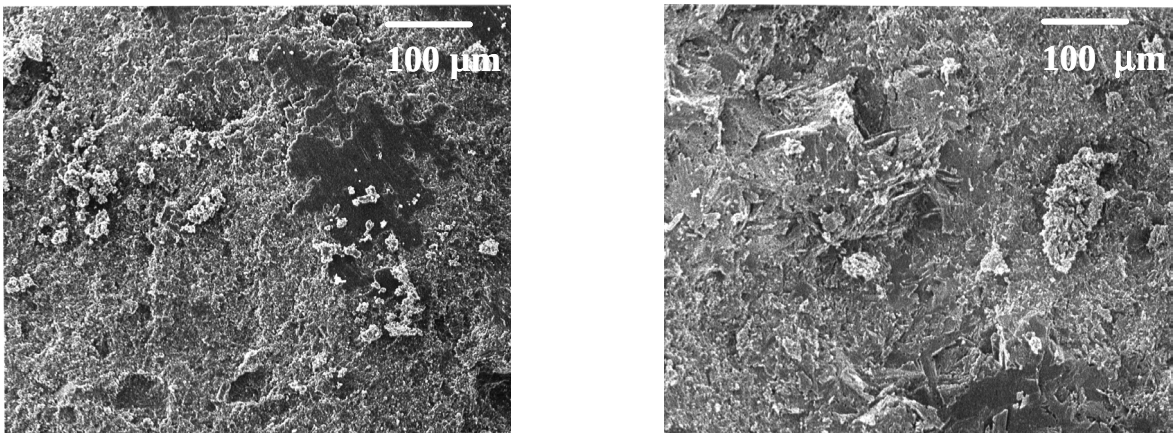

Figure 33: Cross-section of 100% cholesterol matrix before implantation (left) and excised at day 35 (right), both 150x.

Implants containing DSPC showed distinct swelling and erosion in both ratios, demonstrated through both an increase in wet weight and a loss in weight after freeze drying of the implants (Figures 34,35). The strong adherence of some connective tissue that could not be removed caused a very high standard deviation in the measured implant masses of the 50% DSPC implants at day 28.

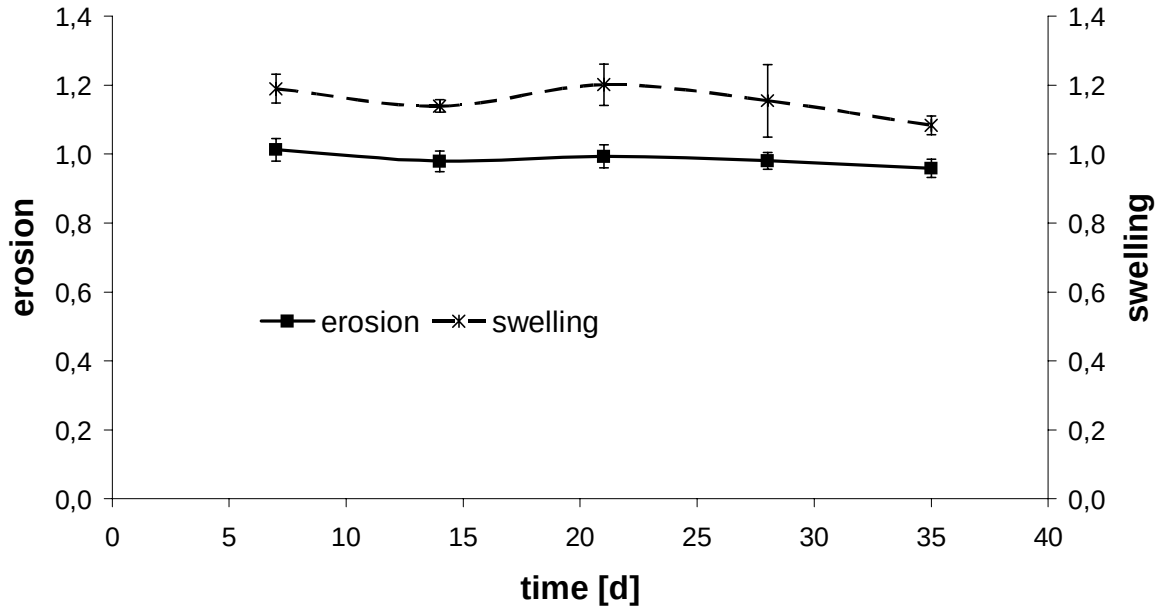

Figure 34: In vivo erosion (—) and swelling (- -) of triglyceride matrices containing 10% DSPC, normalized to 1.0 by pre-implantation mass; values are expressed as mean ± SD (n=4).

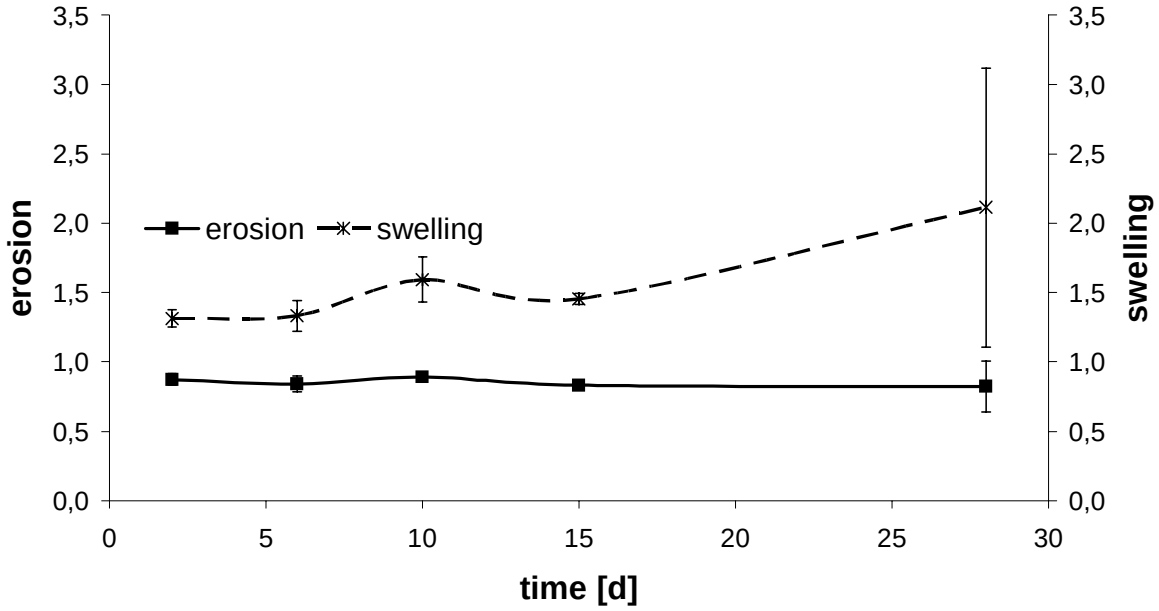

Figure 35: In vivo erosion (—) and swelling (- -) of triglyceride matrices containing 50% DSPC, normalized to 1.0 by pre-implantation mass; values are expressed as mean ± SD (n=4).

The constructs with the higher phospholipid content had already lost their cylindrical shape 6 days post-implantation and distinct signs of erosion like pore formation were observed by SEM throughout the course of the study. Figures 36-39 show the changes in these matrices over the course of the study. show the changes in these matrices over the course of the study. Two days after implantation, a few pores and slight changes in microstructure of the implants were already observed; the implant collapsed at day 6 and distinct cavities were still visible at day 28.

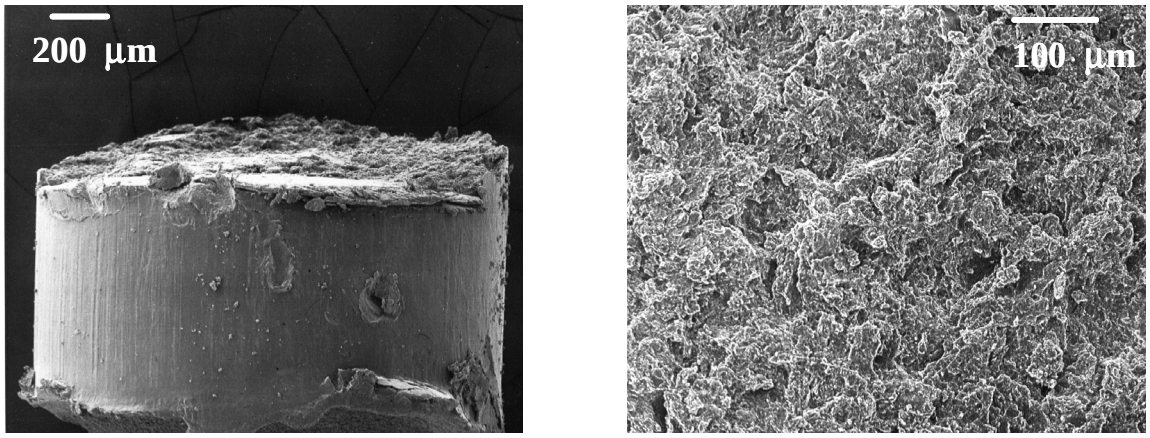

Figure 36: SEM images of the top view (left, 40x) and cross-section (right, 150x) of 1:1 glyceroltripalmitate:DSPC matrix before implantation.

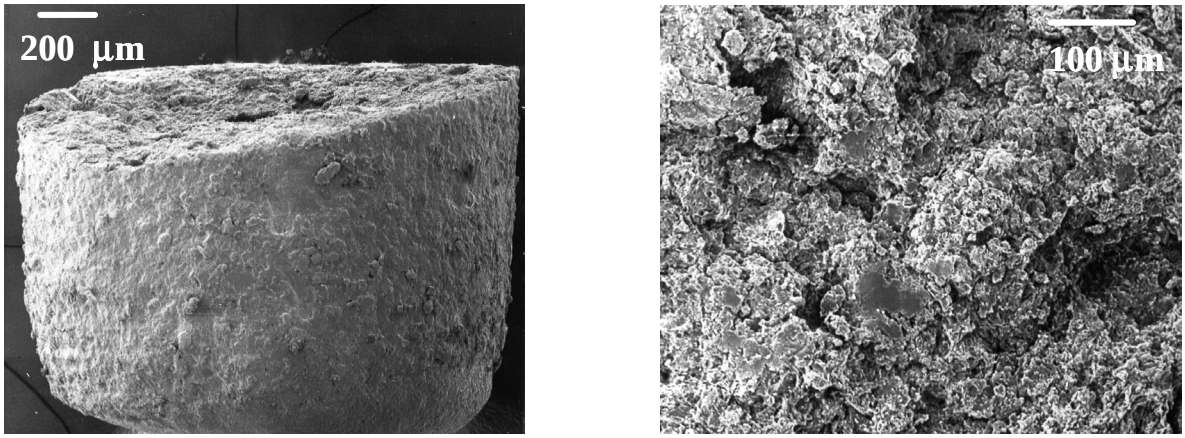

Figure 37: SEM images of the top view (left, 40x) and cross-section (right, 150x) of 1:1 glyceroltripalmitate:DSPC implant excised at day 2.

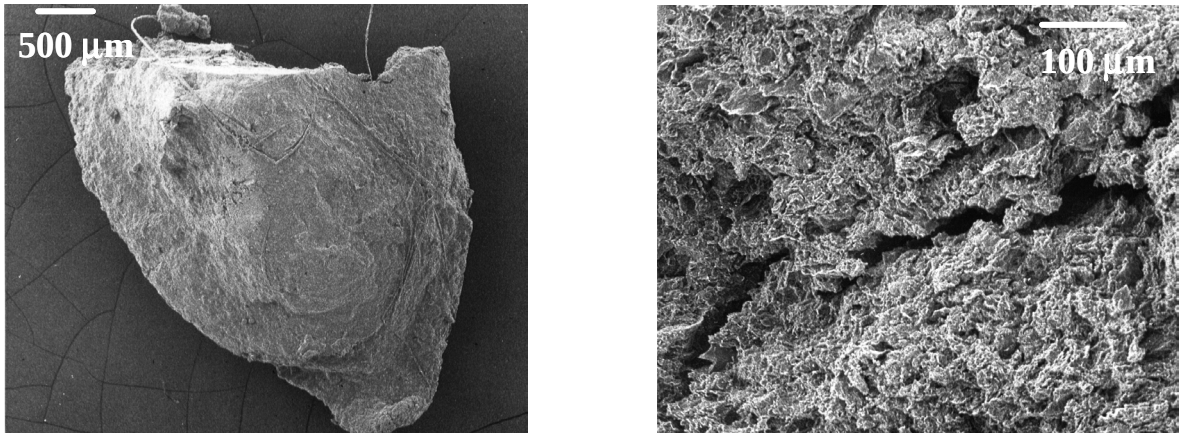

Figure 38: SEM images of the top view (left, 25x) and cross-section (right, 150x) of 1:1 glyceroltripalmitate: DSPC implant excised at day 6.

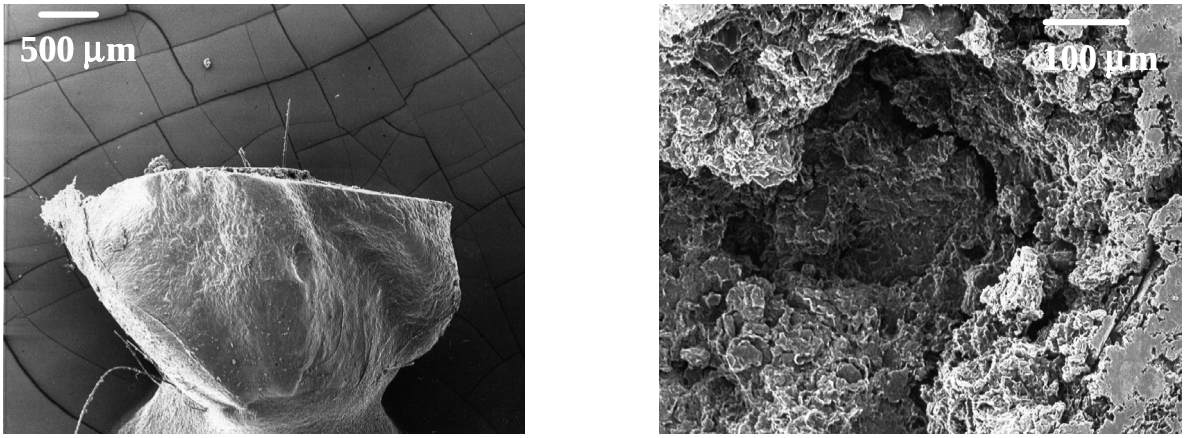

Figure 39: SEM images of the top view (left, 25x) and cross-section (right, 150x) of 1:1 glyceroltripalmitate:DSPC implant excised at day 28.

These observations clearly demonstrated the influence of the DSPC on the accelerated erosion of the triglyceride implants. However, a foreign body reaction at the implantation site was observed when DSPC was incorporated into the matrices. This mild tissue response was

seen in the form of a slight increase in the presence inflammatory cells, such as foreign body giant cells, and was not evident in the implants containing only 10% DSPC. At the end of the study, only connective tissue producing fibroblasts were observed, which indicates that the inflammatory reaction was an acute tissue response (Figure 40). Comparable tissue reactions showing a slight foreign body reaction, noticeable through the appearance of a few inflammatory cells, primarily foreign body giant cells, have already been reported for biodegradable polymers [179-181], whose biocompatibility is accepted to be at least satisfactory. Implants containing 50% phospholipid resulted in a more persistent inflammatory reaction, in which both foreign body giant cells and granylocytes were visible and a chronic tissue response with an increase of inflammatory cells and mononuclear infiltrates (Figure 41) was observed. Thus, this inflammatory reaction appears to be dependent on the amount of the phospholipid present and the tissue response is not related to the triglyceride. It might be caused by the surfactant characteristics of the DSPC or due to the increased roughness of the implant surface followed by increased mechanical irritations, which might also lead to an increase in foreign body reactions [178].

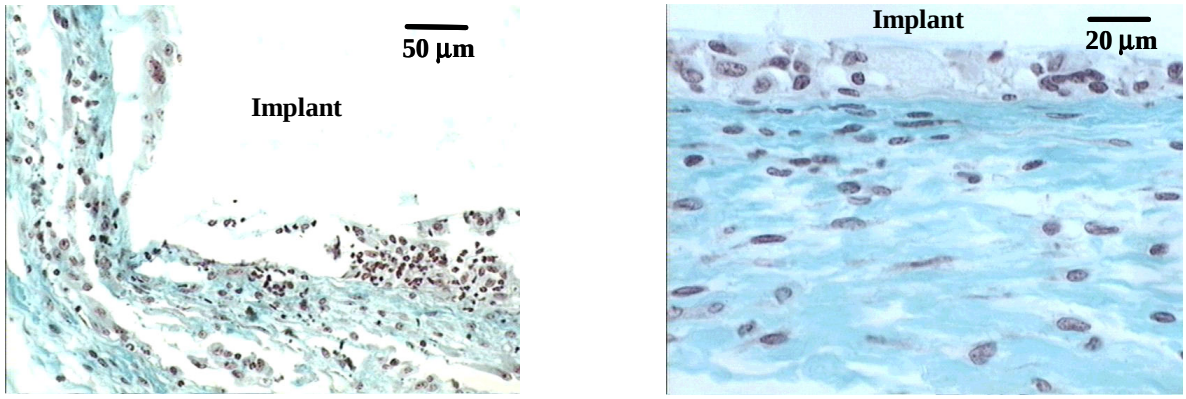

Figure 40: Light microscopy images of histological sections of implants containing 10% phospholipid at day 7 (left, 200x) and day 35 (right, 400x), Masson & Goldner stained, region of the implant marked.

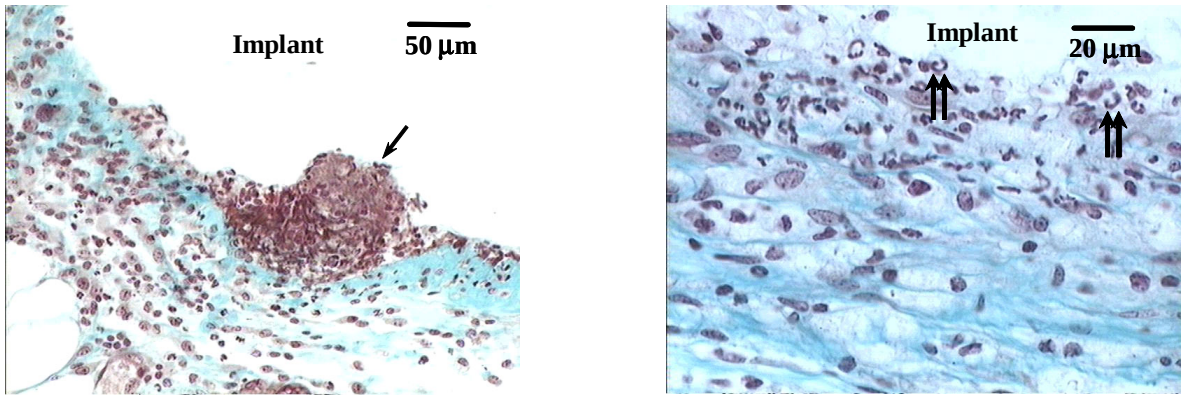

Figure 41: Light microscopy images of histological sections of 50% phospholipid containing implant at day 2 (left, 200x) and day 28 (right, 400x), both Masson & Goldner stained, arrow marks a local connective tissue proliferation, double arrows mark granulocytes.

Summary

Glyceroltripalmitate was shown to be biocompatible in vivo, since neither a significant inflammatory response nor a cytotoxic reaction was observed in mice over a period of 2 months. Furthermore, cholesterol emerged as a well-tolerated material when implanted subcutaneously, although the attempt to influence the (very slow) erosion rate of the triglyceride by mixing it with cholesterol failed. Distinct signs of implant degradation were achieved by using 1:1 mixtures of DSPC with glyceroltripalmitate, but in these concentrations a foreign body reaction was observed. As further aspects influencing the degradation time of the triglyceride, the size of the implanted material, crystallinity, and surface structure are discussed in the following. Additionally, the influence of phospholipids with shorter fatty acid chains and other molecules, such as hydrogel-forming substances, which could function as erosion modifiers on the in vitro release, was investigated.

Chapter 6

Excipients for the Modification of Triglyceride Erosion - Influence on the in vitro Release from Triglyceride Matrices

Introduction

Since in vivo degradation of macroscopic lipid matrices occurred only slowly, investigations were carried out with the goal of accelerating the erosion of the triglyceride. As the experiments described in chapter 5 showed, one possibility to overcome the problem of slow matrix degradation might be the incorporation of excipients, such as the phospholipid DSPC, into the triglyceride matrices. Thereby different strategies can be followed depending on the chosen release modifier.

(i) The use of amphiphilic molecules might accelerate the degradation of the lipid matrices by increasing the weakness of the matrix material (e.g. through a decrease in melting point) and facilitating the emulsification of the triglyceride. (ii) Hydrogel forming agents, which show swelling in contact with water, can serve as disintegrating excipients, which cause breaking of the matrices. Since in the literature indications can be found that lipid microparticles show faster erosion than matrices in the described investigations [118], (iii) incorporation of hydrophilic porogens could be another possibility to accelerate the erosion of the cylindrical triglyceride matrices. Such excipients decrease the stability of the matrix, when leached out, and thus can lead to the collapse of the cylinder into smaller particles upon exposure to mechanical stress, as occurs in vivo. Afterwards these fragments may undergo faster in vivo degradation than solid cylinders.

Hydrogel forming agents and hydrophilic porogens both cause a fragmentation of the matrices into smaller particles with eventually accelerated erosion. However, the differences in these strategies follow from the mechanisms that cause the collapse of the matrix. Hydrogel forming agents show swelling and thus lead to the disintegration of the matrix, whereas the leaching of a hydrophilic porogen from a triglyceride matrix only decreases its mechanical stability. Collapse of the matrix will then be caused by mechanical stress, such as that occurring in vivo after subcutaneous implantation. On the other hand, these two strategies will result additionally in different sizes of the remaining matrix fragments. Resulting triglyceride particles will be smaller when hydrophilic porogens are used due to the higher amount of the excipient necessary to achieve a disintegration of the matrix.

In order to investigate which of these strategies allows for a prolonged release from cylindrical lipid matrices and to get information on the ratios in which the respective excipient can be incorporated while still achieving release over several weeks, in vitro release

experiments were carried out. Thereby the number of animals needed for the following in vivo experiment on the erosion of triglyceride particles could be minimized.

Results and discussion

In vitro release of phospholipid-containing matrices

For the in vitro tests the phospholipids DMPC and DPPC, the hydrogel forming agents agarose and sucrose were chosen as excipients. Since DSPC showed effects in in vivo investigations described above, phospholipids were used to investigate the strategy followed up with the amphiphilic molecules. Thus the three phosphatidyl-cholines DMPC, DPPC and DSPC were incorporated into glyceroltripalmitate cylindrical matrices by the emulsion method described in section 2.17 and [37]. As Figure 42 shows, the incorporation of any ratio of DMPC and DPPC (Figure 43) via the emulsion method led to complete release of the model drug within a few hours, as did the use of 25% and 50% DSPC (Figure 44). Only matrices with ratios of 5% and 10% of the phospholipid with the longest fatty acid chain were capable of sustained release over 10 days (Figure 44).

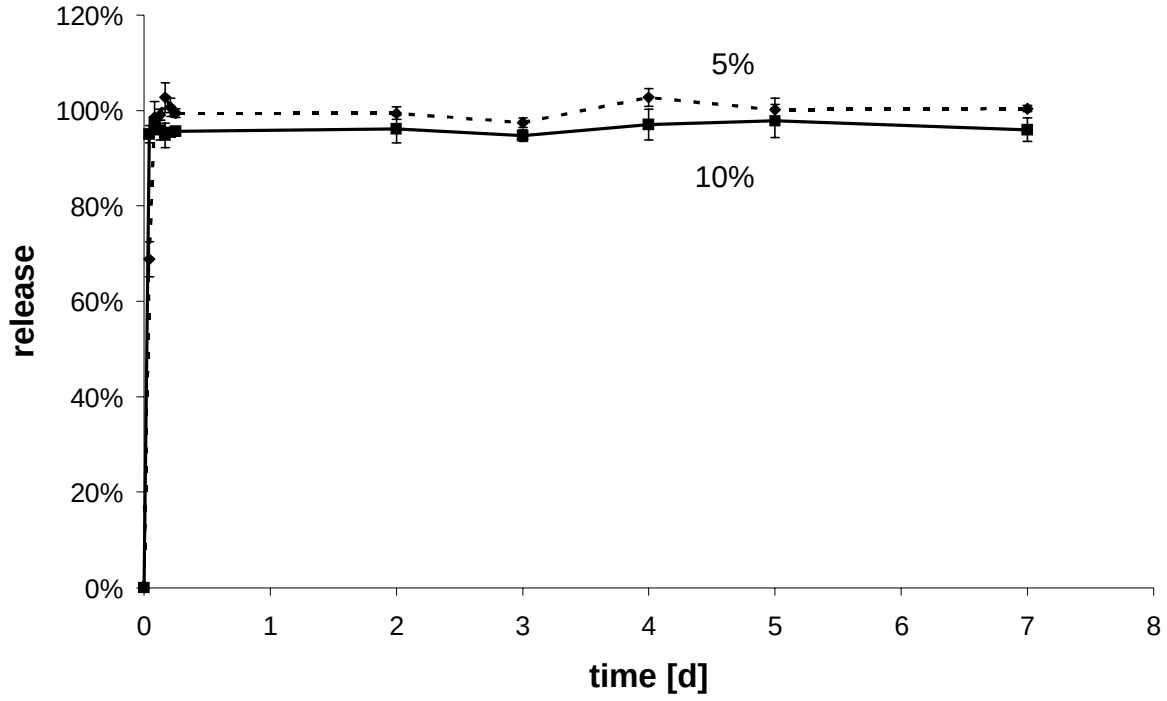

Figure 42: Influence of DMPC on the release profiles of pyranine from glyceroltripalmitate matrices prepared by using the emulsion method, cylinders contained 5% and 10% of the phospholipid; values represent mean ± SD (n=5).

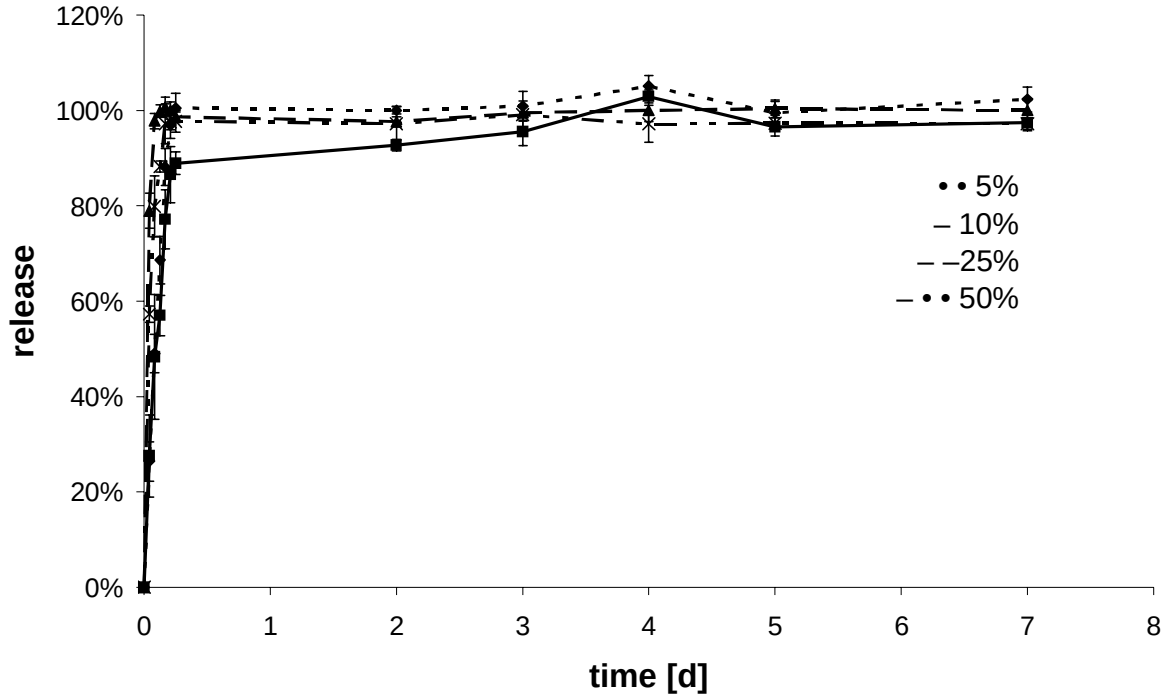

Figure 43: Influence of DPPC on the release profiles of pyranine from glyceroltripalmitate matrices prepared by using the emulsion method; cylinders contained ratios of 5% to 50% of the phospholipid; values represent mean ± SD (n=5).

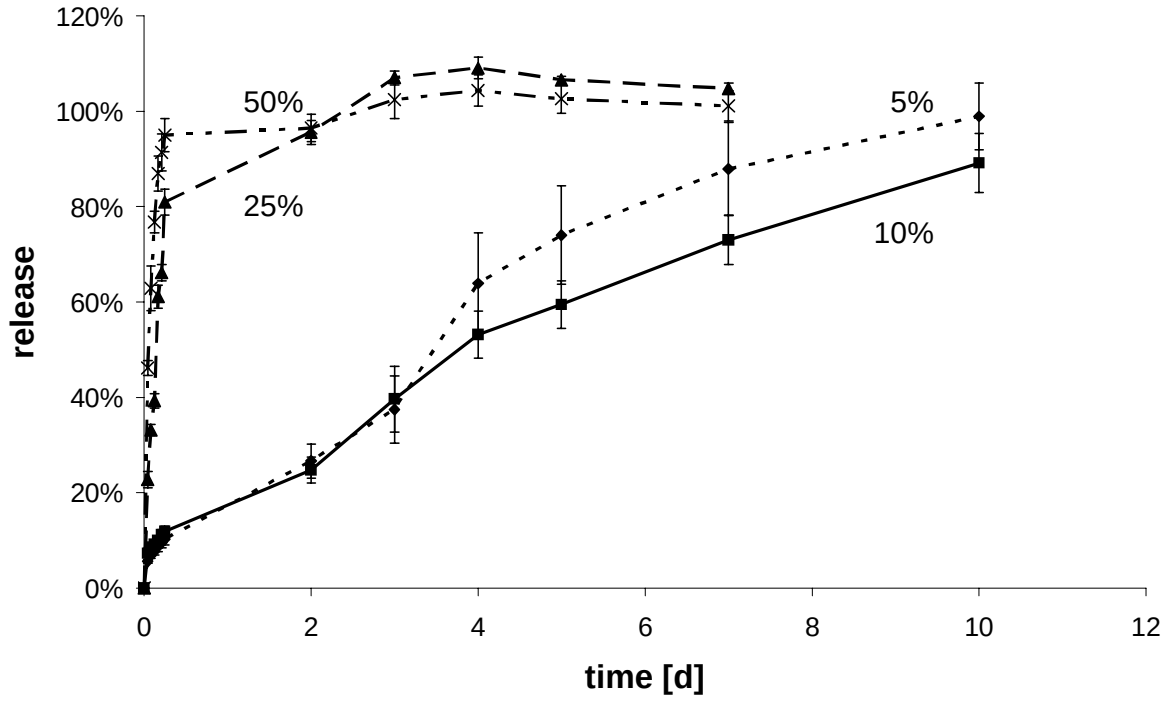

Figure 44: Influence of DSPC on the release profiles of pyranine from glyceroltripalmitate matrices prepared by using the emulsion method; cylinders contained ratios of 5% to 50% of the phospholipid; values represent mean ± SD (n=5).

These results indicate that the goal of prolonged release over several weeks from the triglyceride matrices cannot be achieved by using the emulsion method, because the influence of the erosion modifier on release properties of the matrices was too severe. Thus, a method was developed, which consists of two-steps. First, glyceroltripalmitate was loaded, as described in section 2.6, with the model drug. In a second step, the respective excipient was mixed with the drug loaded triglyceride powder. Thus, the influence of the excipients on the release was minimized, whereas their effect on the erosion of the lipid matrices should be maintained. For the drug loading it must be considered that the total drug content is decreased by incorporation of the modifying component, but can easily be adjusted by increasing the mass of the matrix.

In the following, firstly DPPC and DMPC, the two phospholipids with shorter fatty acid chains of 16 and 14 C-atoms, respectively, were incorporated into glyceroltripalmitate matrices to investigate the strategy, followed up with the newly developed two-step method. In the case of DPPC, 5%, 10%, 25% and 50% of the phospholipid were investigated, whereas the ratio of 50% was not tested with DMPC.

In Figures 45 and 46, release profiles of pyranine from lipid matrices containing phospholipid are shown. Regarding the results with DMPC, a prolongation of drug liberation of up to at least three days was observed for all ratios. This means an approximately 35 fold longer release period when using the two-step method, compared to matrices prepared with the emulsion method. The 5% DMPC containing matrices showed slightly slower release properties than the two other groups (Figure 45). For the phospholipid with the longer fatty acid chain yet more prolonged release periods were achieved and even with the very high ratio of 50% DPPC controlled release was realized (Figure 46). Drug release was completed in 10 days and 14 days, respectively, for the 50% and 25% DSPC containing matrices, whereas the two lower amounts of the erosion modifier, incorporated via the two-step method, led controlled release over a period of 7 weeks.

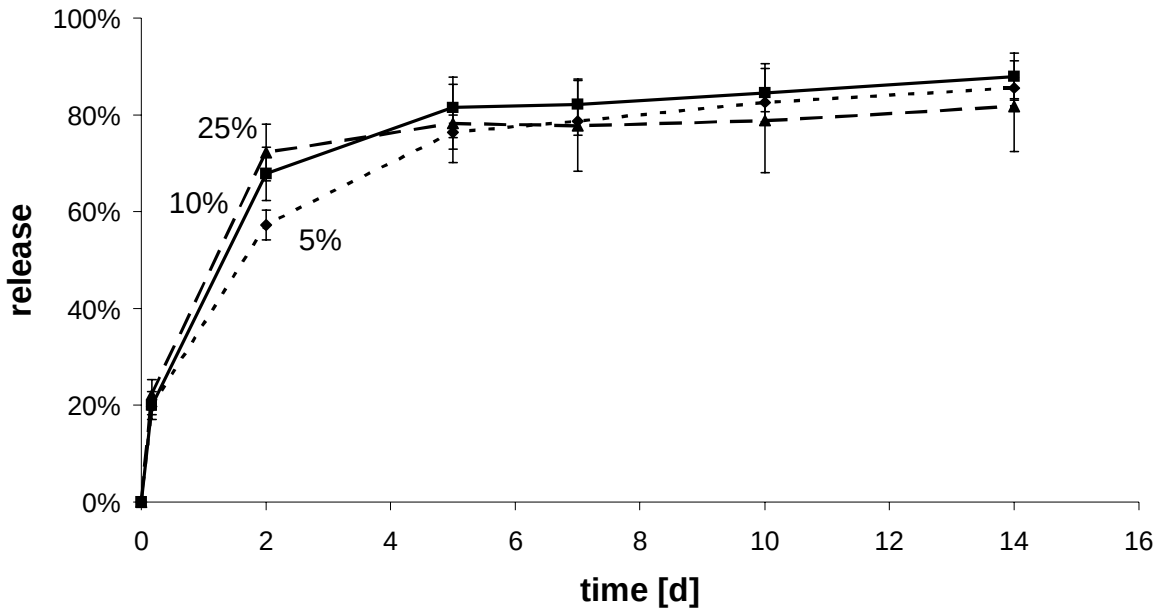

Figure 45: Release profiles of pyranine from glyceroltripalmitate matrices containing DMPC in ratios from 5% to 25%; cylinders were prepared by using the two-step method, data shown as a mean ± standard deviation (n=5).

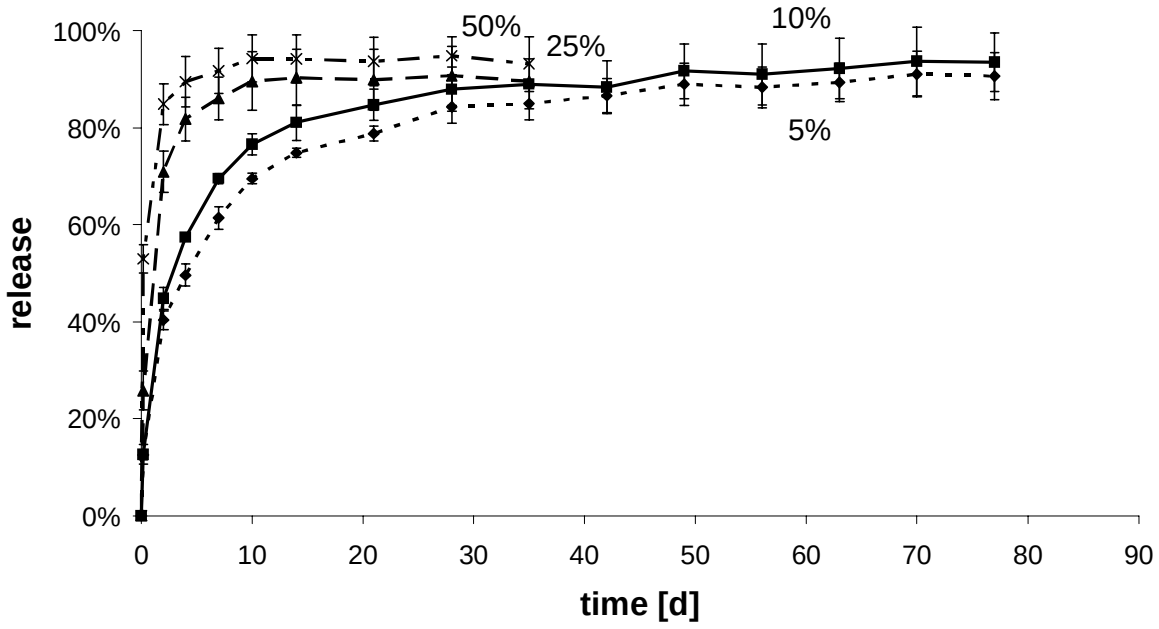

Figure 46: Release profiles of pyranine from glyceroltripalmitate matrices containing DPPC in ratios from 5% to 50%; cylinders were prepared by using the two-step method, data shown as a mean ± standard deviation (n=5).

Since the two-step method emerged as very useful to maintain sustained release properties of glyceroltripalmitate, it was used for all following in vitro investigations on possible erosion modifying components.

In vitro release of agarose-containing matrices

In the next study, agarose was chosen as a hydrogel-forming and disintegrating agent. It was used in concentrations of 5%, 10% and 15%. Results for these experiments are shown in Figure 47. Due to high standard deviations of approximately 6.5%, which appeared for the 5% agarose containing group in this experiment, no significance in the differentiation of release profiles was observed. Nevertheless a tendency towards slower release with decreasing ratios of agarose was obvious. When 15% of the excipient was incorporated into the matrices, pyranine was liberated over 4 weeks, whereas the release period was prolonged to 6 and 7 weeks, in case of 5% and 10% agarose containing matrices, respectively.

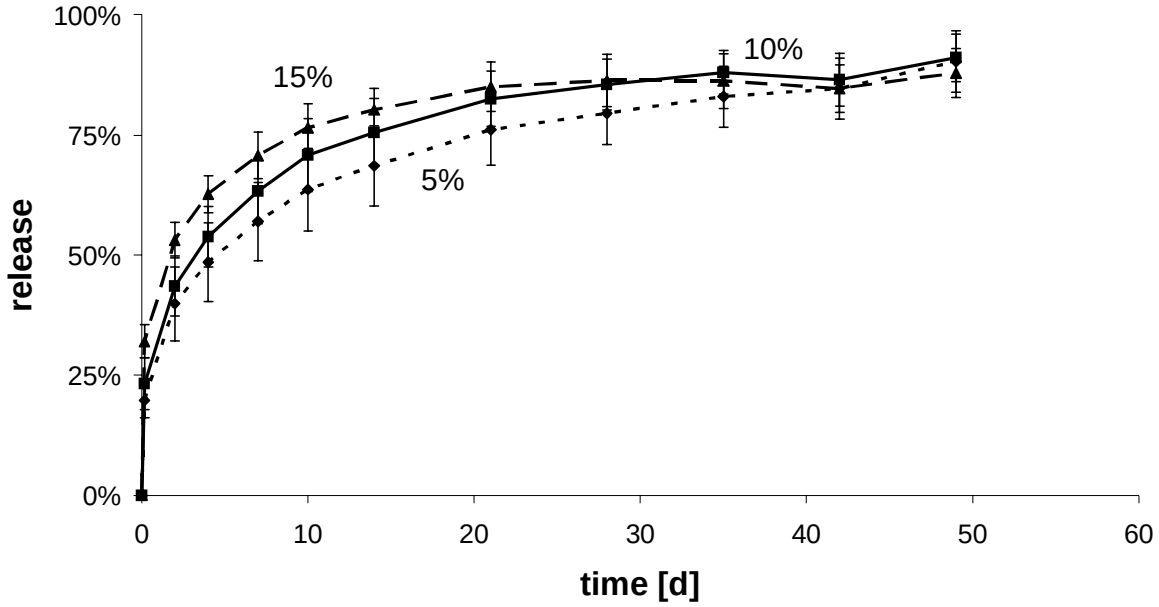

Figure 47: Release profile of pyranine from glyceroltripalmitate matrices containing agarose as an erosion modifier in different ratios; values are expressed as mean ± standard deviation (n=5).

In vitro release of sucrose-containing matrices

In addition to the phospholipids and agarose, sucrose was investigated for its in vitro suitability to serve as an erosion modifier for glyceroltripalmitate matrices, which would provide for the maintenance of the sustained release properties of the triglyceride. The followed strategy thereby was the formation of a network of sucrose crystals within the matrix, which should be leached out immediately at the beginning of the incubation or application, respectively. The resulting pores should decrease the stability of the matrix, lead

to the collapse of the cylinder into smaller fragments and thus accelerate the erosion. A schematic of this strategyis depicted in Figure 48.

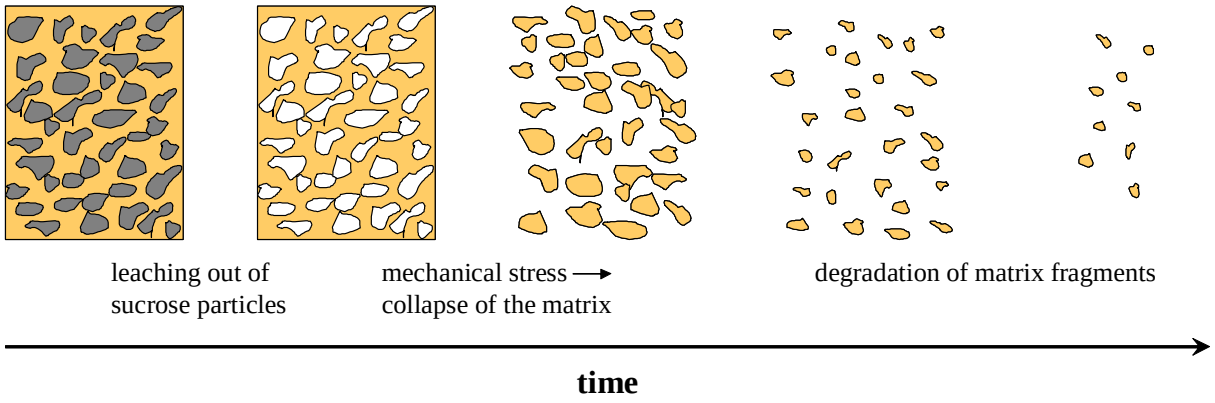

Figure 48: Schematic of the strategy followed with the use of sucrose (gray regions) as an erosion modifier for drug loaded (orange regions) triglyceride matrices.

For these investigations, different particle sizes of the porogen were tested. To this end, sucrose was sieved into fractions with different crystal sizes and incorporated into the lipid implants in ratios of 5%, 10%, 25% and 50%, respectively. In Table 9, the particle sizes of the sucrose and the abbreviations, which will be used in the following to succinctly describe the obtained fractions, are depicted. The particle sizes of the sucrose crystals incorporated into triglyceride matrices were in good agreement with the expected values, as SEM pictures showed (Figure 49).

Table 9: Particle sizes of sucrose incorporated into glyceroltripalmitate matrices as pore-forming agents.

fraction of sucrose	**particle size**
S25-45	25µm – 45µm
S150-180	150µm - 180µm
S250-355	250µm - 355µm
S560-710	560µm - 710µm

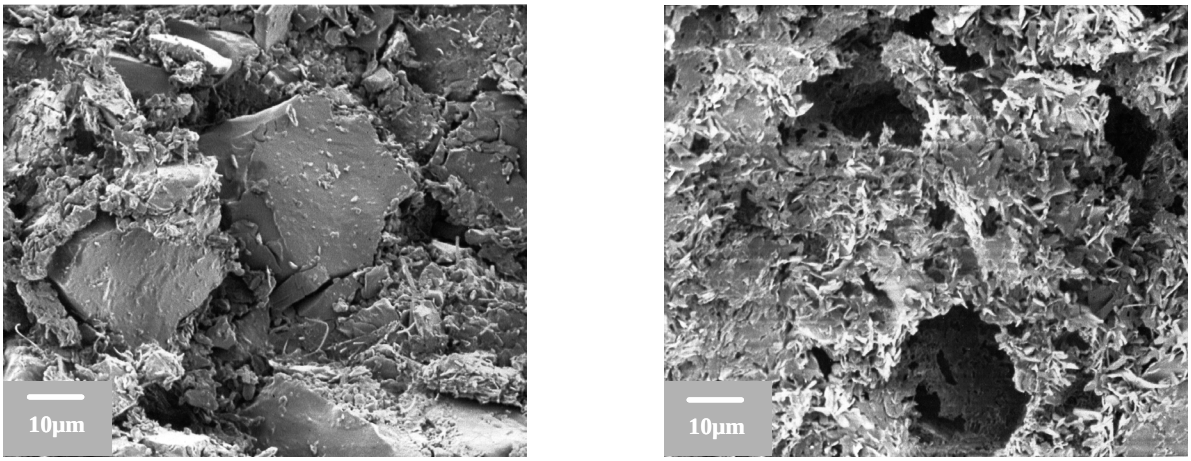

Figure 1: SEM images of glyceroltripalmitate matrices in which 25% (w/w) sucrose from the S25-45-fraction was incorporated; the left picture shows the cylinder before and right picture after incubation of 12 days in phosphate buffer, both 1000x. The sucrose crystals and resulting pores confirm particle sizes of the sieved fractions.

In Figure 50, the effects of sucrose of varying particle size incorporated into glyceroltripalmitate matrices in ratios from 5% to 50% are shown. Regarding the ratio of 5% sucrose, no major differences in release profiles of pyranine from the lipid matrices of S25-45 and S150-180 were observed (Figure 50). Regarding the larger sucrose fractions, pyranine was released almost similarly from matrices of the groups S250-355 and S560-710 over approximately 8 weeks, but after this time, liberation of the dye from cylinders containing sucrose of bigger crystal size occurred slower.

When 10% sucrose was incorporated into the triglyceride matrices (Figure 51), release from the matrices modified with the biggest particle sizes showed nearly no alteration in comparison to that from 5% containing cylinders of the same group. In contrast, the three other sucrose fractions displayed an increase in the initial burst release of the model drug within the first day. Furthermore, liberation of the dye from matrices prepared with the S250-355-fraction of sucrose aligned with that prepared with the two smaller particle sizes, which means a faster release compared to the 5% ratio or to the S560-710-group, respectively. Concerning the matrices containing 10% sucrose from the fractions S25-45 and S150-180, again no major differences in the shape of the resulting release profiles were observed.

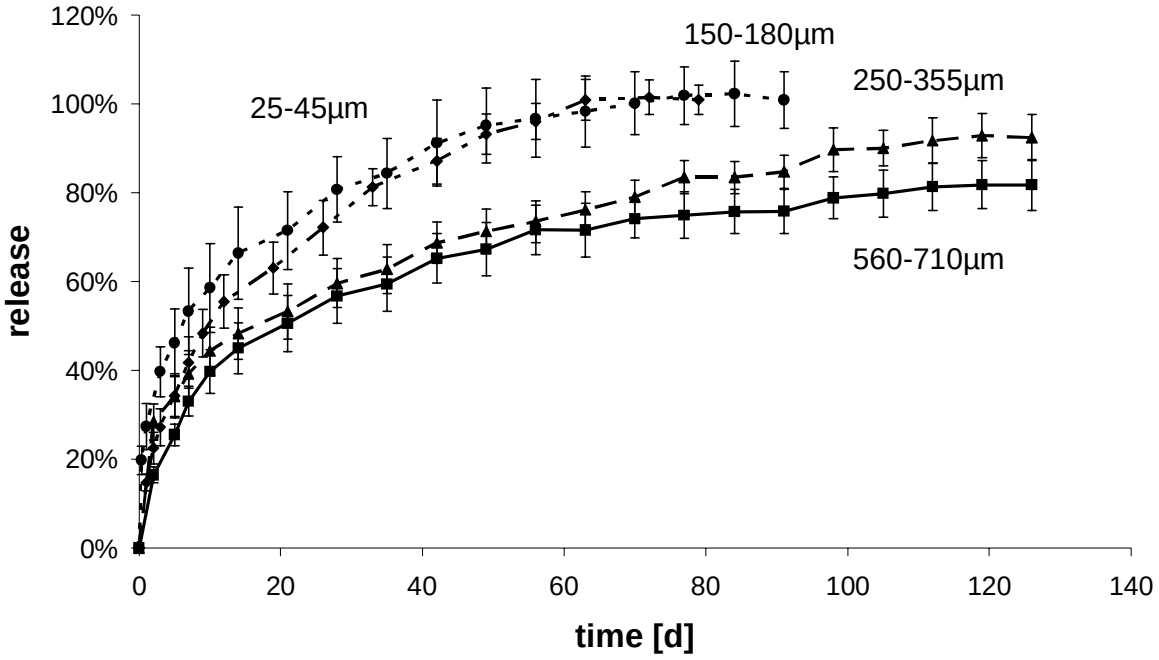

Figure 50: Comparison of release profiles of pyranine from glyceroltripalmitate matrices containing 5% (w/w) sucrose crystals of different particle size as erosion modifier; data show mean ± SD (n=5).

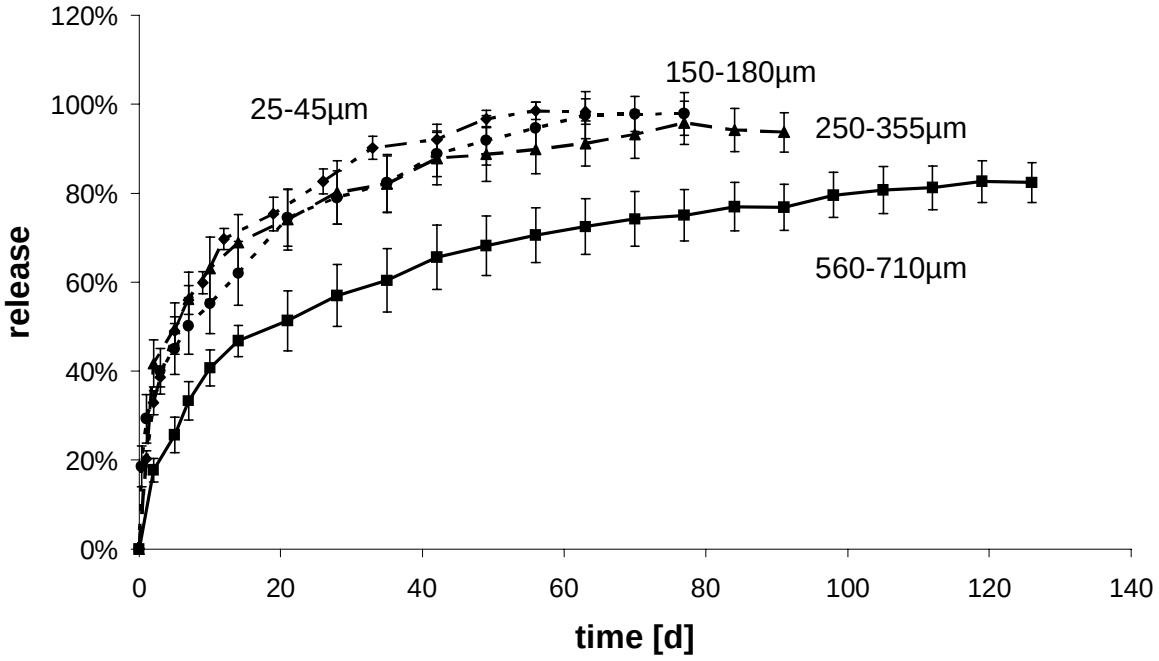

Figure 51: Comparison of release profiles of pyranine from glyceroltripalmitate matrices containing 10% (w/w) sucrose crystals of different particle size as erosion modifier; data show mean ± SD (n=5).

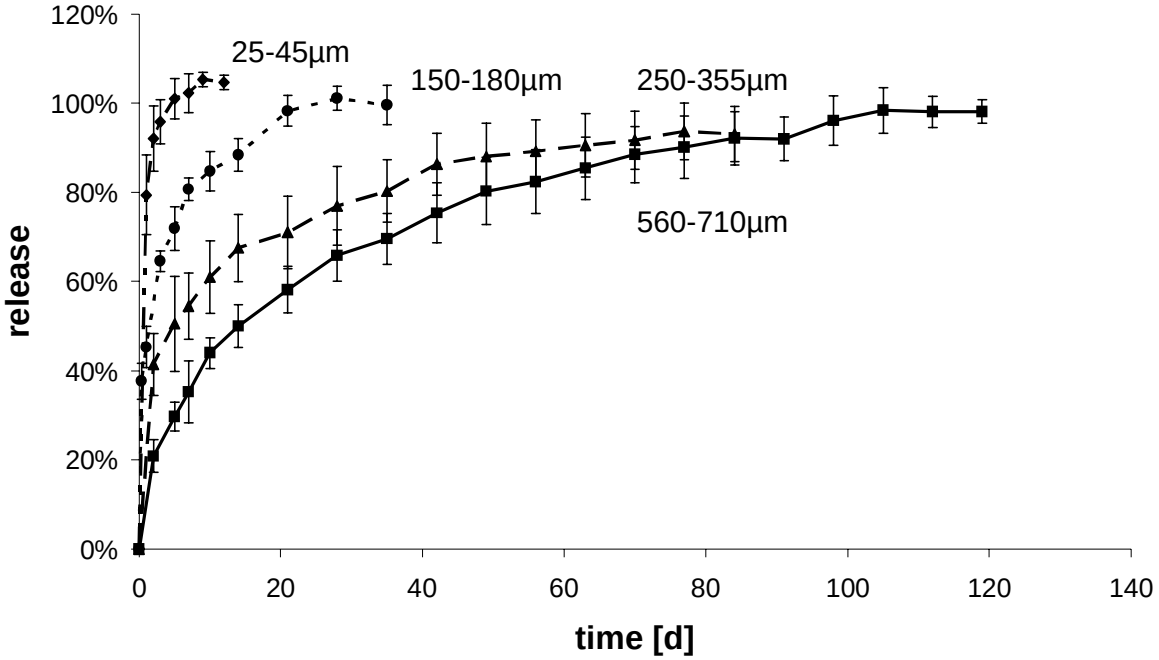

Figure 52: Comparison of release profiles of pyranine from glyceroltripalmitate matrices containing 25% (w/w) sucrose crystals of different particle size as erosion modifier; data show mean ± SD (n=5).

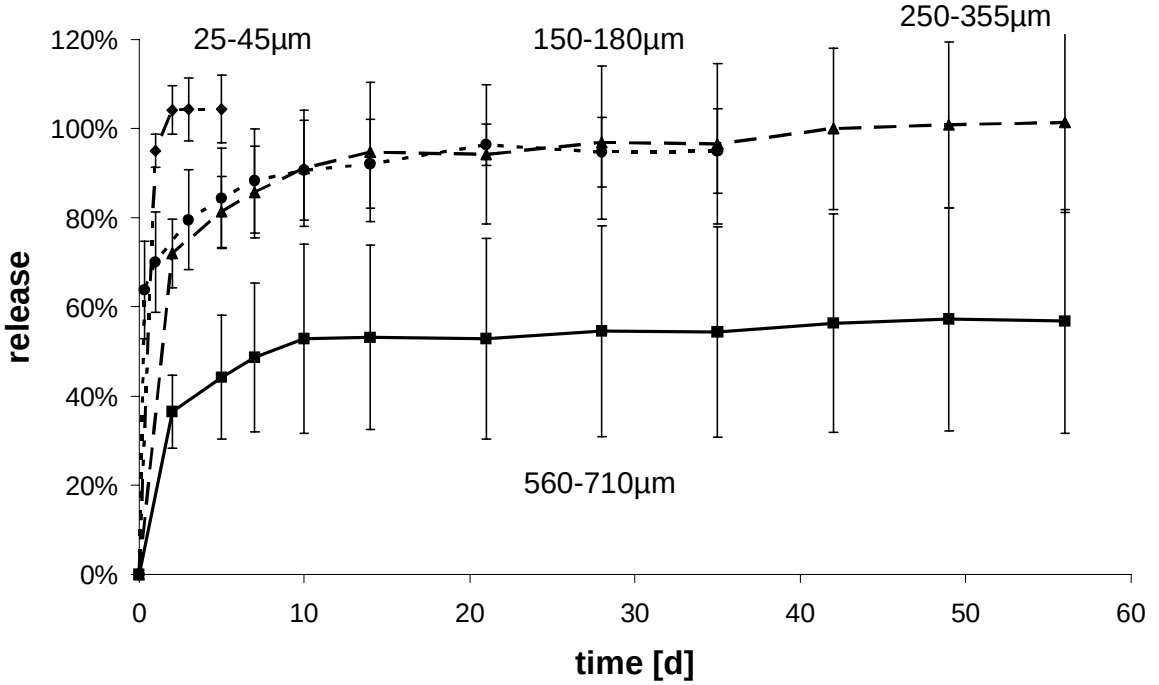

Figure 53: Comparison of release profiles of pyranine from glyceroltripalmitate matrices containing 50% (w/w) sucrose crystals of different particle size as erosion modifier; data show mean ± SD (n=5), (please note the time scale of only 60 days).

The differences between the crystal size fractions were most obvious when the matrices were formulated with 25% sucrose (Figure 52). As expected, cylinders prepared with the smallest particle size of the erosion modifier showed fastest release of the dye (within 9 days), followed by matrices containing sucrose of the S150-180-fraction, which liberated the model drug over 4 weeks. Incorporation of 25% sucrose with particle sizes ranging from 250µm to 355µm into lipid matrices led to a similar release profile compared to that obtained from the cylinders containing 10% of the erosion modifier of this fraction. Concomitantly, it was observed, that the ratio of 25% of the largest sucrose crystals led to a faster release than the two lower ratios.

Regarding the release profiles resulting from an incorporation of 50% of sucrose into glyceroltripalmitate matrices (Figure 53), much faster liberation of the dye, and, with exception of the two smaller particle sizes, much larger standard deviations were observed. Matrices of the S25-45-group released the entire model drug within 2 days, whereas the release period from cylinders containing the S150-180-fraction of sucrose was three weeks. For the matrices prepared with the particle size fraction from 250µm to 355µm, the time of release of approximately 2 to 4 weeks could only be estimated with regard to continuously increasing mean value and standard deviations until day 56. No conclusions on the release period were drawn from results obtained from the S560-710-group, due to the very high standard deviations and incomplete release of the dye. Repetition of in vitro experiments on the latter two groups showed no alteration in the obtained release profiles. These problems, concerning the very high standard deviations, seemed to be due to difficulties during the incorporation of the erosion-modifying component, when both a high ratio and a big particle size, compared to the diameter of 2mm of the manufactured matrix, should be realized.

The other results concerning the effects of incorporation of sucrose with varying particle size in different ratios into glyceroltripalmitate matrices are in good agreement with percolation theory. Since the goal of the incorporation of sucrose crystals into triglyceride matrices is the formation of a network, percolation theory can be applied to understand the results of the described investigations. Due to the preparation method of the matrices, in which the excipient was added to the dye-loaded lipid in a second step (see section 2.17), it must be considered, that an increase in the sucrose content did not lead to any change in the pyranine loading of the triglyceride. This means that alterations in release profiles from triglyceride matrices were caused by changes in the surface area, which was accessible for release. Since this surface area directly depended on the network formed by the hydrophilic

porogen, both the extension of the pore network as well as the time needed to leach out the porogen were of great importance for the resulting release profiles.

Leuenberger et al. [166,167] described the existence of a so-called percolation threshold of a porogen within a matrix, below which no network will be formed. Figure 54 schematically shows the effect of an increased amount of sucrose particles incorporated into pyranine-loaded glyceroltripalmitate matrices. With increasing amount of excipient (Figure 54b), the number of porogen particles that are localized on the surface of the matrix increases. Unlike porogen particles that are completely surrounded by triglyceride (Figure 54a), the particles on the surface are immediately leached out and thus lead to an increased surface area of the dye-loaded triglyceride. A further increased ratio of the porogen results in the formation of a pore network (Figure 54c), thereby increasing the surface area of matrix fragments accessible for release and thus accelerating the release of the dye from the triglyceride matrix.

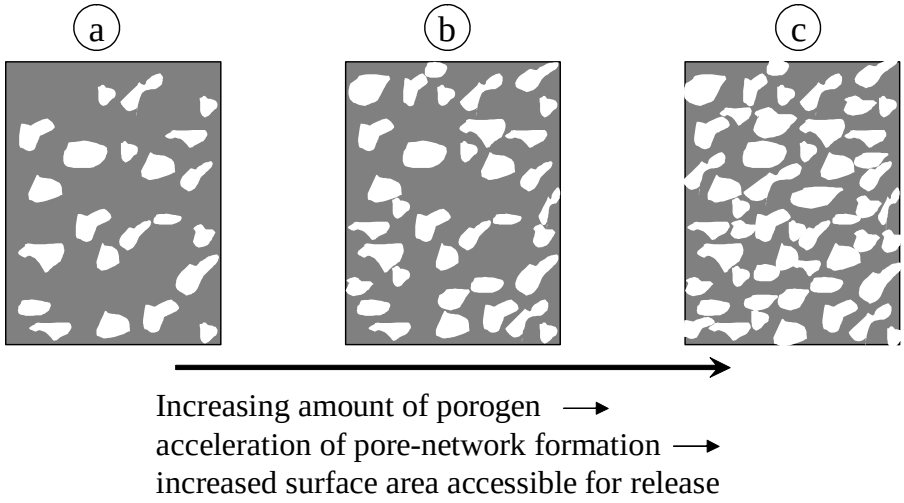

Figure 54: Schematic for alteration of pore network formation caused by increasing the amount of sucrose crystals incorporated into pyranine-loaded glyceroltripalmitate matrices; a higher ratio of porogen also leads to increased number of particles localized on the surface of the matrix.

Fernández-Herváz et al. examined the direct dependence of the percolation threshold on the particle size of the porogen [182]. They found lower percolation thresholds when the particle size of the porogen was decreased. This effect is schematically visualized for sucrose crystals incorporated into pyranine-loaded glyceroltripalmitate matrices in Figure 55. Decreasing the sucrose particle size leads to a higher surface area of the incorporated amount of the excipient. Thus again the amount of particles localized at the surface of the pyranine loaded matrix increases (Figure 55b) and with further decreasing of the sucrose particle size, a porogen network can be formed within the matrix (Figure 55c).

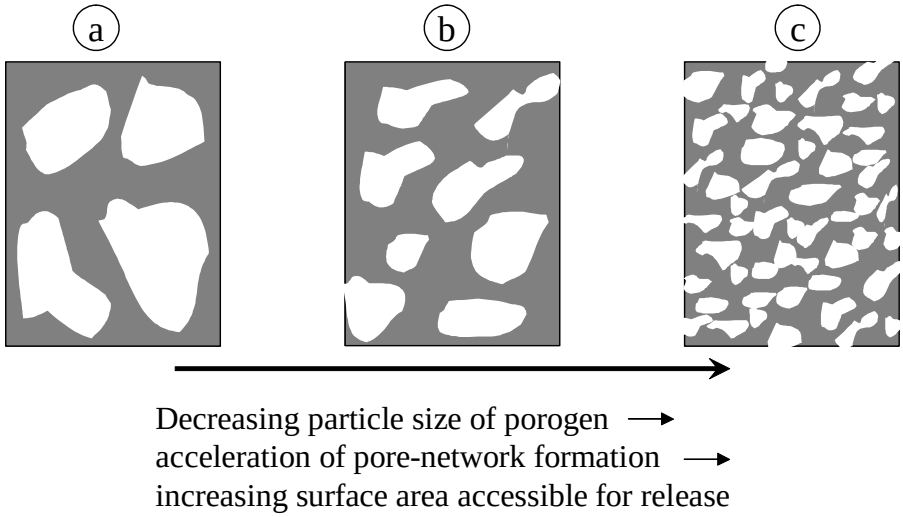

Figure 55: Schematic of sucrose particle size changing pore network formation within pyranine-loaded glyceroltripalmitate matrices.

Release profiles of the pyranine from matrices, containing 5% sucrose can be explained by the number of particles localized at the surface of the matrices. In the case of the two smaller sucrose particle sizes (S25-45 and S150-180), at least a few particles should have had contact with the surface of the matrix. The percolation threshold of sucrose was not yet reached and thus no difference between these two groups was observed. The bigger sucrose particles might have been completely encapsulated into the triglyceride in the ratio of 5%. This would explain on the one hand why there was no difference in release profiles between the matrices prepared with the S250-355- and the S560-710-fractions of the sucrose, since the surface area of the dye-loaded glyceroltripalmitate, which was accessible for release, would have been comparable. On the other hand, the slower release of matrices from these groups compared to that of matrices prepared using the two smaller sucrose particles also becomes understandable.

Increasing the amount of sucrose to 10% of the matrix lead to no major differences in the release profile compared to the matrices containing 5% of the excipientfor the largest sucrose particle size. This may again be explained by a complete encapsulation of the excipient, which consequently resulted in comparable surface areas for both ratios of sucrose. In the case of the S250-355-fraction, the ratio of 10% seemed to be enough that few particles were localized at the surface of the matrix, leading to a faster release compared to the lower ratio of 5%. But since there was no difference observed between any release profiles of matrices prepared with 10% of the three smaller sucrose particle sizes, this amount did not seem sufficient to reach the percolation threshold.

When regarding the release profiles from matrices with ratios of 25% of the porogen, the fast release rates for S25-45 - and the S150-180- group show that the percolation threshold is reached for these two sucrose particle sizes at this ratio. Since the release profile of matrices containing 25% sucrose of the S250-355-fraction is comparable to that from 10% containing matrices, the percolation threshold is not yet reached for this particle sizes. The faster release of matrices containing 25% sucrose of the biggest particle size can be explained by the contact of the excipient to the surface of the matrix.

Examination of the microstructure of the matrices after release confirmed the existence and the interconnectivity of a pore network for the two smaller sucrose particle sizes at the ratio of 25%. Figure 56 shows the results observed by scanning electron microscopy.

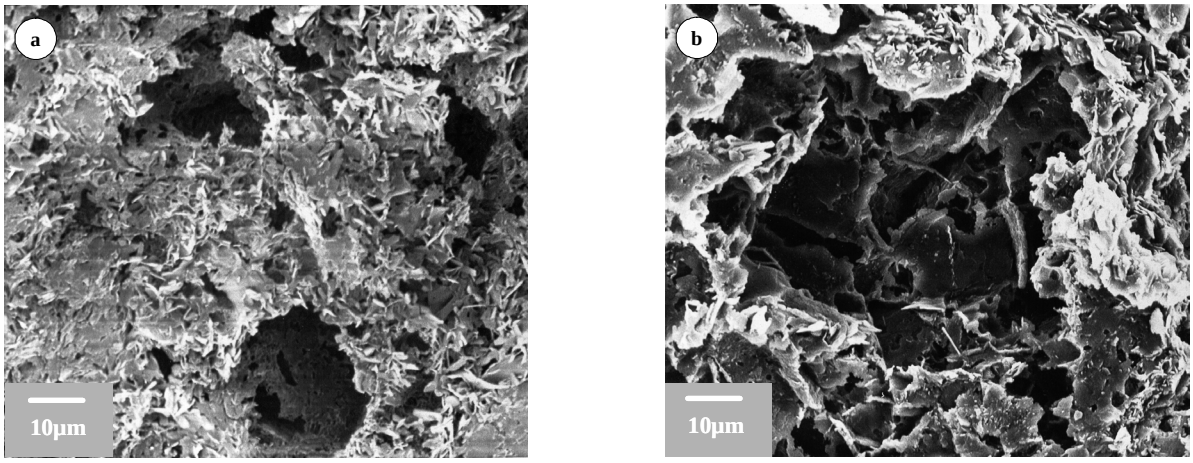

Figure 56: SEM images of triglyceride matrices containing 25% of sucrose with varying crystal size after incubation; interconnectivity of the pores was observed
a) 25µm - 45µm particle size of the erosion modifier, 1000x
b) 150µm - 180µm particle size of the erosion modifier, 1000x.

As Figure 57 shows, no pore network, but contact of the sucrose particles to the surface of the matrices were observed by SEM for matrices containing 25% sucrose of the two bigger particle sizes.

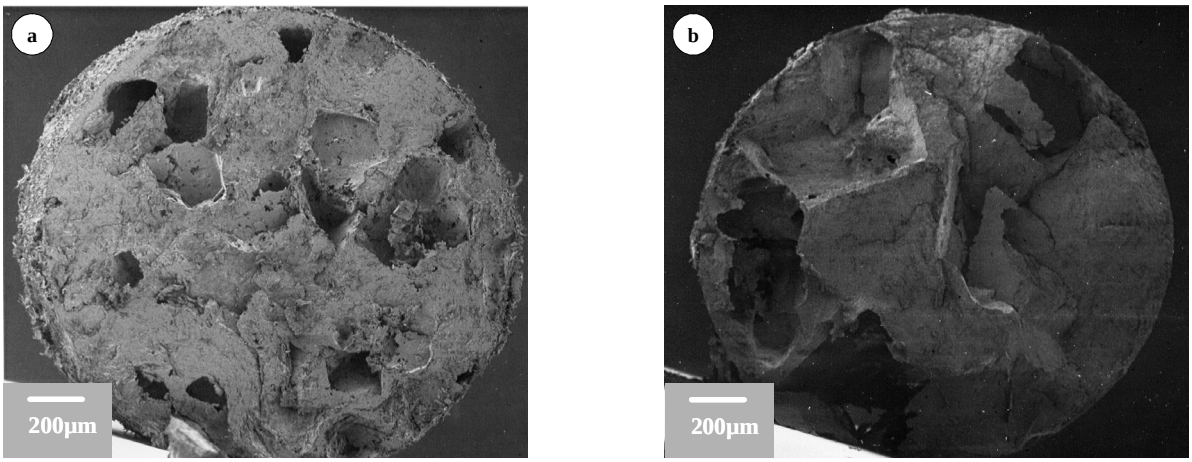

Figure 57: SEM images of triglyceride matrices containing 25% of sucrose with varying crystal size after incubation
c) 250µm - 355µm particle size of the erosion modifier, 40x
d) 560µm - 710µm particle size of the erosion modifier, 40x.

Summary

These in vitro release experiments were carried out to characterize and quantify the effects of excipients on the release profile of triglyceride matrices. Substances should be found that allow for both the acceleration of the erosion and the prolonged controlled release from the lipid cylindrical matrices. Therefore, two methods for the incorporation of the excipients were tested. With regard to the resulting very fast release from the modified glyceroltripalmitate matrices, the emulsion method was demonstrated to be unsuitable for the incorporation of any erosion modifier. Thus, a new two-step method was developed and established, which resulted in much longer release periods from the triglyceride matrices. Applying this method, the phospholipids DMPC and DPPC, the hydrogel-forming agent agarose, and the hydrophilic porogen sucrose were investigated for their use as erosion modifiers for lipid matrices. Matrices containing the phospholipid DMPC showed a release of the model drug within 3 days and this excipient was thus deemed unsuitable for use as an erosion modifier. When agarose or DPPC were incorporated in ratios of 5-15% and 5-50%, respectively, release periods from 2 to 7 weeks were achieved. Concerning the phospholipid DPPC, a dependence between the ratio of the modifying component and release period was visible, whereas matrices containing agarose showed no significant correlation between the

ratio of the disintegrating agent used and the duration of release. Thus, higher ratios of agarose may also be useful.

To summarize the results obtained from the in vitro release investigations on sucrose, it can be said that release from triglyceride matrices containing this excipient depended on both the amount of sucrose incorporated into the matrix and the particle size of the excipient used. For sucrose, the dependence of release period extension on the used amount of the erosion modifier was more distinct using smaller particles sizes. Controlled release was realized for all crystal sizes and release periods of 2 to 15 weeks were achieved; only a ratio of 50% of the smallest sucrose particles led to a fast release within three days.

To judge the suitability of a hydrophilic porogen, such as sucrose, as an erosion modifier, the percolation threshold is of great importance. This is the lowest concentration of sucrose within the matrix at which the formation of a network of the porogen can be observed. Sucrose ratios above the percolation threshold avoid encapsulation of the sucrose crystals within the dye-loaded triglyceride and thus enable the leaching of the excipient and consequently lead to a decrease of the mechanical stability of the matrix, which is the requirement for an acceleration of the in vivo erosion when the matrix is implanted and exposed to mechanical stress. The percolation threshold was reached for the two smaller particle sizes (25-45µm and 150-180µm) at a ratio of 25% of the excipient. 25% sucrose of the two bigger particle sizes (250-355µm and 560-710µm) was at least sufficient to avoid a complete encapsulation of the excipient.

With regard to the high deviations, observed for the two biggest particle sizes (250µm-355µm, 560µm-710µm), the ratios of 50% of these two sucrose fractions was considered not to be practicable for the preparation of cylinders with a diameter of only 2mm, but may be of good use, when larger implants should be prepared.

In conclusion, the obtained results demonstrated that the phospholipid DPPC, the hydrogel-forming agent agarose and the hydrophilic porogen sucrose are suitable to modify the erosion of triglyceride matrices, since these three excipients allow for both a decrease in the stability of triglyceride matrices, which should result in faster erosion, and the maintenance of prolonged release from these matrices.

Chapter 7

In vivo Investigation on the Erosion of Triglyceride Particles

Introduction

Since the in vitro experiments, presented in chapter 6, showed promising results concerning the possibility of prolonged, controlled release from triglyceride matrices containing a considerable amount of an excipient as erosion modifier, the next goal was to verify the hypothesis that the in vivo erosion of smaller lipid particles is faster than that of solid, macroscopic cylinders. In this in vivo study, glyceroltripalmitate microparticles and two groups of glyceroltripalmitate powders were implanted subcutaneously to immunocompetent NMRI-mice. In addition to the size effect of the lipid, the influence of triglyceride crystallinity was investigated by using two glyceroltripalmitate powder groups, which showed a high and low degree of crystallinity. To obtain information into whether small triglyceride particles undergo in vivo degradation, changes in the particle size of the samples were investigated over a period of 8 weeks.

Microparticle and triglyceride-powder characterization

This study was carried out for three groups of glyceroltripalmitate. Lipid microparticles were chosen, because of their smooth surface and very good reproducibility concerning particle size and manufacture. When spray-congealed, the microspheres show the instable β-modification; therefore in addition lipid powders were investigated to clarify the influence of the modification of the triglyceride on its in vivo erosion. Concomitantly, it was considered that the crystallinity of a material may influence its in vivo erosion, and thus two groups with high and low degrees of crystallinity were investigated. Triglyceride powder, which was sterilized in solution by filtration with subsequent freezing in liquid nitrogen and freeze drying, showed low crystallinity, whereas lipid, which underwent hot air sterilization and afterwards was tempered for three days at 55°C showed high degree of crystallinity, similar to that of the bulk material. Results obtained by X-ray diffraction analysis are shown in Figures 58-60. No major differences were observed between the bulk material (Figure 58) and the lipid powder sterilized by hot air and subsequently tempered for 3 days at 55°C (Figure 59). The peaks within the obtained graphics are distinct signs for a high degree of crystallinity. For the freeze-dried glyceroltripalmitate (Figure 60) peak formation was much less distinct, which indicates a lower degree of crystallinity compared to the heat sterilized varient.

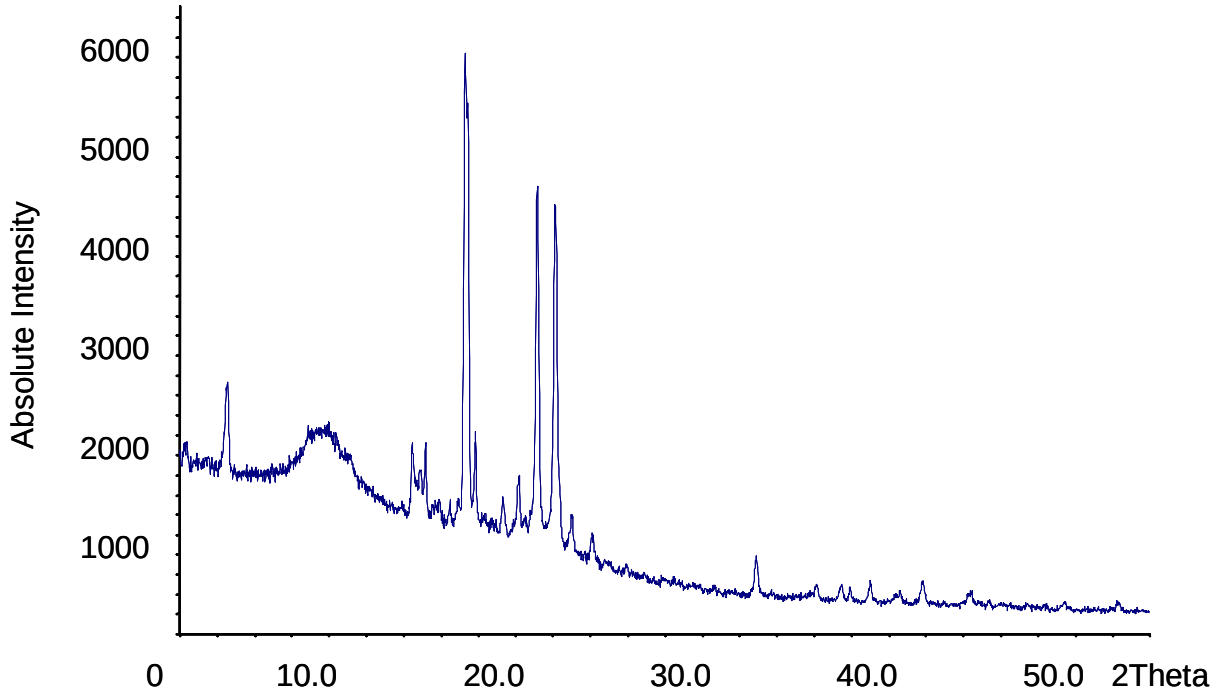

Figure 58: Wide-angle X-ray diffractogram of glyceroltripalmitate bulk material; clearly visible peaks show high degree of crystallinity

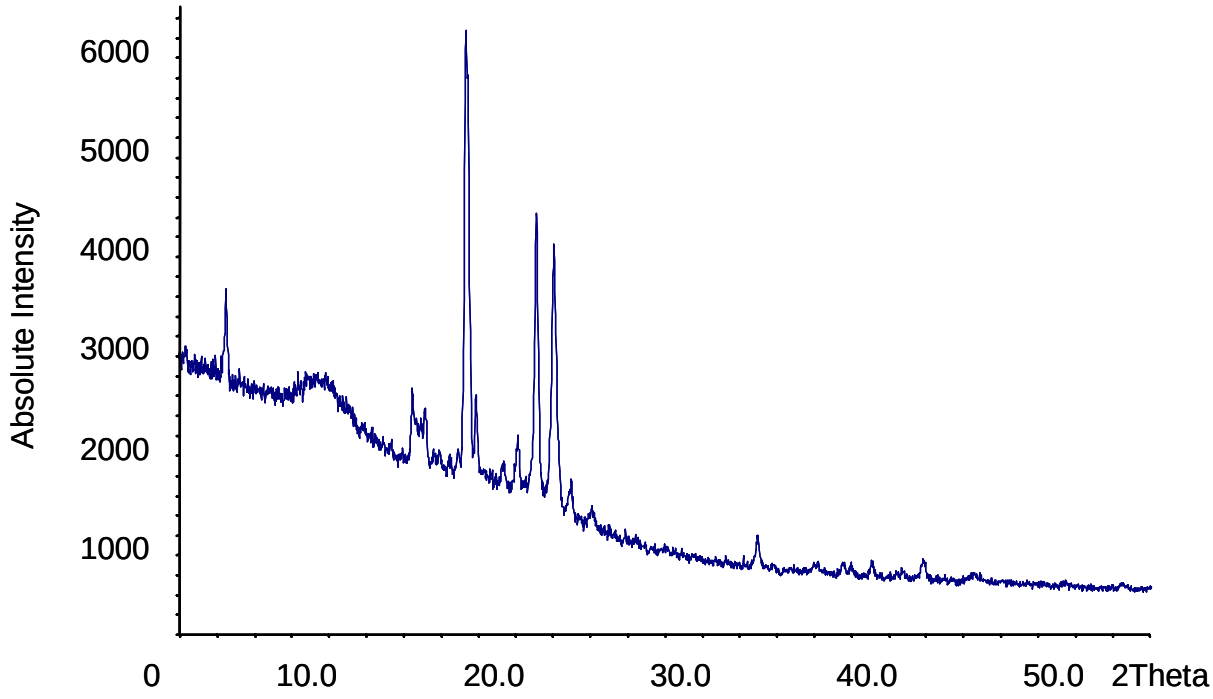

Figure 59: Wide-angle X-ray diffractogram of glyceroltripalmitate; material underwent sterilization for 2h at 110°C and tempering (3days at 55°C), peaks show high degree of crystallinity.

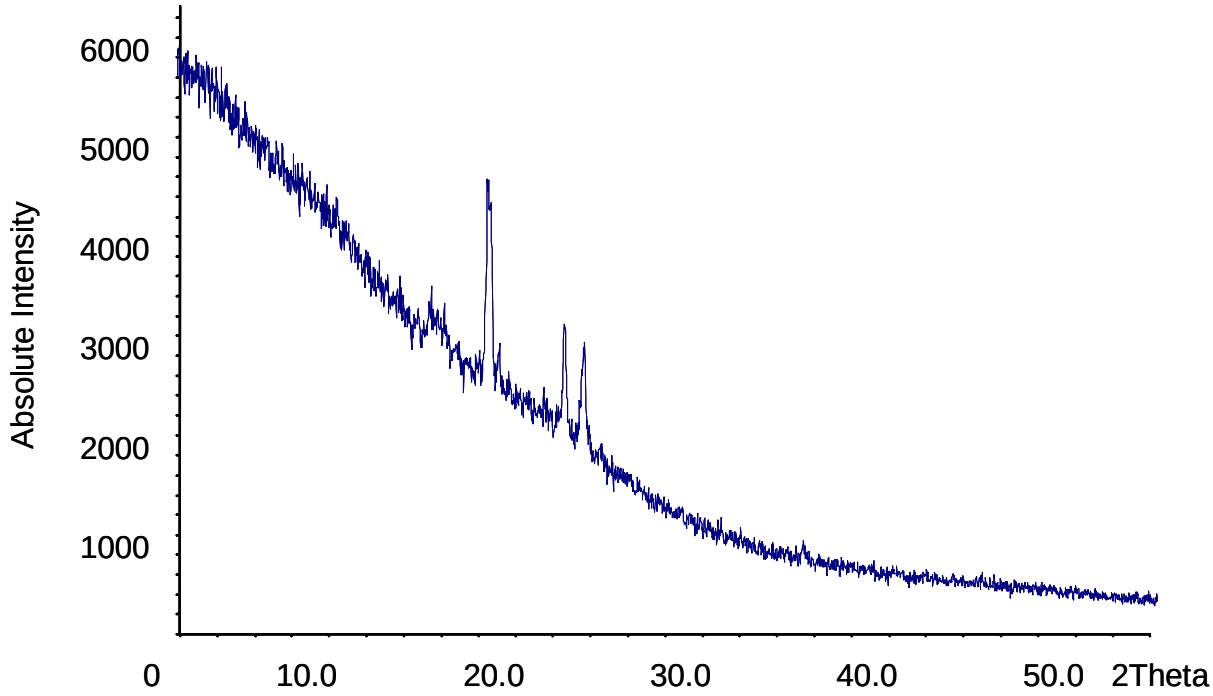

Figure 60: Wide-angle X-ray diffractogram of glyceroltripalmitate; material was dissolved in THF, filtrated, frozen in liquid nitrogen and freeze dried, absence of peaks, respectively less distinctive peaks show low degree of crystallinity

Particle sizes of the investigated lipid samples were determined with laser diffractometry, without the application of ultrasonication. Results are shown in Figure 61. For lipid microparticles a mean diameter of 176µm was determined, whereas both lipid powders showed a multimodal distribution with peaks at particle sizes of 10µm to 20µm and approximately 100µm. All observed particle sizes were confirmed by SEM analysis (Figures 62,63). In the case of the heat-sterilized and freeze-dried triglyceride, the particle size distributions indicate the formation of aggregates, which was also confirmed by results obtained from SEM analysis 63).

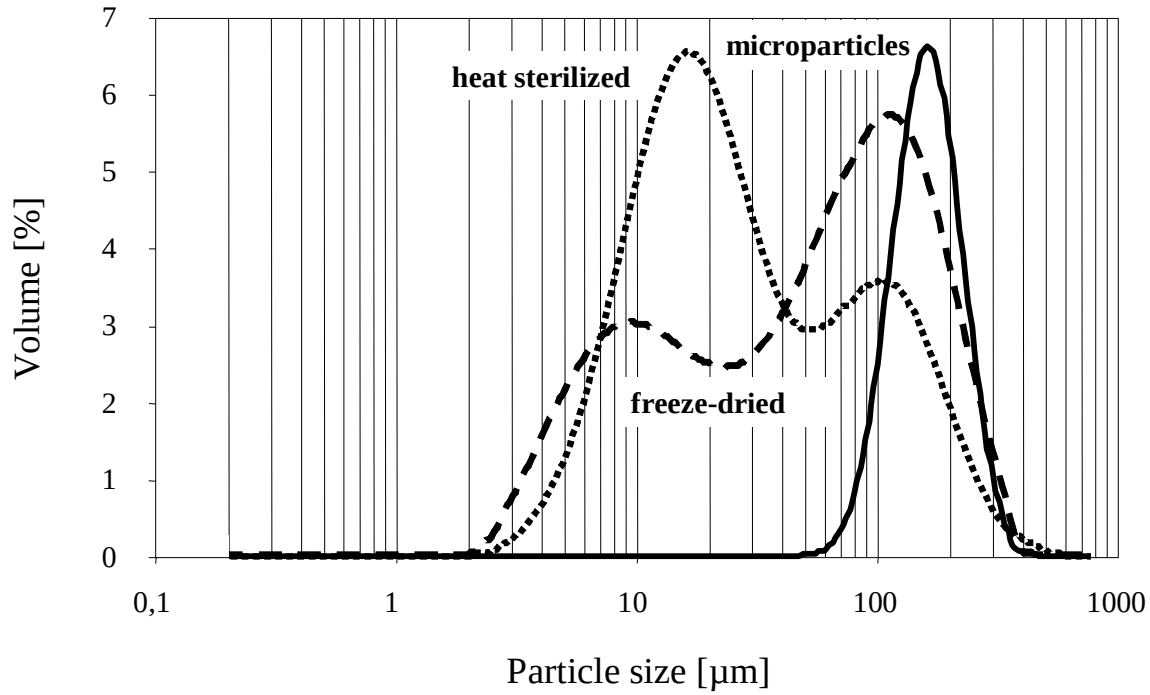

Figure 61: Particle size distribution of lipid microparticles (—) and freeze dried (- -) and heat sterilized (▪▪) glyceroltripalmitate powders for in vivo erosion study, determined by laser diffractometry.

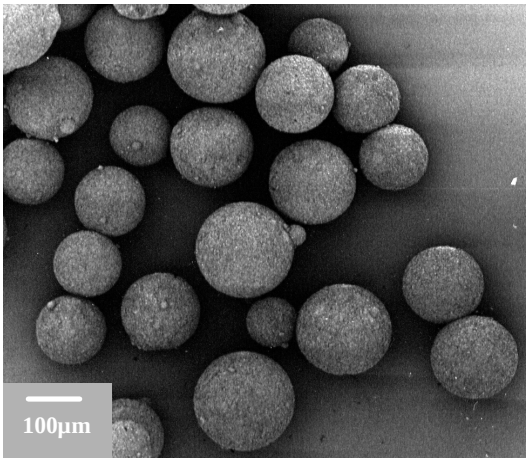

Figure 62: SEM image of glyceroltripalmitate microparticles prior to in vivo investigation (50x).

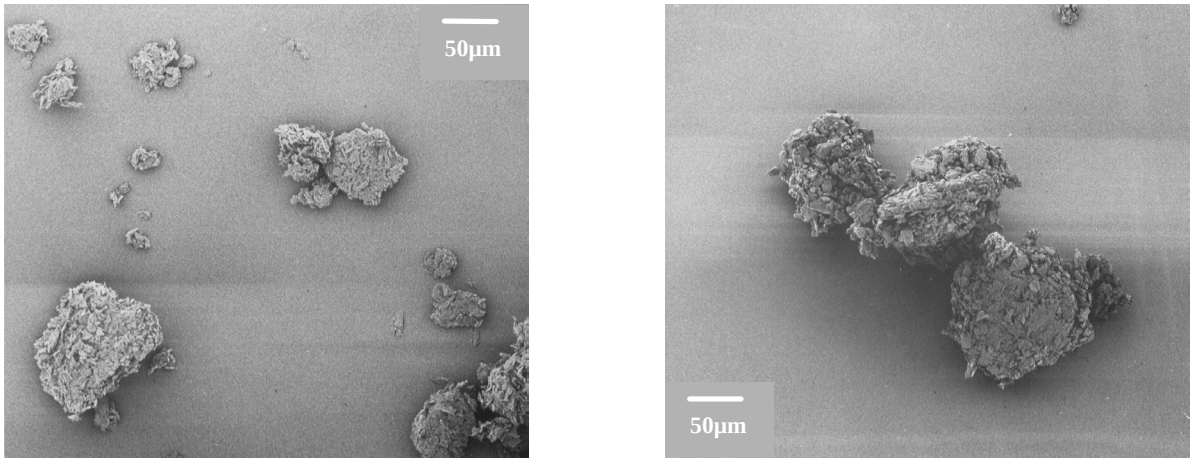

Figure 63: SEM images of freeze-dried (left) and heat-sterilized and tempered (right) triglyceride powders prior to in vivo investigation, both 200x.

For the investigation of the particle size of the glyceroltripalmitate samples and its alteration during the course of the study, histological sections were examined and holes stemming from the microparticles and the triglyceride powder were measured by light microscopy as described in section 2.21. Since the deformation of the holes, which was observed for the microsphere group, was in similar direction in every investigated slice (Figures 3,65), it may not have arisen during in vivo study, but could also be an artifact of the sectioning process. This would also be confirmed by the absolutely round shape of the microparticles prior to the in vivo investigation observed by SEM (Figure 62).

In vivo erosion study

As Figure 63 shows, the two lipid powders were not of spherical shape. Since the described estimator for the real particle diameter (see equation (1) in section 2.21) is only valid for spherical particles, quantitative results can only be reported for the lipid microspheres in our in vivo experiment. For the lipid powder groups, only qualitative conclusions on the degradation were drawn, because of their irregurar shape.

Concerning the freeze-dried triglyceride powder at day 7, larger and smaller particles were seen in histological investigations (Figure 64a), which can be explained by the determined particle size distribution (Figure 61) and SEM results for this group (Figure 63). Days 17 (data not shown) and 28 showed comparable results, which can be distinguished from those from day 7 by a decreasing number of the lipid powder particles and fewer particles of bigger size (Figures 64b,c). 42 days after implantation, no particles were found in any section of all 4 mice, whereas at day 56 in one single slide of one animal particles were seen (Figure 64d),

which had a decrease in size compared to the other excision time points during the study (Figures 64a-c). Since only in one mouse, out of four, particles were found after 8 weeks and these particles were very small, it could be considered that the lipid powder seemed to be compeletly degraded during the in vivo study.

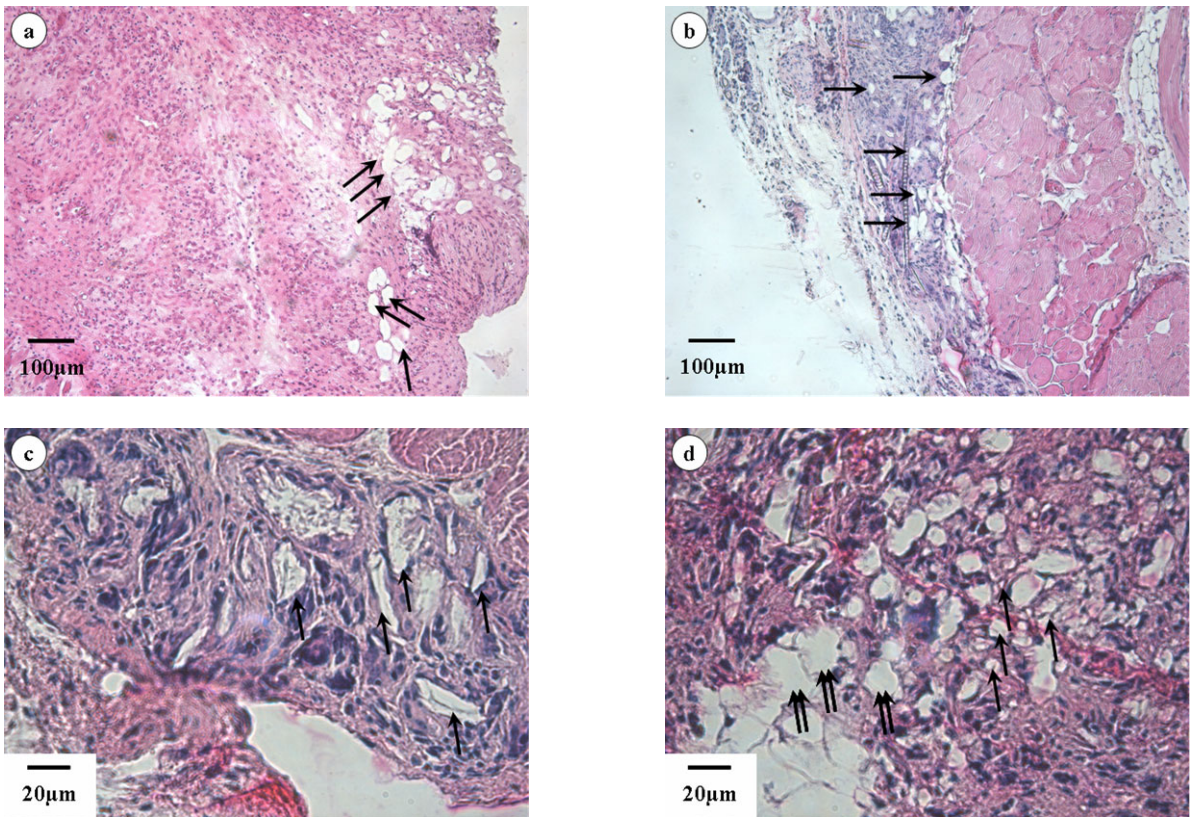

Figure 64: Light microscopy pictures of histological sections of the freeze-dried glyceroltripalmitate powder at different time points of the study, single arrows mark lipid powder particles, all pictures HE stained,
a) histological section of a sample excised at day 7, 100x
b) histological section of a sample excised at day 28, 100x
c) histological section of a sample excised at day 28, 400x
d) picture of the only particle containing histological section in samples excised at day 56, 400x; double arrows mark adipocytes at the interface between adipose tissue and other tissue containing the lipid powder particles.

The results for the heat-sterilized and tempered glyceroltripalmitate powder were almost identical with these obtained for the freeze-dried lipid powder. Large particles were observed after 7 days, but their number decreased with time. After 42 and 56 days, no particles were found in any mouse, which indicated the complete degradation of the triglyceride powder.

Concerning the group of lipid microparticles, the implanted samples were not completely degraded during the investigated period of 8 weeks. At day 56, every examined animal displayed a considerable number of microspheres (Figure 65).

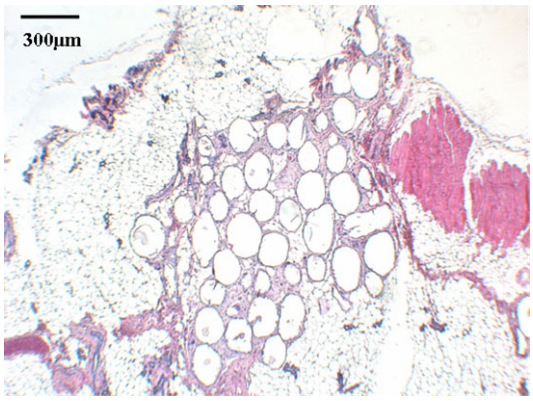

Figure 65: Light microscopy image of a histological section of lipid microparticles containing the tissue sample excised at day 56, HE stained, 100x.

The determination of the lipid microparticle diameters and the subsequent application of the estimator (see equation (1) in chapter 2) made it possible to visualize changes in particle size occurring during the course of the in vivo study. In Figure 66, the particle sizes of the microspheres, which were observed for each excision time point, are depicted.

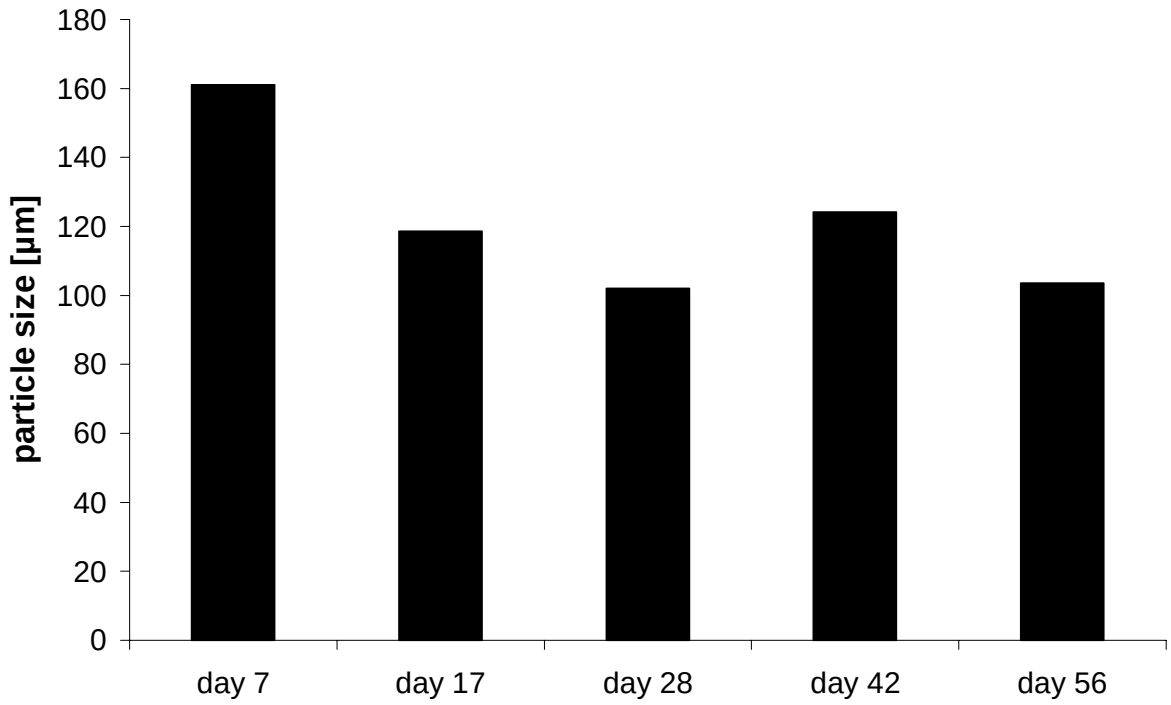

Figure 66: Changes in size of glyceroltripalmitate microparticles over 8 weeks in vivo; values calculated from the measured diameters by use of the estimator depicted in equation (1) (see section 2.21)

Although the lipid microparticles were not completely eroded within the duration of the in vivo study of 8 weeks, a trend is visible. The decrease in the estimated mean diameter from approximately 160µm at day 7 to 100 µm at day 56 suggests that the lipid was not inert in vivo, but seemed to be degraded with time. To investigate whether complete erosion of the triglyceride microparticles occurs, a long term in vivo study has to be carried out, to confirm these early results.

The faster degradation of the triglyceride powder compared to the microparticles can be explained by two factors. Firstly, the microstructure, examined by SEM, indicated a much higher apparent density of the microparticles (Figure 67) compared to the two lipid powders (Figure 68). Glyceroltripalmitate microparticles appear to be much more compact than the lipid powders, as is visible throughout the more loose-packed crystal structure of the triglyceride powders. Therefore, samples of the microparticle group might have been more stable against in vivo degradation. Consequently, this led to longer erosion times for the glyceroltripalmitate microparticles compared to the powder groups and confirmed the in vivo findings.

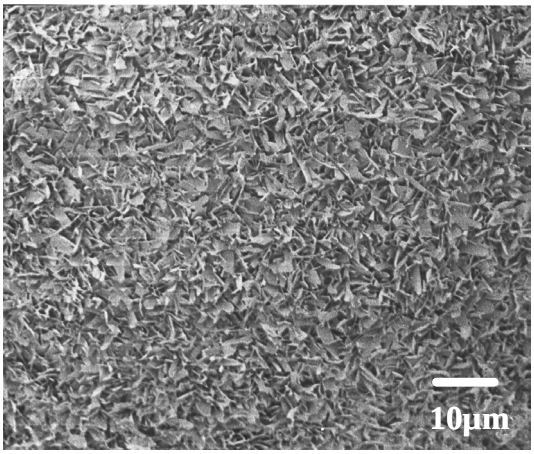

Figure 67: SEM images of lipid microparticles prepared by spray congealing for in vivo erosion study, 1000x, dense structure and high crystallinity were seen.

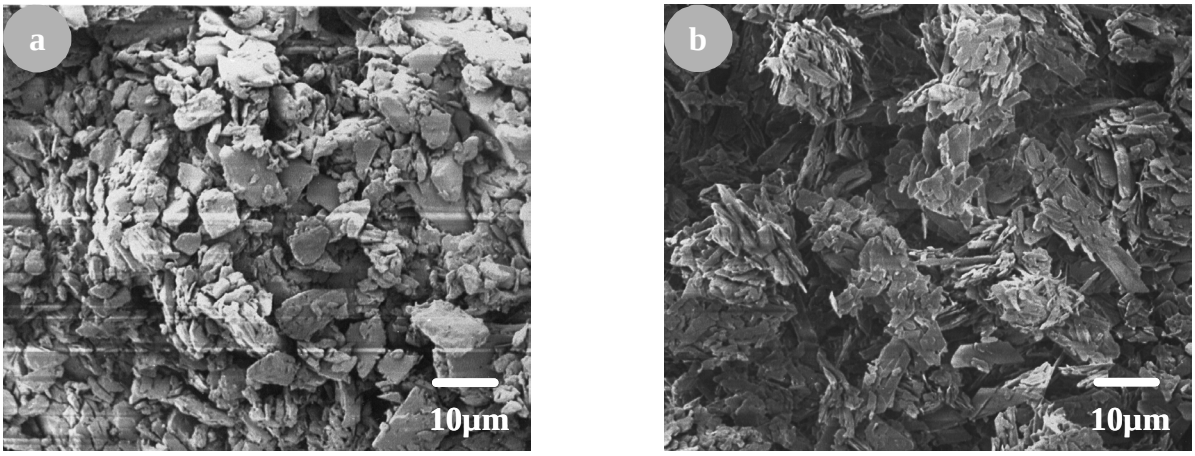

Figure 68: SEM images of lipid powders prepared by using variable sterilization methods for in vivo erosion study, both 1000x
a) heat sterilized triglyceride powder, arrangement of glyceroltripalmitate crystals revealed less dense compared to the microparticles
b) freeze-dried triglyceride powder, glyceroltripalmitate crystal formation was not loose-packed.

Secondly, the lipid microparticles were larger in size (Figure 62) compared to the two glyceroltripalmitate powder groups at the beginning of the study. To confirm the hypothesis of these in vivo investigations, which was the direct dependence of the in vivo erosion time of the triglyceride on its particle size, additional investigations that are long enough to allow for the complete erosion of the triglyceride powers will be necessary. However, first positive results were obtained from these investigations.

Summary

This in vivo study was carried out to investigate the hypothesis of a correlation between the triglyceride particle size and the in vivo erosion time of the material. Concomitantly, the influence of the degree of crystallinity on the in vivo erosion was examined. Therefore glyceroltripalmitate microparticles and two groups of glyceroltripalmitate powders with a high and low degree of crystallinity, respectively, were investigated in vivo. The results showed the degradation of both types of implanted triglyceride powders. No differences in the in vivo erosion were observed due to the varying degree of crystallinity of the triglyceride powders. Due to the non-spherical shape of the glyceroltripalmitate powder material, no quantitative results were obtained, but only qualitative conclusions were drawn. After 56 days, the glyceroltripalmitate powders disappeared.

Although the lipid microparticles were not completely eroded by the end of the 56 day study period, the decreasing diameter clearly indicated that degradation processes were occurring in vivo. These results gave the first positive hints towards the investigated hypothesis of a correlation between the particle size of the triglyceride and the in vivo erosion time.

Chapter 8

Programmable Implants
–
From Pulsatile to Controlled Release

Introduction

In recent years “intelligent” drug delivery systems, such as microchip devices, have been developed [183,184]. The advantage of such systems is their ability to release a plethora of individual doses of one or even several substances from a multitude of drug reservoirs. Due to the pulsatile release of individual doses, any desirable release profile can be ‘generated’ by repetitively releasing dose after dose. According to the literature, ‘pulsatile drug delivery’ denotes the release of drugs, peptides or proteins with high rates within a narrow time interval [185]. Such delivery systems are classified as single- or multiple-pulse systems. They are frequently based on polymeric materials that release a drug almost instantly [186-187]. Many different delivery systems have been developed, such as microchip based devices [183,189] as well as matrices with concentric layers of biodegradable polymer [190,191].

A disadvantage of these systems, however, is that too many pulses would be needed to create a release profile that stretches over extended periods of time, such as several weeks. To overcome this limitation, programmable implants consisting of a drug-loaded polyanhydride core embedded in a drug-free bulk eroding polymer mantle were developed [39]. This system enables a delayed onset of release adjustable by the choice of the mantle material followed by a pulsatile release. However, due to the fast eroding polyanhydride core it was not possible to release drug over an extended time period from these implants. Therefore, in this study we tested different lipophilic core materials with regard to their ability to control drug release [39,192]. In Figure 69 a a comparison of the intended release profiles of this new generation of programmable implants is shown.

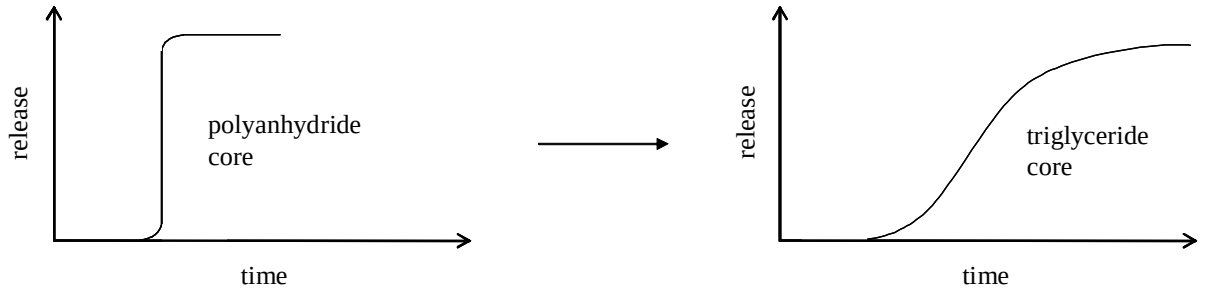

Figure 69: Comparison of release profiles resulting from programmable implants with polyanhydride and triglyceride cores, respectively.

This controlled prolonged release from the prepared systems may be of great benefit when highly potent substances, for example growth factors [193,194], cytokines [195,196] or anti-cancer drugs [197] have to be administered. Such drugs would rapidly exceed therapeutic concentrations during pulsatile release. Concomitantly, controlled prolonged release may be

desirable for an intracranial treatment, since, for example, neurodegenerative diseases or brain tumors frequently require long-term therapy [34,198,199].

The goal of this study was to design programmable implants with a reproducible onset of release and a controlled release once the liberation of the drug has started. Different core and mantle materials were tested for this purpose. Finally, a mathematical model based on convolution theory [159-162] was developed, which allows for the prediction of release profiles, when the release from the core material and the properties of the mantle material are known.

Results

In vitro release

First, the release of pyranine from the lipid core matrices without the polymer mantle was investigated (Figure 70). Cholesterol showed the fastest release within 1.5 hours, whereas glyceroltrilaurate (C12) and glyceroltristearate (C18) released the incorporated dye over a period of 14 days. The triglycerides with the longer fatty acid chains showed continuous release of the model compound over approximately 10 weeks for glyceroltripalmitate (C16) and 16 weeks for glyceroltrimyristate (C14).

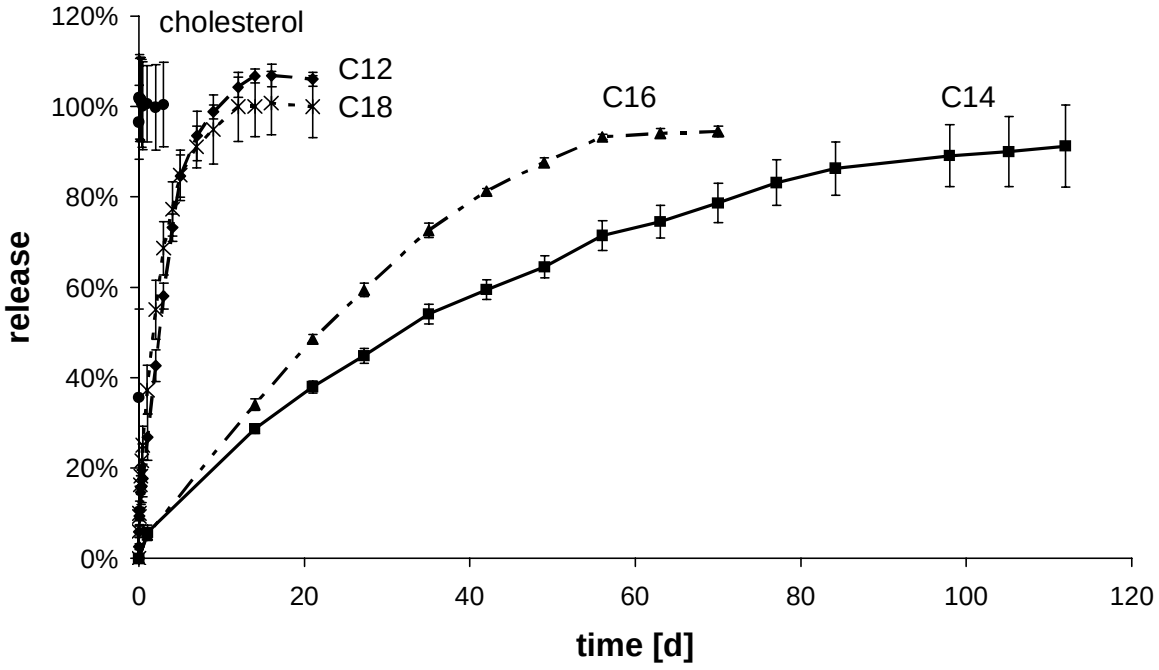

Figure 70: In vitro release profiles of pyranine as model drug from variable lipophilic core materials, for different triglycerides the number of C-atoms of the fatty acid chains is given, data show mean ± standard deviation (n=5).

The first steps to embed the cores into a bulk eroding polymer mantle made of $PLGA_{17}$ were carried out using the manufacturing procedure with the heat treatment at 110°C. Unfortunately, the resulting implants prematurely released their contents in an unpredictable manner, due to incomplete pore closure (data not shown). In addition to this irreproducible onset of release, DSC investigations showed that the heating step might additionally cause an alteration of the modification of the crystalline lipid core materials (data not shown).

A perfectly delayed release with a reproducible onset of all investigated core and mantle materials (Figures 71-73) was obtained by applying a second compression step to the finished implants at temperatures above the glass transition temperature of the respective mantle polymer (see Figure 6 in chapter 2, section 2.22).

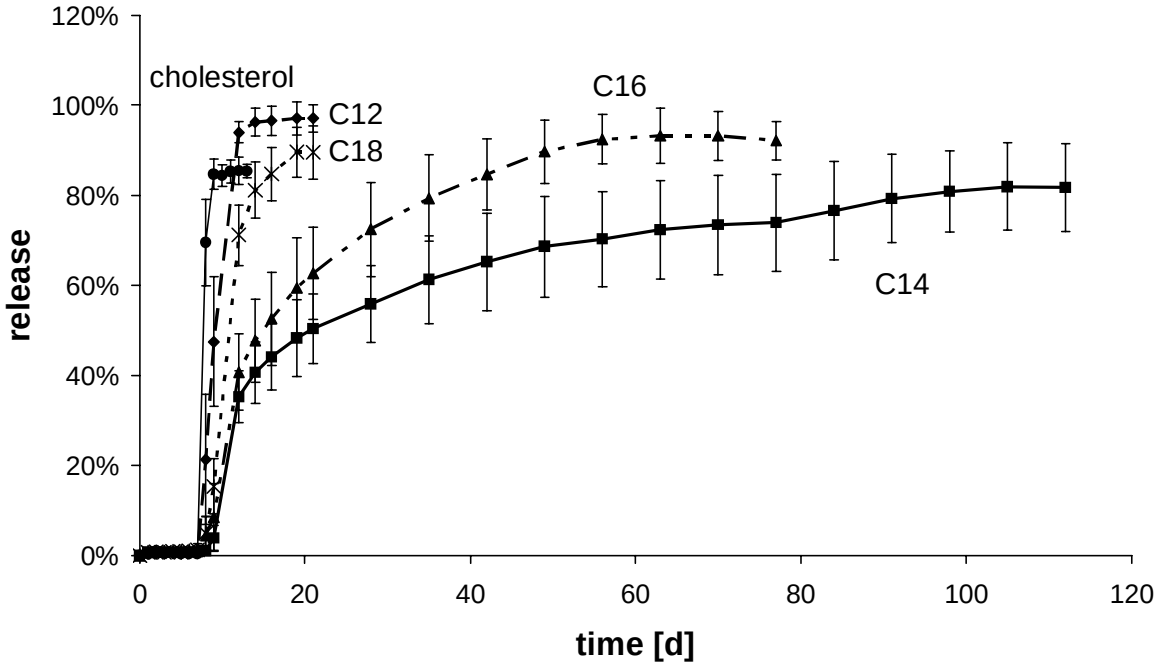

Figure 71: In vitro release from programmable implants with different core materials and $PLGA_{10}$ as polymeric mantle material, for different triglycerides the number of C-atoms of the fatty acid chains is given, values are expressed as mean ± standard deviation (n=4).

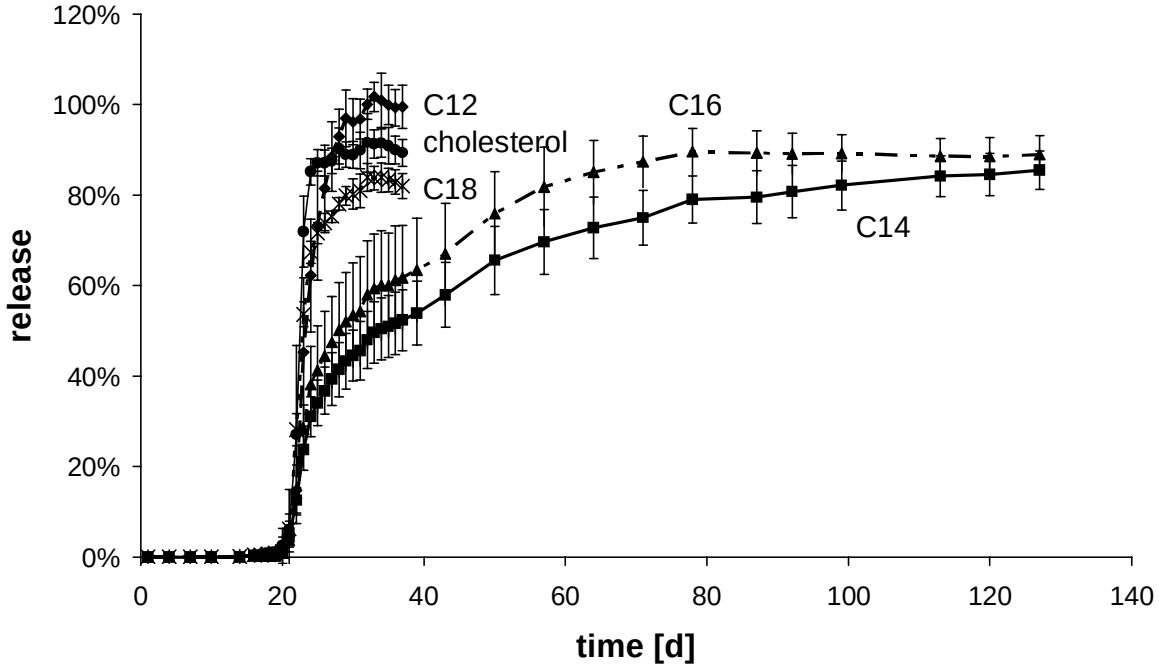

Figure 72: In vitro release from programmable implants with different core materials and $PLGA_{17}$ as polymeric mantle material, for different triglycerides the number of C-atoms of the fatty acid chains is given, values are expressed as mean ± standard deviation (n=4).

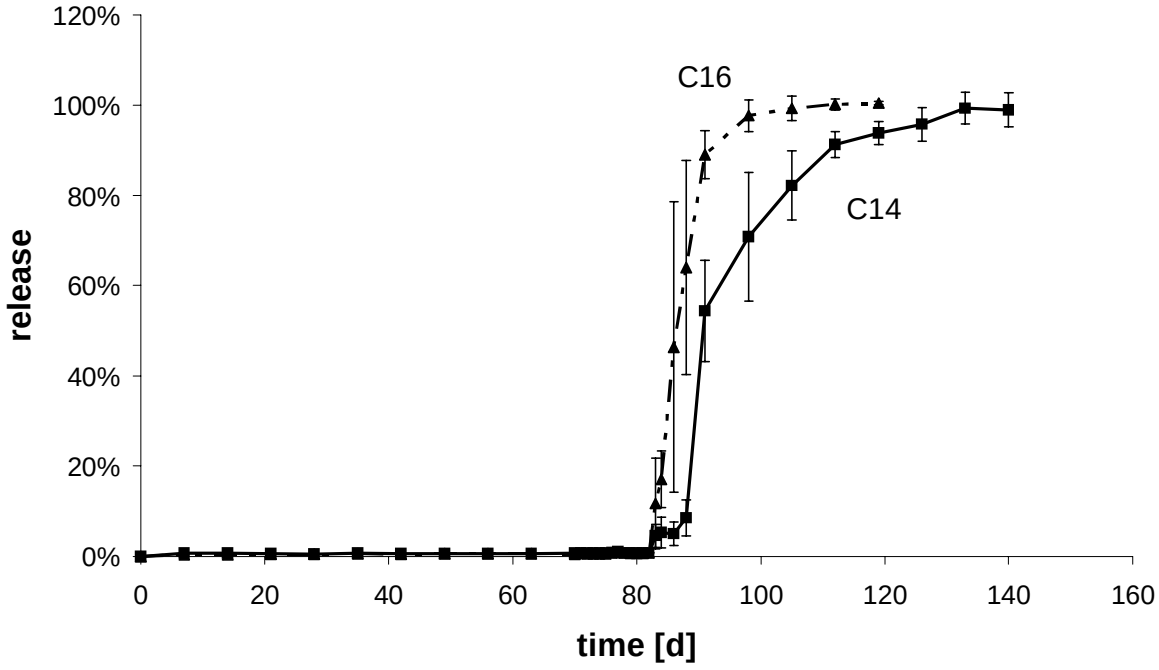

Figure 73: In vitro release from programmable implants with different core materials and PLA_{30} as polymeric mantle material, for different triglycerides the number of C-atoms of the fatty acid chains is given, values are expressed as mean ± standard deviation (n=3).

For all investigated groups, reproducible onset of the release after the degradation of the polymer mantle was achieved (Figures 74-76). Delay times were 8 days for $PLGA_{10}$ (Figure 74), 21 days for $PLGA_{17}$ (Figure 75) and 83 days when the PLA_{30} was used as mantle material (Figure 76) Concomitantly, the desired prolonged release from the programmable implants over periods from 2 weeks (glyceroltrilaurate (C12) and glyceroltristearate (C18)) up to several months (glyceroltrimyristate (C14) glyceroltripalmitate (C16)) was achieved.

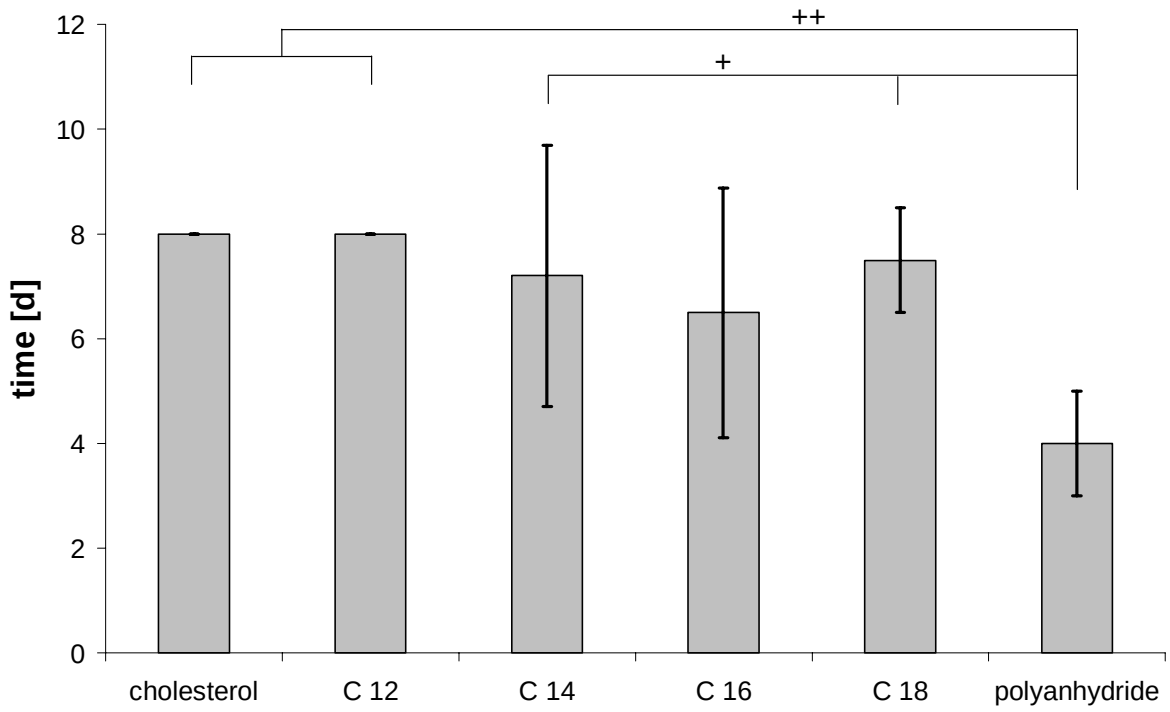

Figure 74: Delay times for the onset of release observed for programmable implants, prepared with varying core materials and with $PLGA_{10}$ as mantle material, data represent mean ± standard deviation, ++ indicates statistical significance with $p<0.01$, + indicates statistical significance with $p<0.05$ (n=4).

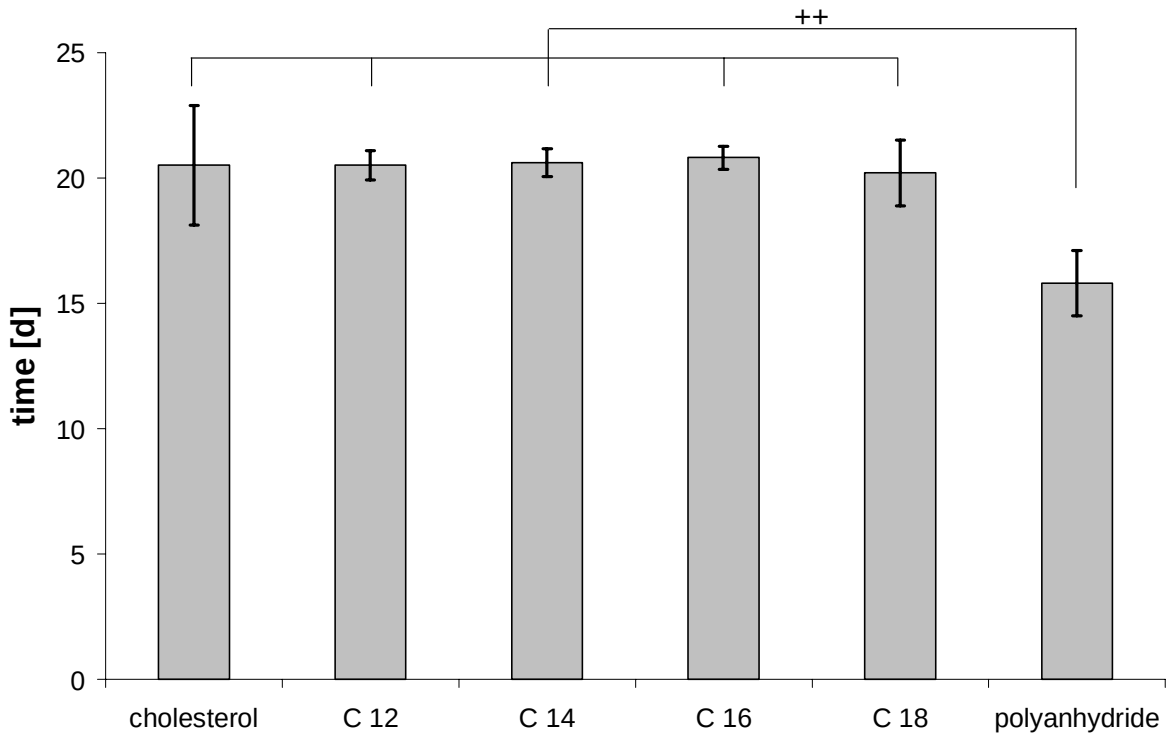

Figure 75: Delay times for the onset of release observed for programmable implants, prepared with varying core materials and $PLGA_{17}$ as mantle material, data represent mean ± standard deviation, ++ indicates statistical significance with $p<0.01$, + indicates statistical significance with $p<0.05$ (n=4).

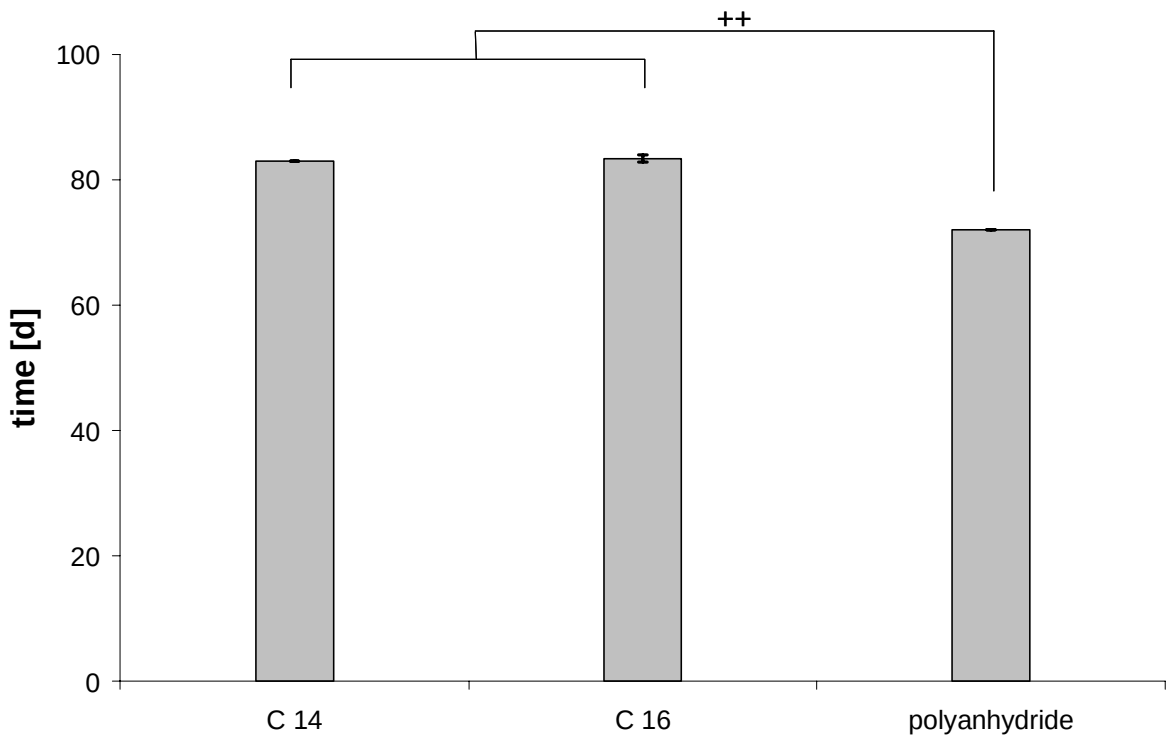

Figure 76: Delay times for the onset of release observed for programmable implants, prepared with varying core materials and with PLA_{30} as mantle material, data represent mean ± standard deviation, ++ indicates statistical significance with $p<0.01$, + indicates statistical significance with $p<0.05$ (n=3).

Mathematical modeling

For the design of programmable implants, it would be desirable to be able to predict the resulting release profile when a core with known release properties is embedded into a polymer mantle. Thus, a convolution model was applied to investigate whether a sensible prediction is possible. For the above-described mathematical modeling, the release of pyranine from a cholesterol core matrix was used as unit impulse function for the matrix materials $PLGA_{10}$ and $PLGA_{17}$. For the investigations carried out with PLA_{30} as polymeric mantle material, release data from polyanhydride cores gathered by Vogelhuber et al. [39] were used as the unit impulse function. Both core materials showed complete release of the incorporated pyranine within one day and can thus be used as unit impulse functions. The release profiles are shown in Figure 77.

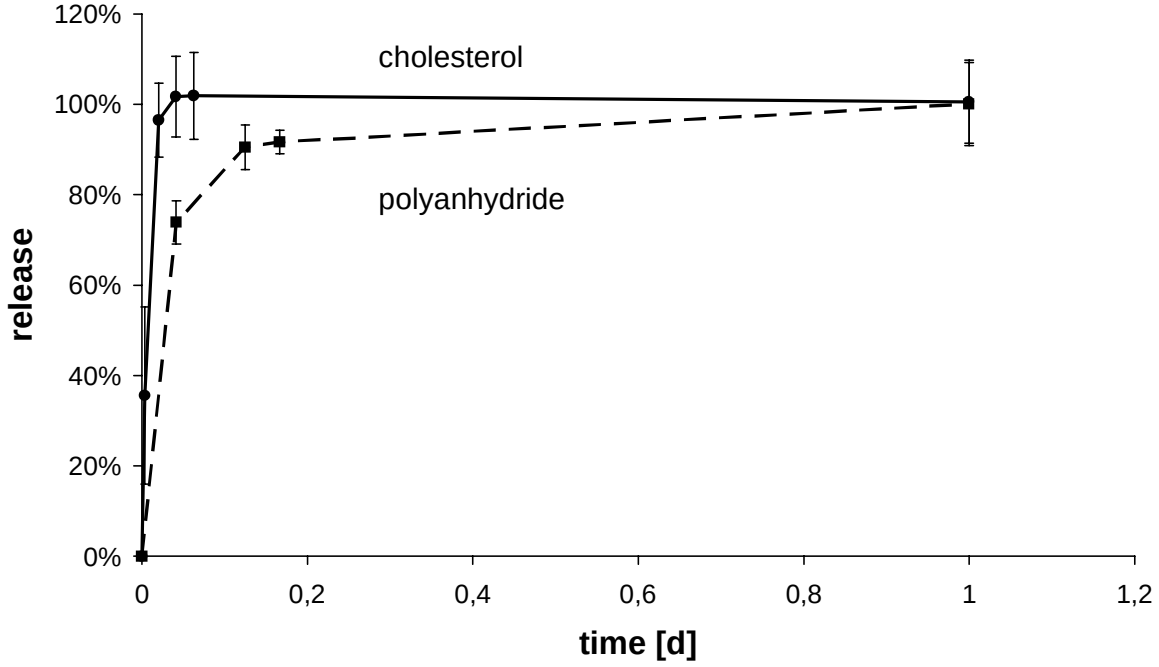

Figure 77: Used unit impulse functions for mathematical modeling, values are expressed as mean ± SD (n=5); Release from cholesterol cores was used for $PLGA_{10}$ and $PLGA_{17}$; Release from polyanhydride cores [39] was used for PLA_{30}.

In Figures 78-87 results of predicted release curves are compared with the experimental release data. When glyceroltrilaurate (C12) core matrices were embedded into a $PLGA_{10}$ mantle (Figure 78), a slightly slower release was determined experimentally, compared to the theoretical profiles. For glyceroltristearate (C18) cores embedded into this polymeric mantle

material, the same effect was observed (Figure 79). Again in vitro release occurred slightly slower than predicted by the convolution model.

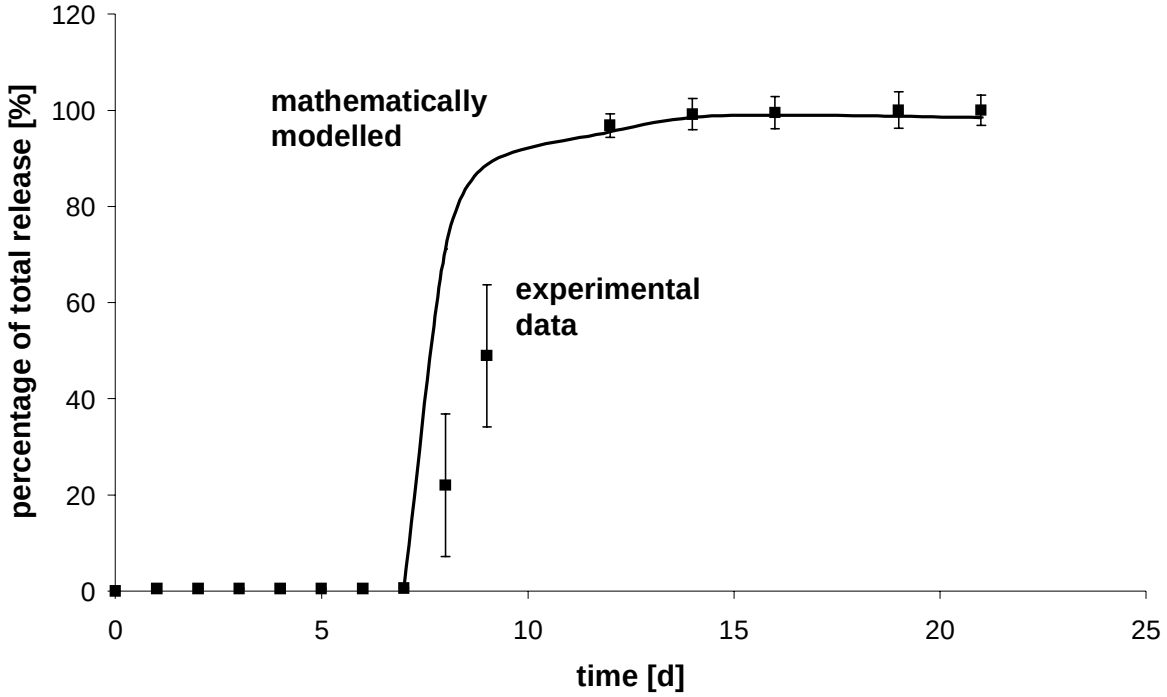

Figure 78: Release profiles from programmable implants, prepared with $PLGA_{10}$ as mantle material and glyceroltrilaurate (C12) as core material;
(■): values of experimental release data are expressed as mean ± SD (n=5),
(–): theoretical release calculated with mathematical model of convolution theory by the use of release data from cholesterol cores as unit impulse function.

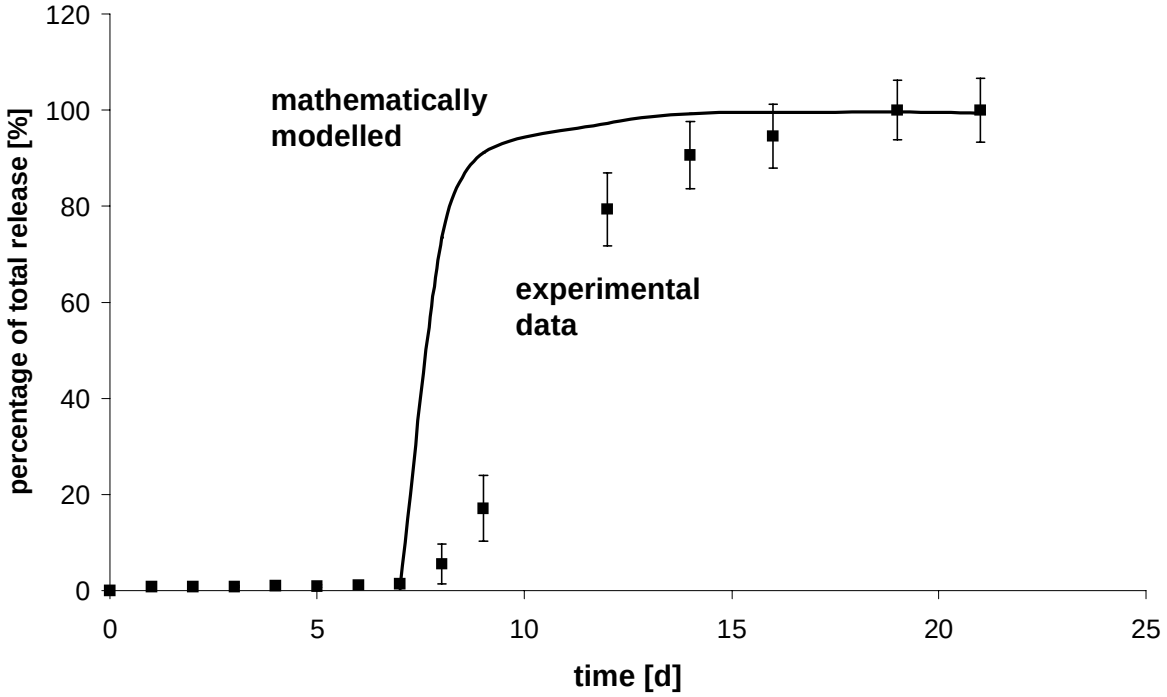

Figure 79: Release profiles from programmable implants, prepared with $PLGA_{10}$ as mantle material and glyceroltristearate (C18) as core material; ,
(■): values of experimental release data are expressed as mean ± SD (n=4),
(–): theoretical release calculated with mathematical model of convolution theory by the use of release data from cholesterol cores as unit impulse function.

Differences between theoretical and experimental release profiles were also observed for the programmable implants prepared with glyceroltrimyristate (C14) as core material and $PLGA_{10}$ as polymer mantle (Figure 80 In this case, programmable implants released the model drug faster than predicted by the model. Deviations between the profiles were higher in the first period of release, but disappeared afterwards. Only minimal differences were observed between theoretically predicted and experimentally determined release profiles after 6-7 weeks and, as could have been expected for the end of the release experiment, good agreement was seen from day 70 to day 112. Figure 81 shows similar results for glyceroltripalmitate (C16) cores. The again visible but less distinctive differences between predicted and in vitro determined release profiles of pyranine from the programmable implants were only visible within the first period of release, but not from day 35 to day 77, which was here the last time point of the experiment.

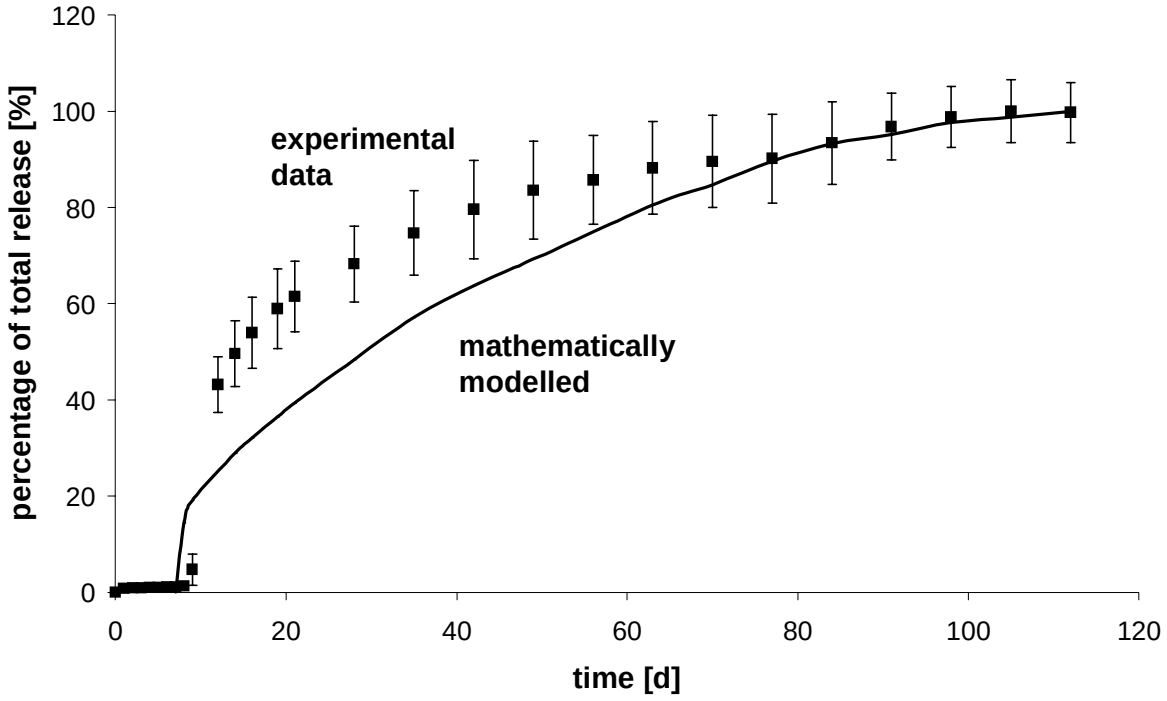

Figure 80: Release profiles from programmable implants, prepared with $PLGA_{10}$ as mantle material and glyceroltrimyristate (C14) as core material;
(■): values of experimental release data are expressed as mean ± SD (n=5),
(–): theoretical release calculated with mathematical model of convolution theory by the use of release data from cholesterol cores as unit impulse function.

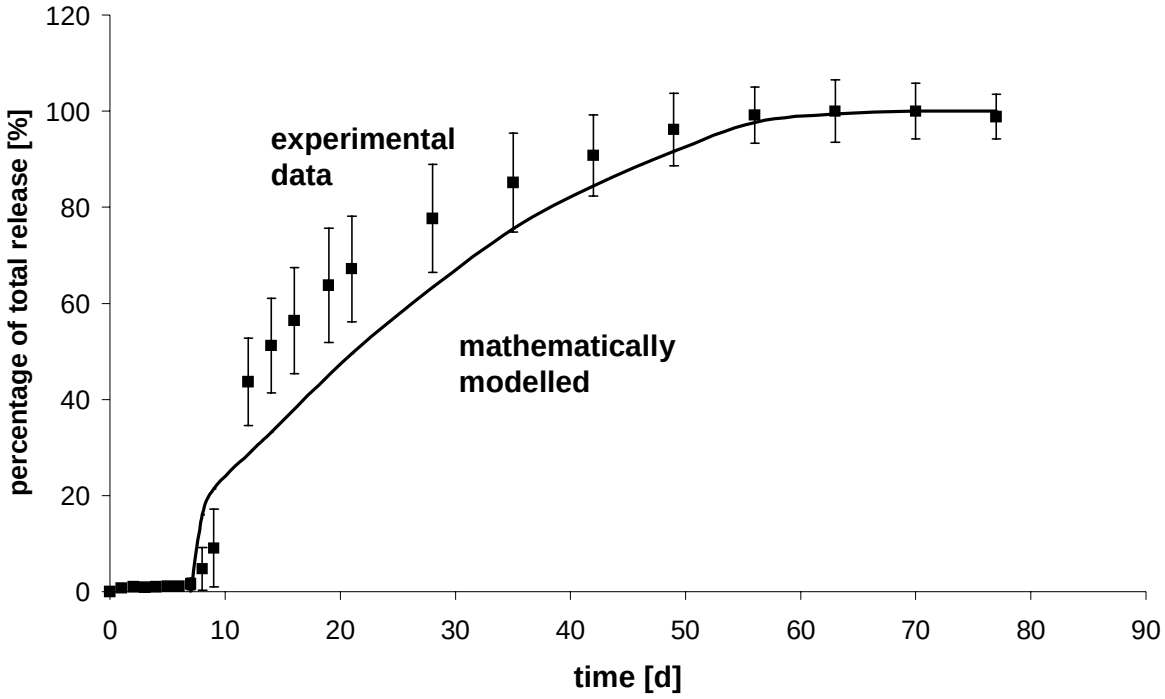

Figure 81: Release profiles from programmable implants, prepared with $PLGA_{10}$ as mantle material and glyceroltripalmitate (C16) as core material;
(■): values of experimental release data are expressed as mean ± SD (n=4),
(–): theoretical release calculated with mathematical model of convolution theory by the use of release data from cholesterol cores as unit impulse function.

Concerning the results observed for programmable implants made with $PLGA_{17}$ as a polymeric mantle material, comparable findings were obtained for the two faster releasing core materials glyceroltrilaurate (C12) and glyceroltristearate (C18) as seen for $PLGA_{10}$. In these groups again the mathematically predicted release was slightly faster than experimentally determined (Figures 82,83). For the slower releasing core materials, glyceroltrimyristate (C14) and glyceroltrilaurate (C12), very good correlations between the theoretically predicted release curves and the experimental data were achieved (Figures 84,85), when these matrix materials were embedded into a mantle of $PLGA_{17}$.

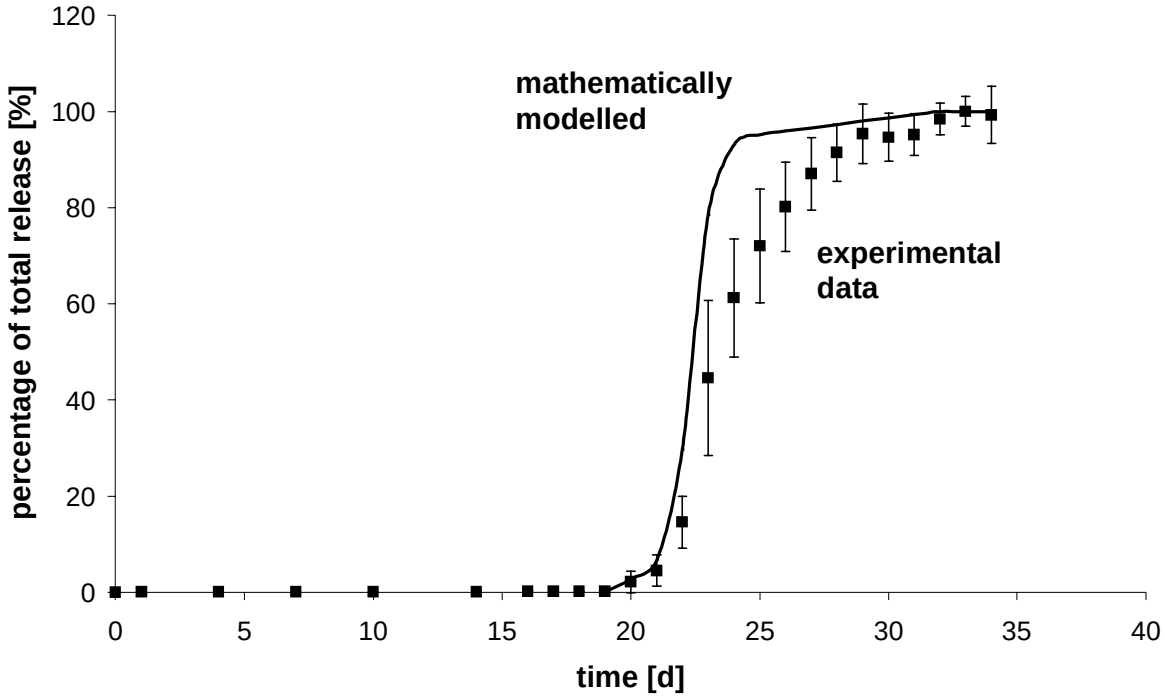

Figure 82: Release profiles from programmable implants, prepared with $PLGA_{17}$ as mantle material and glyceroltrilaurate (C12) as core material;
(■): values of experimental release data are expressed as mean ± SD (n=4),
(–): theoretical release calculated with mathematical model of convolution theory by the use of release data from cholesterol cores as unit impulse function.

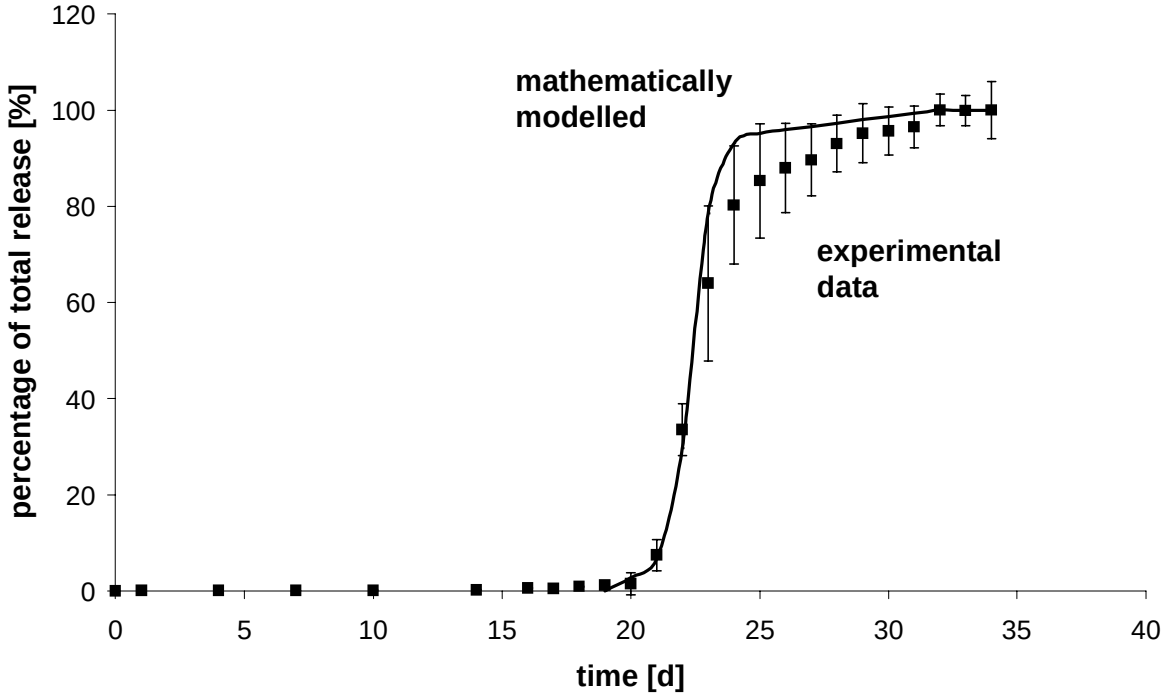

Figure 83: Release profiles from programmable implants, prepared with $PLGA_{17}$ as mantle material and glyceroltristearate (C18) as core material;
(■): values of experimental release data are expressed as mean ± SD (n=4),
(–): theoretical release calculated with mathematical model of convolution theory by the use of release data from cholesterol cores as unit impulse function.

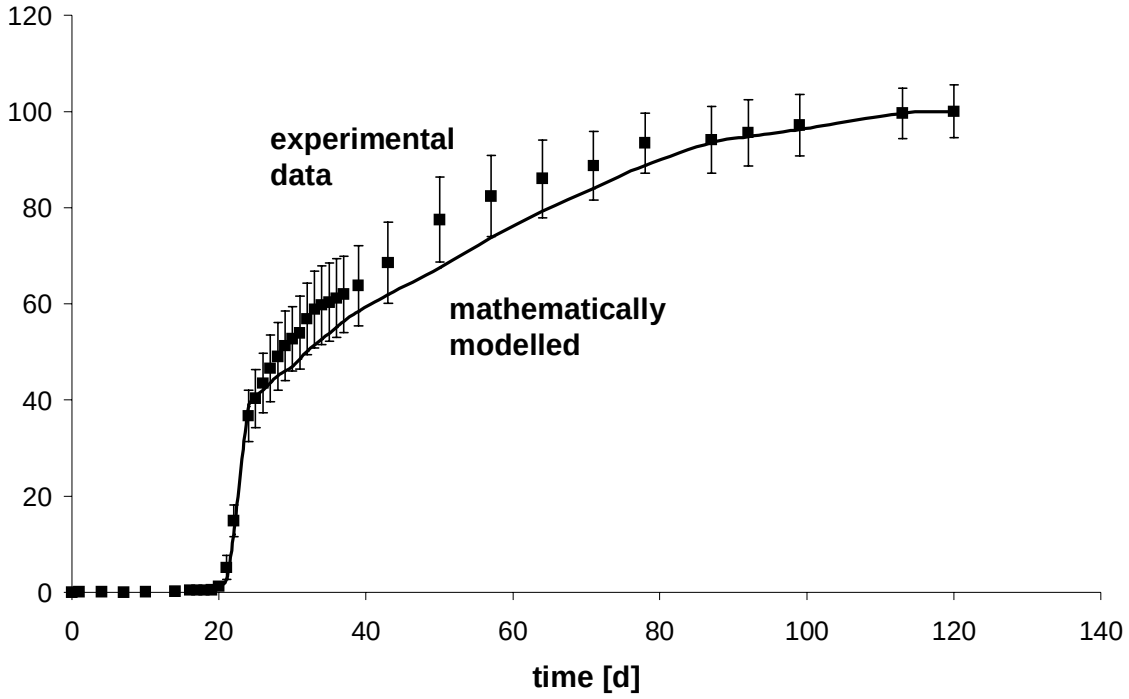

Figure 84: Release profiles from programmable implants, prepared with $PLGA_{17}$ as mantle material and glyceroltrimyristate (C14) as core material;
(■): values of experimental release data are expressed as mean ± SD (n=5),
(–): theoretical release calculated with mathematical model of convolution theory by the use of release data from cholesterol cores as unit impulse function.

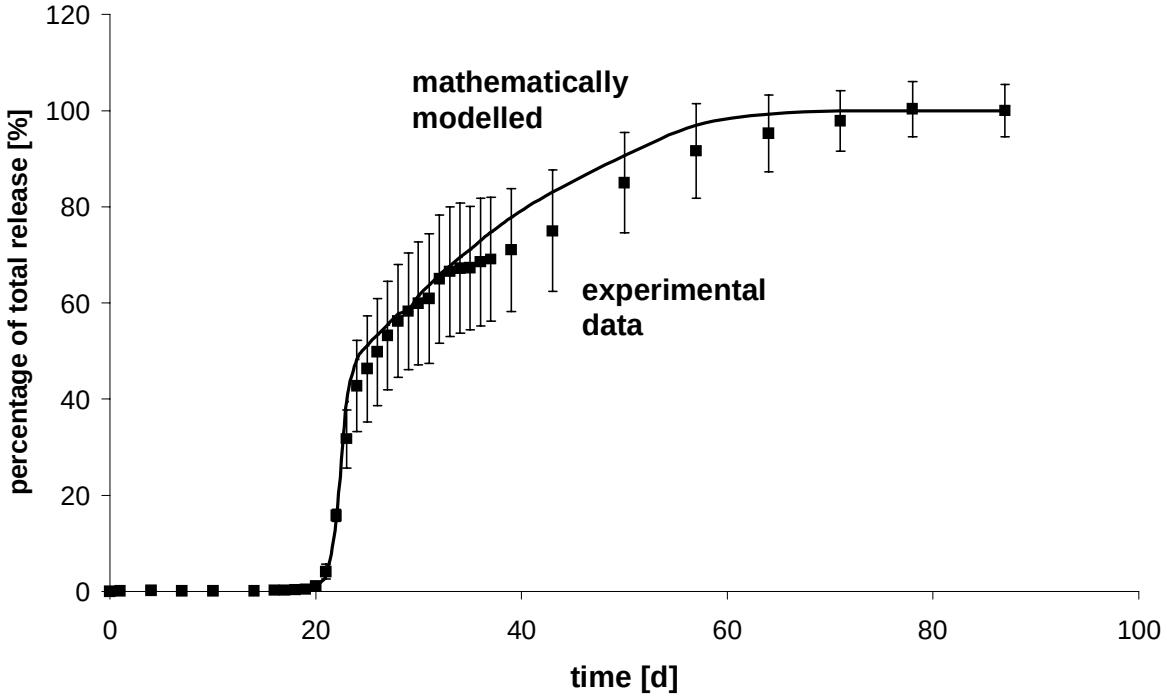

Figure 85: Release profiles from programmable implants, prepared with $PLGA_{17}$ as mantle material and glyceroltripalmitate (C16) as core material;
(■): values of experimental release data are expressed as mean ± SD (n=5),
(–): theoretical release calculated with mathematical model of convolution theory by the use of release data from cholesterol cores as unit impulse function.

When the slowest eroding mantle material (PLA_{30}) was used for the embedding of glyceroltrimyristate (C14) and glyceroltripalmitate (C16), again a faster theoretically predicted release was observed compared to the in vitro findings (Figures 86,87).

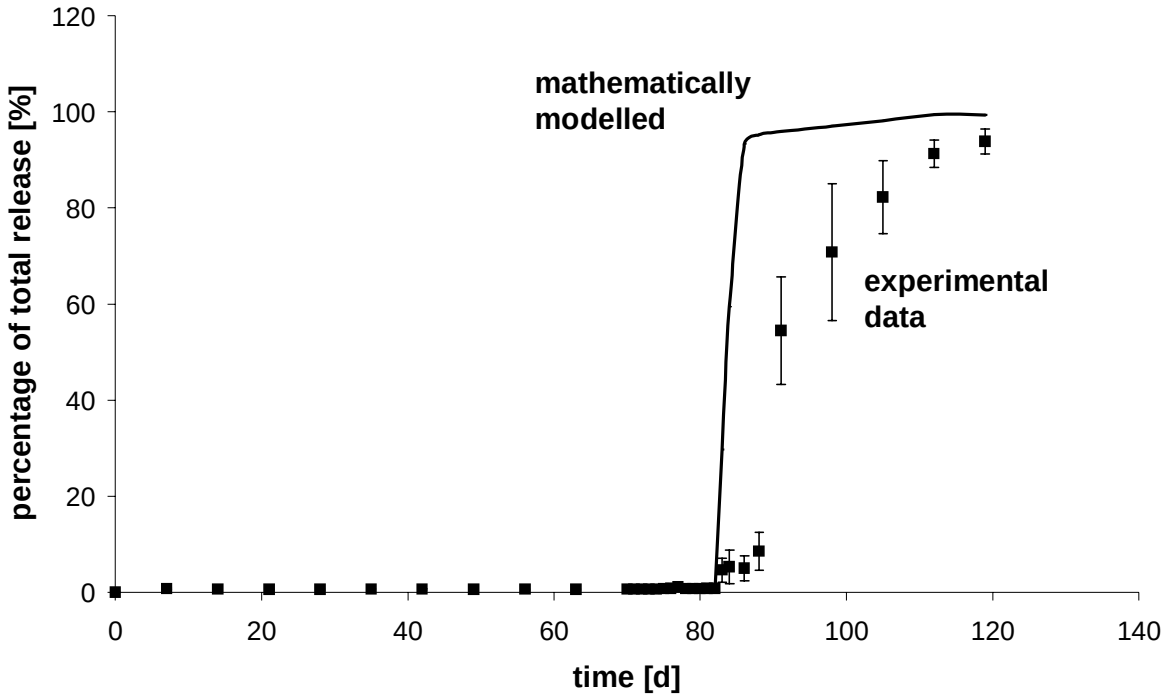

Figure 86: Release profiles from programmable implants, prepared with PLA_{30} as mantle material and glyceroltrimyristate (C14) as core material;
(■): values of experimental release data are expressed as mean ± SD (n=3),
(–): theoretical release calculated with mathematical model of convolution theory by the use of release data from polyanhydride cores as unit impulse function.

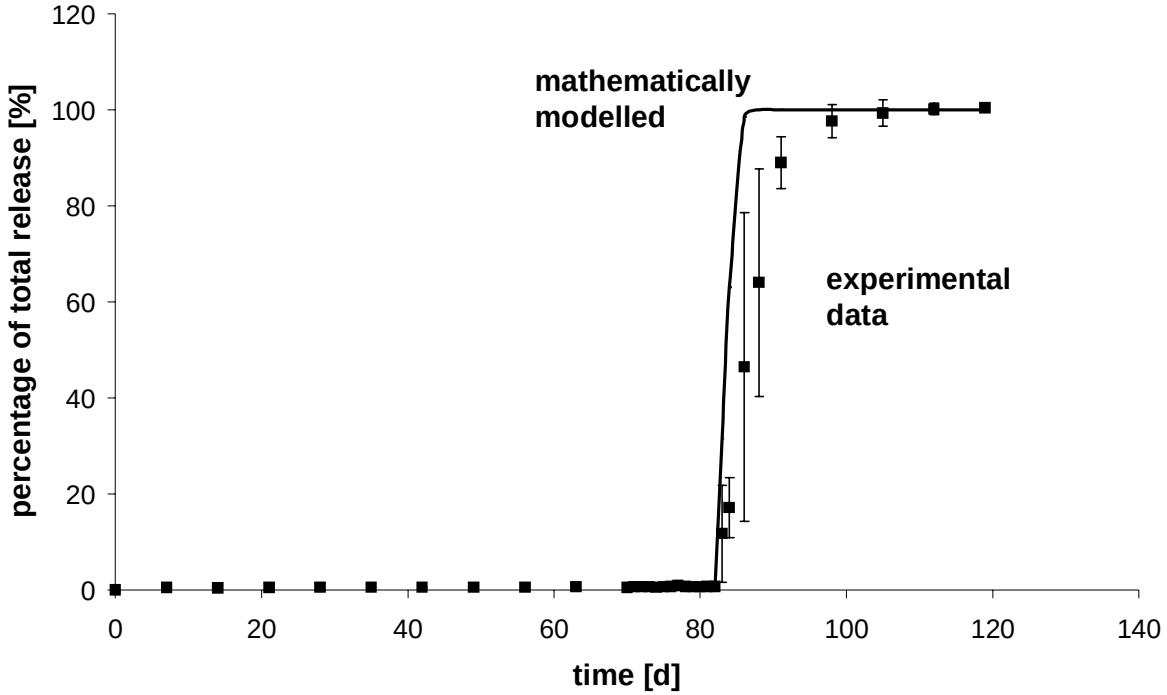

Figure 87: Release profiles from programmable implants, prepared with PLA_{30} as mantle material and glyceroltripalmitate (C16) as core material;
(■): values of experimental release data are expressed as mean ± SD (n=3),
(–): theoretical release calculated with mathematical model of convolution theory by the use of release data from polyanhydride cores as unit impulse function.

Discussion

In vitro release

All three of the mantle materials tested produced programmable implants with a reproducible onset of release. This confirms the suitability of the preparation method with a second compression step at a temperature above the T_g of the respective mantle material to completely close pores, which occur within the polymer mantle. Additionally, the goal of the controlled release after the onset was achieved. Programmable implants containing glyceroltrilaurate (C12) or glyceroltristearate (C18) released the model drug over two weeks, whereas programmable implants prepared with glyceroltrimyristate (C14) or glyceroltripalmitate (C16) as matrix materials showed release periods extending over months (Figures 71-73). This is identical to the results for non-embedded core matrices (Figure 70).

Vogelhuber et al. reported shorter delay times before the start of release for the three polymer materials (see bars of polyanhydride cores in Figures 74-76), which is due to the

different core materials used [39]. The degradation of a polyanhydride core, as it was used previously [39] most likely led to an acidic microclimate, which worked as a catalyst and thus accelerated the degradation of the mantle polymer. This effect did not occur when lipid core materials were used and thus the delay time for the onset of the programmable implants increased significantly in most cases. Only for the group of glyceroltripalmitate cores embedded into $PLGA_{10}$ as mantle material, significance was not reached due to relatively high standard deviations.

Mathematical modeling

Matrices made by embedding glyceroltrilaurate (C12) and glyceroltristearate (C18) in $PLGA_{10}$ displayed slower release profiles experimentally than was predicted using the mathematical modeling (Figures 78,79). This can be explained by the percentage of dye released in the experiment from glyceroltrilaurate and glyceroltristearate core matrices into the polymer mantle during the delay time of the programmable implants and the fact that the onset day of release from programmable implants was chosen as starting point for the mathematical modeling, due to the above mentioned reasons. Regarding the algorithm depicted in equation (11), the consequence for the theoretical prediction can be briefly described as follows: The calculated amount of dye released from the core matrix until the onset ($=I_0$ in equation (11)) is treated in the mathematical model as if it was released in the experiment at day 1 ($=I_0$ of the unit impulse function). Thus, for example when a core matrix would show complete release of the model drug within 7 days or less experimentally, the predicted release profile for the programmable implants would always be exactly the same as it was obtained for the unit impulse function. But since release from the glyceroltrilaurate (C12) and glyceroltristearate (C18) core matrices in fact occurred over a longer period of time (Figure 70), less diffusion of the model drug within the polymer mantle occurred during the delay time and thus explaining the slower in vitro release from the programmable implants compared to the theoretical prediction.

Release of the core matrices had reached approximately 87% at day 7 in the case of glyceroltrilaurate (C12) and glyceroltristearate (C18) core matrices released 91% of the dye within the first 7 days (Figure 70), which was the delay time for $PLGA_{10}$. Thus, differences between the two release profiles were slightly higher in case of the C18 triglyceride compared to glyceroltrilaurate (C12).

But despite the alignment of the calculation method, the modeling resulted in a rather acceptable agreement between predicted and experimentally observed release curves.

The deviations in the first release period when glyceroltrimyristate (C14) was used as core material and $PLGA_{10}$ served as polymer mantle (Figure 80), may be explained by the relatively unsteady onset of release in this group, which was observed by slightly higher standard deviations, compared to the other investigated groups (Figures 74-76). Since a slightly unsteady onset of release was also observed for glyceroltripalmitate cores (Figure 74), the deviations in the early period after the onset (Figure 81) may be explained. Considering these results, a rather acceptable agreement between theory and experiment was observed for $PLGA_{10}$ as mantle material.

Programmable implants made with $PLGA_{17}$ as polymeric mantle material and the two faster releasing core materials, glyceroltrilaurate and glyceroltristearate, lead to slower release of the implants than predicted (Figures 82,83), due to the above described reasons. Nevertheless, when glyceroltrilaurate was used as core material, an acceptable prediction was obtained by convolution and in the glyceroltristearate group two release profiles even showed rather good agreement. Concerning the slower releasing core materials glyceroltrimyristate and glyceroltrilaurate, measured release profiles fitted nearly perfectly into the mathematically modeled prediction of release.

Concerning PLA_{30}, release of pyranine from glyceroltrimyristate cores was approximately 85% at day 83 (Figure 70), which was the onset of the release from programmable implants with this mantle material. Glyceroltripalmitate cores show a complete release of 100% of the dye within an even shorter time period of 70 days (Figure 70). However, the observed deviations between predicted and determined release profiles, which can be explained as aforementioned, were only minute and convolution again resulted in acceptable agreement between theory and experiment.

These results showed that it is possible to make sensible predictions for the release from programmable implants with one of the three investigated polymeric mantle materials when release from the core material is known. Concomitantly, convolution results calculated for PLA_{30} were obtained by using data from a polyanhydride core as unit impulse function. These release data for the pulsatile releasing core material were detailed by Vogelhuber 4 years ago [39], but, nevertheless, a rather good fitting of the theoretical release curves and the

experimental profiles obtained for investigations on triglycerides was observed. This additionally demonstrated the suitability of convolution for the modeling of theoretical release profiles from programmable implants. The prediction of the expected release profile is of great benefit for the design of programmable implants with desired release properties. When release from a core matrix is known, convolution alleviates the need for further in vitro release experiments with programmable implants, due to the possibility to sensibly predict the expected resulting release profile.

Summary

The investigated programmable implants can be described briefly as a drug loaded core matrix embedded into a drug free bulk eroding polymer mantle, which inhibits drug release until its erosion is completed. The aim of this study was to develop a new generation of programmable implants, which allow for prolonged release, since the devices developed by Vogelhuber et al. [39] were limited to pulsatile liberation of incorporated compounds. The goal of controlled release after the onset was realized by using triglycerides as core materials and release periods from 2 weeks up to several months were achieved. The delay time for the release from the programmable implants was varied with the polymeric mantle material from 8 to 83 days. Concomitantly, it was shown that applying a model based on convolution leads to a sensible prediction of the release of a drug from the programmable implants when release rate from the core material is known. This facilitates the design of programmable implants and offers a powerful tool for the adjustment of the resulting drug release to desired profiles.

Chapter 9

Summary and Conclusions

1. Summary

Implants are one of the most important class of devices for the controlled parenteral release of drugs. Therefore, many materials have been investigated for potential use as a matrix material for implantable devices (**chapter 1**). Investigation of crucial parameters during the manufacturing procedures of such an implant as well as the identification of mechanisms that dominate the release of drugs from the chosen material are essential for the design of a controlled release device. Additionally, the in vivo compatibility and erosion behavior of a material play a pivotal role in the suitability of a material for parenteral application. This work focused on lipid materials, primarily triglycerides, for the design of parenterally applicable controlled release implants.

Since triglycerides and other lipid materials are currently being investigated as alternatives to polymeric materials for the delivery of proteins and peptides [118,153,154], the first study served to investigate if release profiles of the two model drugs insulin and somatostatin from triglyceride matrices can be determined directly from the release medium. Therefore, their stability within the release medium, which is essential for a determination of correct controlled release profiles, was investigated (**chapter 3**). Both model drugs underwent distinct degradation when incubated in release medium over 5 weeks and the extent of degradation was quantified to 35% for insulin and even 65% for somatostatin. The resulting degradation products were identified as a deamidation product of somatostatin and the non-covalent dimer of insulin. With these experiments, the necessity of extraction of both model drugs from glyceroltripalmitate matrices for the characterization of long-term in vitro release was shown. Thereby, not only could the residue content be determined, but also the investigation of protein and peptide stability within the matrices was facilitated (**chapter 3**). For the use in further investigations [153,154], a liquid/liquid extraction method developed by Lucke et al. (see section 2.5 in chapter 3 and [141]) was optimized. Concomitantly, a solid/liquid extraction method was newly developed to avoid liquid phase separation and thus protect proteins and peptides from degradation during the extraction process [141]. This will be useful for stability studies of protein and peptide model drugs within the triglyceride matrix material. Extraction yields of 94.5% +/-0.8% and 91.3% +/-5.1% were realized for somatostatin and insulin, respectively, using the newly developed method.

After these experiments on protein and peptide model drugs, the triglyceride material and its cylindrical matrices were characterized to facilitate the design of the desired controlled release device for parenteral drug delivery. Since the following in vitro investigations on the

basic characteristics of triglyceride matrices were mechanistic studies, it was decided that the use of proteins and peptides would have some disadvantages, such as the necessity of re-extraction, lower sensitivity of analytical methods, or possibly occurring degradation processes. Thus, in the following experiments fluorescent dyes were used as model drugs.

The first objective towards the characterization of triglycerides for the design of controlled release matrices was the identification of crucial parameters during the manufacturing procedure and to investigate the extension of their influence on the resulting release profiles (**chapter 4**). To this end, glyceroltripalmitate was loaded with pyranine, a highly water soluble fluorescent dye. Subsequently, cylindrical matrices were manufactured under varying conditions. The investigated parameters for the preparation of the implants were the drug distribution within the matrices, dye loading, compression force and geometry of the cylindrical implants (**chapter 4**). Improving the distribution of the dye within the cylindrical implants led to an increase of the controlled release time period. Varying the pyranine content within the matrix revealed drug loading as one of the most important parameters concerning the expected release profiles. Release properties varied from nearly burst (33% drug loading) to controlled release over 17 weeks (10% drug loading) to a very slow release of only about 13% of the total loaded drug over the investigated time period of 17 weeks (1% drug loading). Compression force was shown as well to have severe influence on release profiles when varied at lower values, but was less decisive when higher forces were applied. This indicated the existence of a threshold for this parameter, which was reached when compressing the implants at 250N. Two parameters were investigated for cylinder geometry. Varying the implant height resulted in no significant influence on release profiles, whereas a decrease in implant diameter accelerated the liberation of the dye. This allows for the adjustment of the dose desired for application without alteration of the release profile.

After the preparation procedure of the triglyceride matrices was characterized, concomitant investigations on release mechanisms and properties of model drugs influencing the release were carried out (**chapter 4**). Three crucial parameters were identified: (i) An acceleration of the release from the matrices was observed when hydrophilicity of the model drug was increased. (ii) Water uptake into the matrices was proved by fluorescence microscopy after incubation of blank triglyceride cylindrical matrices in a solution of fluorescein-di-sodium salt. This indicated clearly the formation of pores and the possibility of diffusion of the incorporated drugs to the surface, where release occurs subsequently. Pore formation directly depended on the particle size of the glyceroltripalmitate used for the preparation of the lipid matrices. (iii) In an in vitro release experiment of fluorescein-di-sodium salt from

glyceroltripalmitate matrices, carried out with release media of increased osmotic pressure, osmosis was shown as well to be involved in the release process of drugs from triglyceride matrices. This indicated that liberation of a drug from glyceroltripalmitate matrices was not purely diffusion-controlled.

Since the in vitro properties of triglyceride matrices were well characterized at this point, the in vivo properties of the material were investigated subsequently. Two studies on the in vivo biocompatibility of glyceroltripalmitate and cholesterol were carried out (**chapter 5**). Concomitantly, the long term in vivo stability, which is a prerequisite for controlled prolonged release, was investigated. In these two experiments both in vivo biocompatibility as well as long term in vivo stability of gloceroltripalmitate and cholesterol was shown. Neither significant inflammatory response nor cytotoxic reactions were observed for any of the two materials. The triglyceride implants were stable and maintained their cylindrical shape over two months. Furthermore, the ability to influence the in vivo erosion of glyceroltripalmitate by the incorporation of the phospholipid DSPC was shown in these in vivo experiments (**chapter 5**).

Due to the in vivo stability of the triglyceride, the erosion behavior of the material was subsequently investigated. Firstly, in vitro experiments on the suitability of several excipients as modifying components for the triglyceride erosion were carried out (**chapter 6**). The strategy taken can briefly be described as a decrease in matrix stability, which would lead to the disintegration of the lipid matrix when it is exposed to mechanical stress, as it occurs in vivo after subcutaneous implantation. In these experiments, the phospholipids DMPC and DPPC, the hydrogel-forming agent agarose, and varying crystal sizes of the hydrophilic porogen sucrose were investigated for their ability to maintain the controlled release properties of glyceroltripalmitate when incorporated in considerable amounts into the triglyceride matrices. For the incorporation of the modifying components, two methods were tested. The emulsion method, previously described [37] for drug loading, could not be applied for the incorporation of any erosion modifier, due to the resulting very fast release of the model drug pyranine from the glyceroltripalmitate matrices within a few hours. Consequently, a two-step method was developed for this purpose (**chapter 6**) with which the suitability of sucrose, agarose and DPPC as erosion modifiers for glyceroltripalmitate matrices was proven in vitro (**chapter 6**). When agarose or DPPC were incorporated in ratios of 5-15% and 5-50%, respectively, release periods from 2 to 7 weeks were achieved. Release from triglyceride matrices containing sucrose depended on both the amount of sucrose incorporated into the matrix and the particle size of the excipient used. Controlled release was realized for all

crystal sizes and release periods of 2 to 15 weeks were achieved; only a ratio of 50% of the smallest sucrose particles led to a fast release within three days.

With regards to these promising in vitro results, the hypothesis for the in vivo use of erosion modifiers for triglyceride matrices, which is the correlation between the in vivo erosion velocity and the particle size of the triglyceride, was subsequently investigated (**chapter 7**). The glyceroltripalmitate microparticles used did not degrade completely within the duration of 8 weeks of the in vivo experiment, but a tendency of decreasing particle size was observed. Since the two glyceroltripalmitate powder groups, which were smaller than the microparticles, were completely degraded within 42 days, this hypothesis could be demonstrated in at least one example. Additionally, the influence of the degree of crystallinity of the triglyceride powder on its in vivo erosion was investigated in this study and shown to have a negligible effect.

In further experiments, the application of triglyceride matrices within programmable implants to achieve controlled prolonged release was investigated (**chapter 8**). These devices were developed by Vogelhuber et al. [39] and comprise a drug-loaded core embedded into a mantle consisting of a bulk eroding polymer, which inhibits release from the system until it starts to erode. Afterwards, the drug is released in a pulsatile manner from the devices described by Vogelhuber et al. [39], due to the polyanhydride, which is used as the core material. With the intent of prolonging the release, glyceroltrilaurate (C12), glyceroltrimyristate (C14), glyceroltripalmitate (C16), glyceroltristearate (C18) and cholesterol were investigated as core materials. The use of the triglycerides as matrix materials for the preparation of the drug-loaded core led to controlled release over several months from the newly developed programmable implants. Cholesterol cores resulted in a pulsatile release. In these experiments, the manufacturing procedure was adapted to and optimized for the triglycerides. By varying the polymeric mantle material, the onset of release was varied from 8 to 83 days. Finally, mathematical modeling using convolution was proven to yield sensible results for the prediction of release profiles from programmable implants when release of the respective drug from the core material itself is known (**chapter 8**). This facilitates the design of programmable implants with any desired release profile.

2. Conclusions

In conclusion, important steps towards the design and understanding of triglyceride matrices as controlled release devices were taken and safety of the biomaterial for parenteral application was proved. Crucial parameters for the manufacture of triglyceride implants were identified and the extension of their influence on the resulting release profiles was cleared up. Basic characteristics of triglycerides as biomaterials for controlled release were elaborated and release mechanisms were identified using glyceroltripalmitate as representative material. Thus, the design of controlled release devices from this material, having desired release profiles was facilitated. Furthermore, biocompatibility, one of the most important characteristics for the suitability of a material to serve as matrix material for parenteral administered devices, was shown for glyceroltripalmitate and cholesterol. Essential knowledge on the in vivo erosion of triglycerides and the potential parameters that influence the degradation was acquired.

In additional experiments, protocols for the extraction of insulin and somatostatin from glyceroltripalmitate matrices for the determination of the residue content and for further experiments on protein and peptide stability within the triglyceride matrix were established. High extraction yields and good reproducibility were achieved.

Finally, release from programmable implants was shifted from pulsatile to controlled prolonged release. The preparation procedure was optimized and reproducible times for the inhibition of release by the polymeric mantle were achieved. Concomitantly, using convolution for mathematical modeling a correlation of the resulting release profiles from programmable implants with the release from the core materials themselves was shown.

References

[1] F.J. Martin, C. Grove, Microfabricated drug delivery systems: concepts to improve clinical benefit, Biomedical Microdevices (2001), 3(2): 97-107.

[2] L.K. Fung, W.M. Saltzman, Polymeric implants for cancer chemotherapy, Advanced Drug Delivery Reviews (1997), 26(2,3): 209-230.

[3] G.P. Carino, E. Mathiowitz, Oral insulin delivery, Advanced Drug Delivery Reviews (1999), 35: 249-257.

[4] R.J. Levy, V. Labhasetwar, C. Song, E. Lerner, W. Chen, N. Vyavahare, X. Qu, Polymeric drug delivery systems for treatment of cardiovascular calcification, arrhythmias and restenosis, Journal of Controlled Release (1995), 36(1-2): 137-47.

[5] C.H. Niu, Y.Y. Chiu, FDA perspective on peptide formulation and stability issues, Journal of Pharmaceutical Sciences (1998), 87: 1331–1334.

[6] K.J. Whittlesey, L.D. Shea, Delivery systems for small molecule drugs, proteins, and DNA: the neuroscience/biomaterial interface, Experimental Neurology (2004), 190: 1-16.

[7] W. Vogelhuber, T. Spruß, G. Bernhardt, A. Buschauer, A. Göpferich, Efficacy of BCNU and paclitaxel loaded subcutaneous implants in the interstitial chemotherapy of U-87 MG human glioblastoma xenografts, International Journal of Pharmaceutics (2002), 238(1-2): 111-121.

[8] A. Maschke, A. Lucke, W. Vogelhuber, C. Fischbach, B. Appel, T. Blunk; A. Goepferich; Lipids: An alternative material for protein and peptide release; ACS Symposium Series 2004, 879 (Carrier-Based Drug Delivery), 176-196.

[9] G. Pauletti, S. Gangwar, G.T. Knipp, M.M. Nerurkar, F.W. Okuma, K. Tamura, T.J. Siahaan, R.T. Borchardt, Structural requirements for intestinal absorption of peptide drugs, Journal of Controlled Release (1996), 41: 3–17.

[10] A. Sharma, C.M. Harper, L. Hammer, R.E. Nair, E. Mathiowitz, N.K. Egilmez, Characterization of cytokine-encapsulated controlled-release microsphere adjuvants, Cancer Biotherapy & Radiopharmaceuticals (2004), 19(6): 764-769.

[11] Y. Yuyama, M. Tsujimoto, Y. Fujimoto, N. Oku, Potential usage of thermosensitive liposomes for site-specific delivery of cytokines, Cancer Letters (Shannon, Ireland) (2000), 155(1): 71-77.

[12] R. J. Duma, M. J. Akers, S. J. Turco, Parenteral Drug Administration: Routes, Precautions, Problems, Complications and Drug Delivery Systems, in Pharmaceutical Dosage Forms: Parenteral Medications Volume 1, Second Edition, Revised and Expanded, Eds. K.E. Avis, H.A. Lieberman, L. Lachman (1992), Marcel Dekker, Inc. pp. 17-58.

[13] H. Brem, S. Piantadosi, P. C. Burger, M. Walzer, R. Selker, N. A. Vick, K. Black, M. Sisti, S. Brem, G. Mohr, P. Muller, R. Morawetz, S. C. Schold, P.-B. T. T. Group, Placebo-controlled trial of safety and efficacy of intraoperative controlled delivery by biodegradable polymers of chemotherapy for recurrent gliomas, Lancet (1995), 345: 1008-1012.

[14] P.M. Black, Brain tumors (first of two parts), New England Journal of Medicine (1991), 324: 1471–1476.

[15] N. Kemeny, D. Civalleri, P. Edman, B. Nilsson, K. Gunnarsson, K. Hakansson, T. Taguchi, K.R. Aiger, Liver cancer: a review of current treatment options, in: N. Kemeny (Ed.), Anupdate of regional treatment of liver cancer. The role of vascular occlusion, Wells Medical: Kent, England, 1992: 7–16.

[16] A.K. Dash, G.C. Cudworth, II. Therapeutic applications of implantable drug delivery systems, Journal of Pharmacological and Toxicological Methods (1998), 40(1): 1-12.

[17] M.F. Haller, W.M. Saltzman, Localized delivery of proteins in the brain: can transport be customized?, Pharmaceutical Research (1998), 15(3): 377-385.

[18] R. Langer, Implantable controlled release systems. In Methods of Drug Delivery. Ed., GM Ihler. (1986) New York: Pergamon Press, pp.121–137.

[19] T. Yasukawa, Y. Ogura, Y. Tabata, H. Kimura, P. Wiedemann, Y. Honda, Drug delivery systems for vitreoretinal diseases, Progress in Retinal and Eye Research (2004), 23(3): 253-281.

[20] R. Sitruk-Ware, M. Small, N. Kumar, Y.-Y. Tsong, K. Sundaram, T. Jackanicz, Nestorone: clinical applications for contraception and HRT, Steroids (2003), 68(10-13): 907-913.

[21] L.J. Gooren, New long-acting androgens, World Journal of Urology (2003), 21(5): 306-310.

[22] V. Baekelandt, B. De Strooper, B. Nuttin, Z. Debyser, Gene therapeutic strategies for neurodegenerative diseases, Curr. Opin. Mol. Ther. (2000), 2: 540– 554.

[23] J.C. Glorioso, M. Mata, D.J. Fink, Therapeutic gene transfer to the nervous system using viral vectors, J. NeuroVirol.(2003), 9: 165– 172.

[24] J. Segovia, Gene therapy for Parkinson's disease: current status and future potential. Am. J. Pharmacogenomics (2002), 2: 135–146.

[25] L. Tenenbaum, A. Chtarto, E. Lehtonen, D. Blum, V. Baekelandt, T. Velu, J. Brotchi, M. Levivier, Neuroprotective gene therapy for Parkinson's disease, Curr. Gene Ther. (2002), 2: 451– 483.

[26] R. Langer, Drug delivery and targeting, Nature (1998), 392: 5 –10.

[27] H. Cohen et al., Sustained delivery and expression of DNA ancapsulated in polymeric nanoparticles, Gene Therapy (2000), 7: 1896-1905.

[28] R. Gref et al., Biodegradable long-circulating polymer nanoshperes, Science (1994), 263: 1600-1603.

[29] M.R. Gasco, Non-stealth and stealth solid lipid nanoparticles (SLN) carrying doxorubicin: pharmacokinetics and tissue distribution after i.v. administration to rats, Pharmacol. Res. (2000), 42: 337–343.

[30] T. Ameller, V. Marsaud, P. Legrand, R. Gref, J.-M. Renoir, In vitro and in vivo biologic evaluation of long-circulating biodegradable drug carriers loaded with the pure antiestrogen RU 58668, Int. J. Cancer (2003), 106: 446-454.

[31] A. S. Ulrich, Biophysical aspects of using liposomes as delivery vehicles, Bioscience Reports (2002), 22(2): 129-150.

[32] M. P. Ramprasad, A. Amini, T. Kararli, N. V. Katre, The sustained granulopoietic effect of progenipoietin encapsulated in multivesicular liposomes, International Journal of Pharmaceutics (2003), 261(1-2): 93-103.

[33] K. Juni, J. Ogata, M. Nakano, T. Ichihara, K. Mori, M. Akagi, Preparation and evaluation in vitro and in vivo of polylactic acid microspheres containing doxorubicin, Chem Pharm Bull (1985), 33:313-318.

[34] J.-P. Benoit, N. Faisant, M.-C. Venier-Julienne, P. Menei, Development of microspheres for neurological disorders: From basics to clinical applications, Journal of Controlled Release (2000), 65(1-2), 285-296.

[35] B. Albertini, N. Passerini, M. L. Gonzalez-Rodriguez, B. Perissutti, L. Rodriguez, Effect of Aerosil on the properties of lipid controlled release microparticles, Journal of Controlled Release (2004), 100(2): 233-246.

[36] W. Vogelhuber, E. Magni, M. Mouro, T. Spruss, C. Guse, A. Gazzaniga, A. Gopferich, Monolithic triglyceride matrixes: A controlled-release system for proteins, Pharmaceutical Development and Technology (2003), 8(1): 71-79.

[37] W. Vogelhuber, E. Magni, A. Gazzaniga, A. Gopferich, Monolithic glyceryl trimyristate matrices for parenteral drug release applications, European Journal of Pharmaceutics and Biopharmaceutics (2003), 55(1): 133-138.

[38] C. B. Packhaeuser, J. Schnieders, C. G. Oster, T.Kissel, In situ forming parenteral drug delivery systems: an overview, European Journal of Pharmaceutics and Biopharmaceutics (2004), 58(2): 445-455.

[39] W. Vogelhuber, P. Rotunno, E. Magni, A. Gazzaniga, T. Spruß, G. Bernhardt, A. Buschauer, A. Göpferich, Programmable biodegradable implants, Journal of Controlled Release (2001), 73 (1): 75-88.

[40] W. Michaeli, O. Pfannschmidt, Microporous, resorbable implants produced by the CESP process, Advanced Engineering Materials (1999), 1(3-4): 206-208.

[41] A. A. LaVan, T. McGuire, R. Langer, Small-scale delivery systems for in vivo drug delivery, Nature Biotechnology (2003), 21(10): 1184-1191.

[42] J.H. Eldridge, J.K. Staas, J.A. Meulbroek, J.R. McGhee, T.R. Tice, R.M. Gilley, Biodegradable microsphere as a vaccine delivery system, Mol. Immunol. (1991), 28: 287–294.

[43] N. J. Medlicott, I. G. Tucker, Pulsatile release from subcutaneous implants, Advanced Drug Delivery Reviews (1999), 38(2): 139-149.

[44] M.E. Akermann, W.C.W. Chan, P. Laakkonen, S.N. Bhatia, E. Ruoslahti, Nanocrystal targeting in vivo, Proc. Natl. Acad. Sci. USA 99, 12617-12621 (2002).

[45] E. Merisko-Liversidge et al., Formulation and anti tumor activity evaluation of nanocrystalline suspensions of poorly soluble anti cancer drugs, Pharm. Res. (1996), 13: 272-278.

[46] A. G. Tkachenko et al., Multifunctional gold nanoparticle –peptide complexes for nuclear targeting, J. Am. Chem. Soc. (2003), 125: 4700-4701.

[47] S.D. Putney, P.A. Burke, Improving protein therapeutics with sustained-release formulations, Nat. Biotechnol. 16 (1998) 153–157.

[48] J.M. Pean, F. Boury, M.C. Venier-Julienne, P. Menei, C. Menei-Montero, J.P. Benoit, Biodegradable PLGA microspheres for the intracerebral administration of neurotrophic factors, Proceed. Int'l. Symp. Control. Rel. Bioact. Mater., Boston 26 (1999) 1048–1049.

[49] P. Menei, M. Boisdron-Celle, A. Croue, G. Guy, J.P. Benoit, Effect of stereotactic implantation of biodegradable 5-Fluorouracil-loaded microspheres in healthy and C6 gliomabearing rats, Neurosurgery 39 (1996) 117–124.

[50] D. A. Edwards et al., Large porous particles for pulmonary drug delivery, Science (1997), 276 : 1868-1871.

[51] D. A. Edwards, C. Dunbar, Bioengineering of therapeutic aerosols, Annu. Rev. Biomed. Eng. (2002), 4: 93-107.

[52] E. Mathiowitz, J.S. Jacob, Y.S. Jong, G.P. Carino, D. Chickering, C. Santos, K. Chaturvedi Vijayaraghavan, M. Bassett, S. Montgomery, C. Morrell, Biologically erodable microspheres as potential oral drug delivery systems, Nature 386 (1997) 410-414.

[53] G.R. Evans, K. Brandt, M. S. Widmer, L. Lu, R. K. Meszlenyi, P. K. Gupta, A. G. Mikos, J. Hodges, J. Williams, A. Gurlek, A. Nabawi, R. Lohman, C. W. Patrick Jr., In vivo evaluation of poly(l-lacticacid) porous conduits for peripheral nerve regeneration. Biomaterials (1999), 20: 1109–1115.

[54] T.W. Hudson, G.R. Evans, C.E. Schmidt, Engineering strategies for peripheral nerve repair, Orthop. Clin. North Am. (2000), 31: 485–498.

[55] M. Oudega, S.E. Gautier, P. Chapon, M. Fragoso, M.L. Bates, J.M. Parel, M.B. Bunge, Axonal regeneration into Schwann cell grafts within resorbable poly(alpha-hydroxyacid) guidance channels in the adult rat spinal cord, Biomaterials (2001), 22: 1125– 1136.

[56] M. Hacker, J. Tessmar, M. Neubauer, A. Blaimer, T. Blunk, A. Göpferich, M.B. Schulz, Towards biomimetic scaffolds: Anhydrous scaffold fabrication from biodegradable amine-reactive diblock copolymers, Biomaterials (2003), 24: 4459-4473.

[57] L.D. Harris, B.S. Kim, D.J. Mooney, Open pore biodegradable matrices formed with gas foaming, J. Biomed. Mater. Res. (1998) 42: 396–402.

[58] W.L. Murphy, D.J. Mooney, Controlled delivery of inductive proteins, plasmid DNA and cells from tissue engineering matrices, J. Periodontal Res. (1999), 34: 413– 419.

[59] L.D. Shea, E. Smiley, J. Bonadio, D.J. Mooney, DNA delivery from polymer matrices for tissue engineering, Nat. Biotechnol. (1999), 17: 551– 554.

[60] Y.D. Teng, E.B. Lavik, X. Qu, K.I. Park, J. Ourednik, D. Zurakowski, R. Langer, E.Y. Snyder, Functional recovery following traumatic spinal cord injury mediated by a unique polymer scaffold seeded with neural stem cells, Proc. Natl. Acad. Sci. U.S.A. (2002), 99, 3024– 3029.

[61] J. Folkman, D. Long, The use of silicone rubber as a carrier for prolonged drug therapy, J. Surg. Res. (1964), 4: 139–142.

[62] J. Folkman, D.M. Long, R. Rosenbaum, Silicone rubber: a new diffusion property useful for general anesthesia, Science (1966), 154: 148–149.

[63] N. Ueno, M.F. Rofojo, L.H.S. Liu, Controlled release rate of a lipophilic drug (BCNU) from a refillable silicone rubber device, J. Biomed. Mater. Res. (1982), 16: 669–677.

[64] T.H. Ferguson, G.F. Needham, J.F. Wagner, Compudose: an implant system for growth promotion and feed efficiency in cattle, J. Contr. Rel. (1988), 8: 45–54.

[65] V. Ranade, Drug delivery systems 4. Implants in drug delivery, J. Clin. Pharm. (1990), 30: 871– 889.

[66] H.W. Buchholz, H. Engelbrecht, Depot effect of various antibiotics mixed with Palacos resins, Chirurg (1970), 40: 511–515.

[67] K. Klemm, Die Behandlung chronischer Knocker-infektionen mit Gentamycin-PMMA-Ketten and Kugelen. In Gentamycin-PMMA-Kette, Gentamycin-PMMA-Kugelin Symposium. Ed., H. Conten. Munchen, Erlaner: VLE Verlag (1977), pp. 20–25.

[68] D.K. Kirkpatric, L.S. Tractenberg, P.D. Mangino, In vitro characteristics of tobramycin-PMMA beads: compressive strength and leaching, Orthopedics (1985) 8: 1130 –1134.

[69] D.H. Robinson, S. Sampath, Release kinetics of tobramycin sulfate from polymethylmethacrylate implants, Drug. Dev. Ind. Pharm. (1989) 15:2339 –2357.

[70] F. Greco, L. Palma, N. Specchia, S. Jacobelli, C. Gaggini, Polymethylmethacrylate-antiblastic drug compounds: an in vitro study assessing the cytotoxic effect in cancer cell lines-a new method for local chemotherapy of bone metastasis, Orthopedics (1992), 15: 189-194.

[71] H. Wahlig, E. Dingeldein, Antibiotics and bone cements. Experimental and clinical long-term observations, Act. Ortho. Scand. (1980), 51: 49 –56.

[72] H. Whalig, Gentamicin PMMA beads, a drug delivery system, basic results. In Local Antibiotic Treatment in Osteomyelitis and Soft Tissue Infections. Eds., Th JG van Rens and FH Kayser, (1981), Amsterdam: Excerpta, pp. 9–17.

[73] A.K. Dash, R. Suryanarayanan, An implantable dosage form for the treatment of bone infections, Pharm. Res. (1992), 9: 993–1002.

[74] D.A. Wood, Biodegradable drug delivery systems, Int J Pharm (1980), 7: 1–18.

[75] D.H. Lewis, Controlled release of bioactive agents from lactide/glycolide polymers, In Biodegradable Polymers as Drug Delivery Systems, Ed., M Chasin R Langer, New York: Marcel Dekker (1990), pp. 1–41.

[76] M. Danckwerts, A. Fassihi, Implantable controlled release drug delivery systems: a Review, Drug. Dev. Ind. Pharm. (1991), 17: 1465–1502.

[77] H. Okada, Y. Inoue, T. Heya, H. Ueno, T. Ogawa, H. Toguchi, Pharmacokinetics of once-a-month injectable microspheres of leuprolide acetate, Pharmaceutical Research 8 (1991): 787–791.

[78] T.R. Tice, D.W. Mason, R.M. Gilley, Clinical use and future of parenteral microsphere delivery systems, in: L.F. Precott, and Nimmo, W.S. (Eds.), Novel Drug Delivery and its Therapeutic Application, Wiley, New York, 1989, p. 223.

[79] B.J.A. Furr, F.G. Hutchison, A biodegradable delivery system for peptides: preclinical experience with the gonadotropin-releasing hormone agonist ZoladexÒ, J. Control. Release 21 (1992) 117–128.

[80] H. Brem, S. Piantadosi, P.C. Burger, M. Walker, R. Selker, N.A. Vick, K. Black, M. Sisti, S. Brem, G. Mohr, P. Muller, R. Morawetz, S.C. Schold, Placebo-controlled trial of safety and efficacy of intraoperative controlled delivery by biodegradable polymers of chemotherapy for recurrent gliomas, Lancet 345 (1995) 1008–1012.

[81] N.B. Graham, Polymeric inserts and implants for the controlled release of drugs, Br. Poly. J. (1978), 10: 260 –266.

[82] H. Okada, Y. Inoue, T. Heya, H. Ueno, T. Ogawa, H. Toguchi, Pharmacokinetics of once-a-month injectable microspheres of leuprolide acetate, Pharmaceutical Research (1991), 8: 787–791.

[83] B.J.A. Furr, F.G. Hutchison, A biodegradable delivery system for peptides: preclinical experience with the gonadotropin-releasing hormone agonist Zoladex®, J. Control. Release (1992), 21: 117–128.

[84] T.R. Tice, D.W. Mason, R.M. Gilley, Clinical use and future of parenteral microsphere delivery systems, in: L.F. Precott, and Nimmo, W.S. (Eds.), Novel Drug Delivery and its Therapeutic Application, Wiley, New York, 1989, p. 223.

[85] Kissel T, Li Y, Unger F. ABA-triblock copolymers from biodegradable polyester A-blocks and hydrophilic poly(ethyleneoxide) B-blocks as a candidate for in situ forming hydrogel delivery systems for proteins. Adv Drug Delivery Rev (2002), 54(1): 99-134.

[86] S. Kyotani, Y. Nishioka, M. Okamura, T. Tanaka, M. Miyazaki, S. Ohnishi, Y. Yamamoto, K. Ito, T. Ogiiso, S. Tanada, M. Terao, A study of embolizing materials for chemo-embolization therapy of hepatocellular carcinoma: antitumor effect of cis-diaminedichloroplatinum(II) albumin microspheres, containing chitin and treated with

chitosan on rabbits with VX2 hepatic tumors, Chemical & Pharmaceutical Bulletin (1992), 40(10): 2814–2816.

[87] P.K. Gupta, C.T. Hung, F.C. Lam, Application of regression analysis in the evaluation of tumor response following the administration of adriamycin either as a solution or via albumin microspheres to the rat, J. Pharm. Sci. (1990), 79(7): 634–637.

[88] J. Novotny, K. Zinek, Application of epirubicin containing albumin microspheres in the experimental therapy of breast cancer, Neoplasma (1994), 41: 201–204.

[89] J.A. Goldberg, N.S. Willmott, J.H. Anderson, G. McCurrach, R.G. Bessent, J.H. McKillop, C.S. McArdle, The biodegradation of albumin microspheres used for regional chemotherapy in patients with colorectal liver metastasis, Nuclear Medicine Communications (1991), 12(1): 57–63.

[90] J.C. Doughty, J.H. Anderson, N. Willmott, C.S. Asardle, Intra-arterial administration of adriamycin-loaded albumin microspheres for locally advanced breast cancer, Posttissue graduate Medical Journal (1994), 71(831): 47–49.

[91] D. Maysinger, K. Krieglstein, J. Filipovic-Grcic, M. Sendtner, K. Unsicker, P. Richardson, Microencapsulated ciliary neurotrophic factor: physical properties and biological activities. Exp. Neurol. (1996), 138: 177–188.

[92] H.H. Tonnesen, J. Karlsen, Alginate in drug delivery systems, Drug Development and Industrial Pharmacy (2002), 28(6): 621-630.

[93] M.Z.I. Khan, I.G. Tucker, J.P. Opdebeeck, Evaluation of cholesterol-lecithin implants for sustained delivery of antigen: release in vivo and single-step immunisation of mice, International Journal of Pharmaceutics (1993),90(3);255-262.

[94] D. Boison, L. Scheurer, J.L. Tseng, P. Aebischer, H. Mohler, Seizure suppression in kindled rats by intraventricular grafting of an adenosine releasing synthetic polymer. Exp. Neurol. (1999), 160: 164-174.

[95] W. Bechtel, K.C.Wright, S.Wallace, B. Mosier, D. Mosier, S. Mir, S. Kuo, An experimental evaluation of microcapsules for arterial chemoembolization, Radiology (1986), 161: 601–604.

[96] D. S. Kohane, N. Plesnila, S. S. Thomas, D. Le, R. Langer, M. A. Moskowitz, Lipid-sugar particles for intracranial drug delivery: safety and biocompatibility, Brain Research (2002), 946(2): 206-213.

[97] D.R. Parker, P.K. Bajpai, Effect of locally delivered testosterone on bone healing. 19th Annual Meeting of the Society for Biomaterials April 28–May 2 (1993): p. 276.

[98] L. Illum, I. Jabbal-Gill, M. Hinchcliffe, A.N. Fisher, S.S. Davis, Chitosan as a novel nasal delivery system for vaccines, Advanced Drug Delivery Reviews (2001), 51(1-3): 81-96.

[99] A.C. Lee, V.M. Yu, J.B. Lowe 3rd, M.J. Brenner, D.A. Hunter, S.E. Mackinnon, S.E. Sakiyama-Elbert, Controlled release of nerve growth factor enhances sciatic nerve regeneration, Exp. Neurol. (2003), 184: 295– 303.

[100] S.E. Sakiyama-Elbert, A. Panitch, J.A. Hubbell, Development of growth factor fusion proteins for cell-triggered drug delivery. FASEB J. (2001), 15: 1300– 1302.

[101] P.Y. Wang, Lipids as excipient in sustained release insulin implants, International Journal of Pharmaceutics (1989), 54(3): 223-230.

[102] P.T. Golumbek, R. Azhari, E.M. Jaffe, H.I. Levitsky, A. Lazenby, K. Leong, D.M. Pardoll, Controlled release, biodegradable cytokine depots: a new approach in cancer vaccine design, Cancer Res. (1993), 53: 5841–5844.

[103] Z. Zhao, E.M. Jaffe, M.C. Thomas, D.M. Pardoll, K.W. Leong, GM-CSF microspheres in cancer immunotherapy - a mechanistic study of the vaccine site, Proceedings of International Symsposium on Controlled Release of Bioactive Materials (1996), 23: 91–92.

[104] Y. Tabata, K. Uho, S. Muramatsu, Y. Ikada, In vivo effects of recombinant interferon alpha A/D incorporated in gelatin microspheres on murine tumor cell growth, Jpn. J. Cancer Res. (1989), 80: 387–393.

[105] X. Chen,Y.Wu, D. Zhong, L. Li, T. Tan, X. Xie, C.Yan, X. Li, Hepatic carcinoma treated by hepatic arterial embolization using I and chemotherapeutic agent gelatin microspheres report of 9 cases, Journal of West China University of Medical Sciences (1992), 23(4): 420–423.

[106] P.Y. Wang, Sustained delivery of bioactive polypeptide by compression in lipid admixture, Mat. Res. Soc. Symp. Proc. (1989), 110: 407-412.

[107] M. Acemoglu, Chemistry of polymer biodegradation and implications on parenteral drug delivery, International Journal of Pharmaceutics (2004), 277(1-2): 133-139.

[108] L. Illum, N.F. Farraj, A.N. Fisher, I. Jabbal-Gill, M. Miglietta, L.M. Benedetti, Hyaluronic acid ester microspheres as a nasal delivery system for insulin, J. Control. Release (1994), 29: 133–141.

[109] I. R. Dos Santos, J. Richard, B. Pech, C. Thies and J. P. Benoit, Microencapsulation of protein particles within lipids using a novel supercritical fluid process, International Journal of Pharmaceutics (2002), 242(1-2): 69-78.

[110] I.S.Wollner, S.C.Walker-Andrews, J.E. Smith, W.D. Ensminger, Phase II study on hepatic arterial degradable starch microspheres and mitomycin, Cancer Drug Delivery (1986), 3(4): 279–284.

[111] M. Kitamura, K. Arai, K. Miyashita, G. Kosaki, Arterial infusion chemotherapy in patients with gastric cancer in liver metastasis and long-term survival after treatment, Japanese Journal of Cancer & Chemotherapy (1989), 16(8 Pt 2): 2936–2939.

[112] A.K. Thom, E.R. Sigurdson, M. Bitar, J.M. Daly, Regional hepatic arterial infusion of degradable starch microspheres increases fluorodeoxyuridine (FUdR) tumor uptake, Surgery (1989), 105(3): 383–392.

[113] D. Civalleri, J.C. Pector, L. Hakansson, J.P. Arnaud, N. Duez, M. Buyse, Treatment of patients with irresectable liver metastates from colorectal cancer by chemo-occlusion

with degradable starch microspheres, British Journal of Surgery (1994), 81(9): 1338-1341.

[114] T.P. Foster, E.L. Parrott, Release of highly water-soluble medicinal compounds from inert, heterogenous matrices. I: Physical mixture, Journal of Pharmaceutical Sciences (1989), 79(9): 806-810.

[115] M. S. Espuelas, P. Legrand, J. M. Irache, C. Gamazo, A. M. Orecchioni, J. -Ph. Devissaguet and P. Ygartua, Poly([ε]-caprolacton) nanospheres as an alternative way to reduce amphotericin B toxicity, International Journal of Pharmaceutics (1997), 158(1): 19-27.

[116] M.Z.I. Khan, I. G. Tucker, J. P. Opdebeeck, Cholesterol and lecithin implants for sustained release of antigen: release and erosion in vitro, and antibody response in mice, International Journal of Pharmaceutics (1991), 76(1-2): 161-170.

[117] S. El-Shanawany, Sustained release of nitrofurantoin from inert wax matrixes, Journal of Controlled Release (1993), 26(1): 11-19.

[118] H. Reithmeier, J. Herrmann, Achim Göpferich, Lipid microparticles as a parenteral controlled release device for peptides, Journal of Controlled Release (2001), 73(2-3): 339-350.

[119] C. Jollivet, A. Aubert-Pouessel, A. Clavreul, M.C. Venier-Julienne, S. Remy, C.N. Montero-Menei, J.P. Benoit, P. Menei, Striatal implantation of GDNF releasing biodegradable microspheres promotes recovery of motor function in a partial model of Parkinson's disease, Biomaterials (2004), 25: 933–942.

[120] R. Bodmeier, O. Paeratakul, Process and formulation variables affecting the drug release from chlorpheniramine maleate-loaded beads coated with commercial and self-prepared aqueous ethyl cellulose pseudolatexes, International Journal of Pharmaceutics (1991), 70(1-2): 59-68.

[121] V.G. Roullin, L. Lemaire, M.C. Venier-Julienne, N. Faisant, F. Franconi, J.P. Benoit, Release kinetics of 5-fluorouracil-loaded microspheres on an experimental rat glioma, Anticancer Res. (2003), 23: 21–25.

[122] H. Okada, T. Heya, Y. Ogawa, T. Shimamoto, One-month release injectable microcapsules of a luteinizing hormone-releasing hormone agonist (leuprolide acetate) for treating experimental endometriosis in rats, J. Pharmacol. Exp. Ther. (1988), 244: 744–750.

[123] H. Toguchi, Pharmaceutical manipulation of leuprorelin acetate to improve clinical performance, J. Int. Med. Res. (1990), 18(Suppl. 1): 35–41.

[124] S. Li, M. Lepage,Y. Merand, A. Belanger, F. Labrie, Growth inhibition of 7,12-dimethylbenz(a)anthracene-induced rat biomammary tumors by controlled-release low-dose medroxyprogesterone acetate, Breast Cancer Res. Treat. (1992), 24: 127–137.

[125] S. Kyotani, Y. Nishioka, M. Okamura, T. Tanaka, M. Miyazaki, S. Ohnishi, Y. Yamamoto, K. Ito, T. Ogiiso, S. Tanada, M. Terao, A study of embolizing materials for chemo-embolization therapy of hepatocellular carcinoma: antitumor effect of cis-diaminedichloroplatinum(II) albumin microspheres, containing chitin and treated with

chitosan on rabbits with VX2 hepatic tumors, Chemical & Pharmaceutical Bulletin (1992), 40(10): 2814–2816.

[126] J. Yang, X.C. Ma, Z.J. Zon, S.L. Wei, Experimental maxillofacial arterial chemoembolization with encased-cisplatin ethylcellulose microspheres, Am. J. Neuroradiol. (1995), 16: 1037–1041.

[127] M.A. Burton, Y. Chen, H. Atkinson, J.P. Codde, S.K. Jones, B.N. Gray, In vitro and in vivo responses of doxorubicin ion exchange microspheres to hyperthermia, Int. J. Hyperthermia (1992), 8: 485–494.

[128] J.P. Codde, A.J. Lumsden, S. Napoli, M.A. Burton, B.N. Gray, A comparative study of the anticancer efficacy of doxorubicin carrying microspheres and liposomes using a rat liver tumour model, Anticancer Res. (1993), 13: 539-543.

[129] H. Teder, C.J. Johansson, The effect of different dosages of degradable starch microspheres (Spherex) on the distribution of doxorubicin regionally administered to the rat, Anticancer Res. (1993), 13: 2161–2164.

[130] N. Chiannilkulchai, N. Ammoury, B. Caillou, J.P. Dementvissaguet, P. Couvreur, Hepatic tissue distribution of doxomedulloblastomarubicin-loaded nanoparticles after i.v. administration in reticulosarcoma M 5076 metastasis-bearing mice, Cancer Chemother. Pharmacol. (1991), 26: 122–126.

[131] A. Sintov, W.A. Scott, R. Siden and R.J. Levy, Efficacy of epicardial controlled-release lidocaine for ventricular tachycardia induced by rapid ventricular pacing in dogs, J. Cardiovasc. Pharmacol. (1990), 16: 812-817.

[132] R. Siden, A. Kadish, W. Flowers, L. Kutas, B.K. Bieneman, J. DePietro, J.P. Jenkins, K.P. Gallagher and R.J. Levy, Epicardial controlled-release verapamil prevents ventricular tachycardia episodes induced by acute ischemia in a canine model, J. Cardiovasc. Pharmacol. (1992), 19: 798-809.

[133] V. Labhasetwar, T. Underwood M. Gallagher, G. Murphy, J. Langberg and R.J. Levy, Sotalol controlled release systems for arrhythmias: In vitro characterization, in vivo drug disposition, and electrophysiologic effects, J Pharm Sci. (1994), 83: 156-164.

[134] R.J. Levy, G. Golomb, J. Trachy, V. Labhasetwar, D. Muller and E. Topoi, Strategies for treating arterial restenosis using polymeric controlled release implants, in: C.G. Gebelein (Ed.), Biotechnology and Bioactive Polymers, Lionfire, Edgewater, FL, 1994, pp. 259-268.

[135] A. Göpferich, R. Langer, Modeling of polymer erosion in three dimensions: rotationally symmetric devices, AIChE J. (1995), 41: 2292–2299.

[136] J. M. Anderson, M. S. Shive; Biodegradation and biocompatibility of PLA and PLGA microspheres; Advanced Drug Delivery Reviews; 1997; 28; 5-24.

[137] M. A. Royals; S. M. Fujita, G. L. Yewey , J. Rodriguez, P. C. Schultheiss, R. L. Dunn; Biocompatibility of a biodegradable in situ forming implant system in rhesus monkeys; J. Biomed. Mater. Res.; 1999; 45; 231-239.

[138] B. Ronneberger, T. Kissel, J. M. Anderson; Biocompatibility of ABA triblock copolymer microparticles consisting of poly(L-lactic-co-glycolic-acid) A-blocks attached to central poly(oxyethylene) B-blocks in rats after intramuscular injection; European Journal of Pharmaceutics and Biopharmaceutics; 1997; 43; 19-28.

[139] A. Brunner, K. Mäder, A. Göpferich, The chemical microenvironment inside biodegradable microspheres during erosion, Proc. Int. Symp. Control. Release Bioact. Mater. (1998), 25: 154–155.

[140] M. Morlock, H. Koll, G. Winter, T. Kissel, Microencapsulation of rh-erythropoietin, using biodegradable poly(,-lactide-co-glycolide): protein stability and the effects of stabilizing excipients, European Journal of Pharmaceutics and Biopharmaceutics, (1997), 43(1): 29-36.

[141] A. Lucke, J. Kiermaier, A. Goepferich, Peptide acylation by poly(ahydroxyesters), Pharm. Res. (2002), 19: 175–181.

[142] T. Eldem, P. Speiser, H. Altorfer, Polymorphic behavior of sprayed lipid micropellets and its evaluation by differential scanning calorimetry and scanning electron microscopy, Pharm. Res. (1991), 8: 178-184.

[143] E.E. Hassen, J.M. Gallo, Targeting anticancer drugs to the brain. I: Enhanced brain delivery of oxantrazone following administration in magnetic cationic microspheres, J. Drug Targeting (1993), 1: 7–14.

[144] J. Yang, X.C. Ma, Z.J. Zon, S.L. Wei, Experimental maxillofacial arterial chemoembolization with encased-cisplatin ethylcellulose microspheres, Am. J. Neuroradiol. (1995), 16: 1037–1041.

[145] N.A. Barekzi, A.G. Felts, K.A. Poelstra, J.B. Slunt, D.W. Grainger, Locally delivered polyclonal antibodies potentiate intravenous antibiotic efficacy against Gram-negative infections, Pharm. Res. (2002), 19: 1801-1807.

[146] K.A. Poelstra, N.A. Barekzi, A.M. Rediske, A.G. Felts, J.B. Slunt, D.W. Grainger, Prophylactic treatment of Gram-positive and Gram-negative abdominal implant infections using locally delivered polyclonal antibodies, J. Biomed. Mater. Res. (2002), 60: 206-215.

[147] I.A. Rojas, J.B. Slunt, D.W. Grainger, Polyurethane coatings release bioactive antibodies to reduce bacterial adhesion, J. Controlled Release (2000), 63: 175–189.

[148] A. Berthold, K. Cremer, J. Kreuter, Collagen microparticles: carriers for glucocorticoids, Eur J Pharm (1998), 45: 23-9.

[149] C.-M. Chang, R. Bodmeier, Low viscosity monoglyceride-based drug delivery systems transforming into a highly viscous cubic phase, International Journal of Pharmaceutics (1998), 173(1-2): 51-60.

[150] R.H. Müller, K. Mäder, S. Gohla, Solid lipid nanoparticles (SLN) for controlled drug delivery - a review of the state of the art, European Journal of Pharmaceutics and Biopharmaceutics (2000), 50(1): 161-177.

[151] S. Morel, M.R. Gasco, R. Cavalli, Incorporation in lipospheres of [D-Trp-6]LHRH, Int. J. Pharm. (1994), 105: R1– R3.

[152] A.J. Almeida, S. Runge, R.H. Müller, Peptide-loaded solid lipid nanoparticles (SLN): influence of production parameters, Int. J. Pharm. (1997), 149: 255– 265.

[153] A. Maschke, T. Blunk, A. Göpferich, Lipid Microparticles for Sustained Release of Peptides and Proteins, Annual meeting of the AAPS, 2003.

[154] S. Koennings, C. Guse, T. Blunk, A. Goepferich, Lipid implants for controlled release of proteins, Annual meeting of the Controlled Release Society, 2003.

[155] Desinfektion mit UV Strahlung: Strahlenquellen, technische Hinweise und Anwendung, UV-Technik, Speziallampen GmbH, Wümbach, Germany, 1999.

[156] S.D. Wicksell, The corpuscle problem. A mathematical study of a biometric problem, Biometrika 1925, XVII: 84-99.

[157] S.D. Wicksell, The corpuscle problem. Second memoir. Case of ellipsoidal corpuscles, Biometrika 1926, XVIII: 151-172.

[158] D. Stoyan, W. S. Kendall, J. Mecke; Stochastic geometry and its applications, p289ff.

[159] E. Stepanek, Praktische Analyse linearer Systeme durch Faltungsoperationen; Akademische Verlagsgesellschaft Geest & Portig K.-G. Leipzig (1976), Issue 23.

[160] R. Suverkrup, Convolution and deconvolution methods, Drugs and the Pharmaceutical Sciences (2000), 106(Oral Drug Absorption): 255-280.

[161] Z.Z. Karu, Signals and Systems, ZiZi Press Cambridge, 1995, pp. 45ff.

[162] P. Langguth, G. Fricker, H. Wunderli-Allenspach, Biopharmazie, Wiley-VCH Verlag GmbH & CoKGaA Weinheim, 2004, pp 242ff.

[163] G. Grimmett, Percolation, Sringer Verlag New York, Berlin, Heidelberg, London, Paris, Tokyo, 1988.

[164] D. Stauffer, Introduction to percolation theory, Taylor & Francis, London and Philadelphia, 1985.

[165] D. Stauffer, A. Coniglio, M. Adam; Gelation and critical phenomena; Adv. Polymer Sci. 1982; 44: 103-158.

[166] H. Leuenberger, R. Leu; Formation of a tablet: A site and bond percolation phenomenon; Journal of pharmaceutical sciences 1992; 81(10): 976-982.

[167] H. Leuenberger, B. D. Rohera, C. Haas; Percolation theory – a novel approach to solid dosage form design; International Journal of Pharmaceutics 1987; 38: 109-115.

[168] S. Tonoli, Rilascio da sistemi lipidici impiantabili: influenza della porosità e delle interazioni tracciante-matrice, Dissertation submitted for Diploma 2005.

[169] I. V. Pech, K. Peterson, J. G. Cairncross; Chemotherapy for brain tumors; Oncology; 1998; 12; 537-553.

[170] P. U. Freda; How effective are current therapies for acromegaly; Growth Hormone & IGF Research, 2003; 13; S141-S151.

[171] M. Konishi, Y. Tabata, M. Kariya, A. Suzuki, M. Mandai, K. Nanbu, K. Takakura, S. Fujii; In vivo anti-tumor effect through the controlled release of cisplatin from biodegradable gelatin hydrogel; Journal of Controlled Release; 2003; 92; 301-313.

[172] S. Brahim, D. Narinesingh, A. Guiseppi-Elie; Bio-smart hydrogels: co-joined molecular recognition and signal transduction in biosensor fabrication and drug delivery; Biosensors and Bioelectronics; 2002; 17; 973-981.

[173] C. Tardi, M. Drechsler, K.H. Bauer, M. Brandl; Steam sterilisation of vesicular phospholipid gels; International Journal of Pharmaceutics; 2001; 217(1-2); 161-172.

[174] D. T. Morehead; N. W. Pankhurst; A. J. Ritar; Effect of treatment with LH-RH analog on oocyte maturation, plasma sex steroid levels and egg production in female striped trumpeter Latris lineata (Latrididae); Aquaculture; 1998; 169(3,4); 315-331.

[175] C. Guse, S. Schreiner, T. Spruß, T. Blunk, A. Göpferich; Phospholipids as a release modifier for triglyceride matrices; DPhG Jahrestagung 2002, Berlin (Germany).

[176] Y. Tabata, A. Nagano, Y. Ikada; Biodegradation of hydrogel carrier incorporating fibroblast growth factor; Tissue engineering 1999; 5(2); 127-38.

[177] Baumans V., The Laboratory Mouse, in: Poole T. (ed) The UFAW Handbook on the Care and Management of Laboratory Animals, Vol. 1 (1999), pp. 282-312, Blackwell Science, Oxford.

[178] J. Hilborn; A new evolving paradigm for biocompatibility; Cytotherapy; 2004; 6; 265.

[179] B. Saad, O. M. Keiser, M. Welti, G. K. Uhlschmid, P. Neueuschwandner, U. W. Suter; Multiblock copolyesters as biomaterials: in vitro biocompatibility testing; J. Mater. Sci.: Mater. Med.1997; 8: 497-505.

[180] J. E. Bergsma, R. R. M. Bos, F. R. Rozema, W. de Jong, G. Boering; Biocompatibility of intraosseously implanted predegraded poly(lactide): an animal study; J. Mater. Sci.: Mater. Med.1996; 7: 1-7.

[181] R. Van Dijkhuizen-Radersma, S. C. Hesseling, P. E. Kaim, K. de Groot, J. M. Bezemer; Biocompatibility and degradation of poly(ether-ester) microspheres: in vitro and in vivo evaluation; Biomaterials 2002; 23: 4719-4729.

[182] M. J. Fernández-Hervás, M. T. Vela, M. J. Arias and A. M. Rabasco, Percolation theory: Evaluation and interest of percolation thresholds determination in inert matrix tablets, Pharmaceutica Acta Helvetiae1996, 71(4): 259-264.

[183] J.T. Santini Jr, M.J. Cima; R. Langer, A controlled-release microchip, Nature 1999, 398(6717): 335-338.

[184] S. Sershen, J. West, Implantable, polymeric systems for modulated drug delivery, Advanced Drug Delivery Reviews, 2002, 54(9): 1225-1235.

[185] N.A. Peppas, Fundamentals of pH- and temperature-sensitive delivery systems, in: R. Gurny, H. Junginger, N. Peppas (eds.), Pulsatile drug delivery, Wissenschaftliche Verlagsgesellschaft mbH, Stuttgart, 1992, pp. 41-56.

[186] T. Bussemer, I. Otto, R. Bodmeier, Pulsatile drug-delivery systems, Critical Reviews in Therapeutic Drug Carrier Systems (2001), 18(5): 433-458.

[187] B.G. Stubbe, S.C. De Smedt, J. Demeester, "Programmed Polymeric Devices" for Pulsed Drug Delivery, Pharmaceutical Research (2004), 21(10): 1732-1740.

[188] A. Kikuchi, T. Okano, Pulsatile drug release control using hydrogels, Advanced Drug Delivery Reviews (2002), 54(1): 53-77.

[189] A.C. Richards Grayson, I.S. Choi, B.M. Tyler, P.P. Wang, H. Brem, M.J. Cima, R. Langer, Multi-Pulse drug delivery from a resorbable polymeric microchip device, Nature Materials 2003, 2: 767-772.

[190] A. Göpferich, Bioerodible implants with programmable drug release, J. Control. Release 1997, 44(2-3): 271-281.

[191] A. Göpferich, Implants with phased release of medicaments, US 6086908, July 11, 2000.

[192] S. Koennings, A. Goepferich, Lipospheres as delivery systems for peptides and proteins Lipospheres in Drug Targets and Delivery, 2005, pp. 67-86.

[193] L.N. Gillespie, G.M. Clark, P.F. Bartlett, P.L. Marzella, BDNF-induced survival of auditory neurons in vivo: cessation of treatment leads to accelerated loss of survival effects, Journal of Neuroscience research 2003, 71: 785-790.

[194] M. Ozeki, Y. Tabata, Promoted growth of murine hair follicles through controlled release of vascular endothelial growth factor, Biomaterials (2002), 23(11): 2367-2373.

[195] A. Sharma, C.M. Harper, L. Hammer, R.E. Nair, E. Mathiowitz, N.K. Egilmez, Characterization of cytokine-encapsulated controlled-release microsphere adjuvants, Cancer Biotherapy & Radiopharmaceuticals (2004), 19(6): 764-769.

[196] Y. Yuyama, M. Tsujimoto, Y. Fujimoto, N. Oku, Potential usage of thermosensitive liposomes for site-specific delivery of cytokines, Cancer Letters (Shannon, Ireland) (2000), 155(1): 71-77.

[197] P.B. Storm, J.T. Moriarity, B. Tyler, P.C. Burger, H. Brem, J. Weingart, Polymer delivery of camptothecin against 9L gliosarcoma: release, distribution, and efficacy. Journal of neuro-oncology 2002, 56(3): 209-17.

[198] A. McRae, A. Dahlstrom, Transmitter-loaded polymeric microspheres induce regrowth of dopaminergic nerve terminals in striata of rats with 6-OH-DA induced parkinsonism, Neurochem. Int. 1994, 25: 27–33.

[199] A. Mc Rae, E.A. Ling, S. Hjorth, A. Dahlstrom, D. Mason, T. Tice, Catecholamine-containing biodegradable microsphere implants as a novel approach in the treatment of CNS neurodegenerative disease. A review of experimental studies in DA-lesioned rats, Mol. Neurobiol. 1994, 9: 191–205.

Appendices

List of Abbreviations

AIDS	acquired immunodeficiency syndrome
ANOVA	analysis of variance
BBB	blood-brain barrier
BGS	Beta Gamma Service
DMPC	dimyristoyl-phosphatidyl-choline
DPPC	dipalmitoyl-phosphatidyl-choline
DSC	differential scanning calorimetry
DSPC	distearoyl-phosphatidyl-choline
Em.	emission
EVAc	Ethylvinylacetate copolymer
Ex.	extinction
GFC	gel filtration chromatography
HCl	hydrochloric acid
HIV	human immunodeficiency virus
HPLC	high performance liquid chromatography
i.m.	intramuscularly
i.v.	intravenously
LC/MS	liquid chromatography coupled with mass spectrometry
M_w	weight average molecular weight
m/z	mass-per-charge
NMRI	Naval Medical Research Institute
pBMA	poly(butylmethacrylate)
pCPP-SA	poly(bis(p-carboxyphenoxy)propane) - sebacic acid
PDMS	poly(dimethylsiloxane)
PEG	poly(ethylene glycol)
PES	polyester

Ph. Eur.	Pharmacopoea Europaea
PLA	poly(D,L-lactic acid)
PLGA	poly(D,L-lactic-*co*-glycolic acid)
PMMA	poly(methylmethacrylate)
PTFE	polytetrafluor-ethylen
s.c.	subcutaneously
SD	standard deviation
SEM	scanning electron microscopy
TFA	trifluoroacetic acid
T_g	glass transition temperature
THF	tetrahydrofurane
% (w/w)	percent, weight per weight
WAXD	wide angle X-ray diffractometry
WHO	World health organisation

Curriculum vitae

Name:	Christian Guse
Date of birth:	25. September 1975
Place of birth:	Landshut
Nationality:	German
Martial status:	married since 28. September 2002

Education:

09/1981 – 07/1983	Elementary School St. Nikola, Landshut
09/1983 – 07/1985	Elementary School Seligenthal, Landshut
09/1985 – 07/1991	Grammar School: Maristengymnasium, Furth bei Landshut
09/1991 – 07/1992	Grammar School: Hans Leinberger Gymnasium, Landshut
09/1992 – 07/1994	Grammar School: Gymnasium Seligenthal, Landshut

Professional Training and Experience:

11/94-02/95 and 04/96-10/99	Study of Pharmacy at the University of Regensburg, Regensburg
11/99-04/00	Traineeship at the “Rosen-Apotheke”, Landshut
05/00-10/00	Traineeship at the “Apotheke im BKR Regensburg”, Regensburg
11/00	Acquisition of the license to practise as pharmacist
01/01-present	PhD program at the Department of Pharmaceutical Technology, University of Regensburg, Regensburg, Prof. Dr. Achim Göpferich

Civilian Service:

03/95-03/96	Patient service at the “Klinikum Landsht”, Landshut

List of Publications

Publications:

W. Vogelhuber, E. Magni, M. Mouro, T. Spruss, C. Guse, A. Gazzaniga, A. Gopferich, Monolithic triglyceride matrixes: A controlled-release system for proteins; Pharmaceutical Development and Technology (2003), 8(1): 71-79.

C. Guse, S. Koennings, F. Kreye, F. Lecomte, A. Goepferich, J.Siepmann, Protein release from lipid-based implants: Elucidation of the underlying mass transport mechanisms; to be submitted to International Journal of Pharmaceutics.

K. Elkharraz, N. Faisant, C. Guse, F. Lecomte, A. Goepferich, R. Gust, J.P. Benoit, J. Siepmann, Paclitaxel-loaded Microparticles and Implants for the Treatment of Brain Cancer: Preparation and Physicochemical Characterization; to be submitted to International Journal of Pharmaceutics.

C. Guse, S. Koennings, A. Maschke, M. Hacker, C. Becker, S. Schreiner, T. Blunk, T. Spruss, A. Goepferich, Biocompatibility and erosion behavior of triglycerides and blends with cholesterol and phospholipids; to be submitted to International Journal of Pharmaceutics (**Chapter 5**).

C. Guse, S. Koennings, T. Blunk, J. Siepmann, A. Goepferich, Programmable Implants – From Pulsatile to Controlled Release; to be submitted to International Journal of Pharmaceutics (**Chapter 8**).

Conference Abstracts:

A. Maschke, C. Guse, J. Herrmann, A. Göpferich, Triglyceride Matrices for Controlled Release of Peptides and Proteins; Proceedings of the 4th World Meeting on Pharmaceutics Biopharmaceutics and Pharmaceutical Technology. Florence 8th-11th April 2002, pp. 891-892.

B. Appel, A. Maschke, C. Guse, H. Sarhan, K. Kellner, T. Blunk, A. Göpferich, 3-D cartilage engineering culture as a test system for growth factor application devices; GZG Jahrestagung, Regensburg, 2002.

B. Appel, A. Maschke, C. Guse, H. Sarhan, K. Kellner, T. Blunk, A. Göpferich, Lipid matrices release bioactive insulin in a 3-D cartilage engineering culture; CRS German local chapter, Vienna, 2002.

C. Guse, S. Schreiner, T. Spruß, T. Blunk, A. Göpferich, Phospholipids as a Release Modifier for Triglyceride Matrices; Archiv der Pharmazie,Vol.335 Sept.(Suppl.1) (2002) 121, DPhG Berlin 2002.

S. Koennings, C. Guse, T. Blunk, A. Goepferich, Lipid implants for controlled release of proteins; Annual meeting of the Controlled Release Society, 2003, Glasgow.

S. Koennings, C. Guse, T. Blunk, A. Goepferich, Lipid implants as delivery system for protein drugs; APV Annual Meeting 2004, Nuremberg.

C. Guse, S. Koennings, T. Blunk, A. Goepferich, Preprogrammable Implants with a Lipid Core; APV Annual Meeting 2004, Nuremberg.

S. Koennings, C. Guse, T. Blunk, A. Goepferich, Preparation method for protein-loaded lipid implants intended for long-term release; CRS Annual Meeting 2004, Honolulu.

C. Guse, S. Koennings, T. Blunk, A. Goepferich, Factors influencing the release from triglycerid matrices; Annual Meeting AAPS 2004, Baltimore (ML, USA).

Danksagung

Zum Schluss möchte ich mich bei allen herlzich bedanken, die zum Gelingen meiner Doktorarbeit beigetragen haben.

Herrn Prof. Göpferich danke sehr ich für die Überlassung des Themas und die Unterstützung der Arbeit. Die kostruktiven Diskussionen und Anregungen während der „FAH“- und „EU“-Meetings waren sehr hilfreich und motivierend. Außerdem möchte ich mich dafür bedanken, meine Ergebnisse auf nationalen und internationalen Kongressen und Meetings präsentiert haben zu dürfen.

Frau Dr. Michaela Schulz, Herrn Dr. Torsten Blunk und Herrn Dr. Jörg Tessmar möchte ich ebenfalls danken für die vielen Beiträge zu meiner Arbeit im Rahmen der zahlreichen Projektbesprechungen.

Für die finanzielle Förderung der durchgeführten Projekte gilt mein Dank der Forschungsgemeinschaft der Arzneimittelhersteller (FAH) und der Europäischen Union (EU).

Desweiteren möchte ich mich bei allen derzeitigen und ehemaligen Kollegen am Lehrstuhl bedanken. Mein herzlicher Dank gilt insbesondere:

- Sigrid Drotleff für ihr allzeit offenes Ohr, ihre Freundschaft, viele hilfreiche und motivierende Diskussionen, sowie für das „Sitten“ meiner Implantate.
- Dr. Thilo Spruss für die hilfreiche und freundliche Unterstützung bei der Durchführung der Tierversuche.
- Herrn Wiesenmayr und Herrn Baumann für die praktische Unterstützung bei den Tierversuchen, die Pflege der Mäuse und die netten Unterhaltungen.
- Dr. Martina Andratschke für die Hilfe bei der Röntgendiffraktometrie
- Stefanie Könnings für die freundschaftliche Zusammenarbeit im Rahmen des „EU-Projektes“, sowie ebenfalls für das „Sitten“ der Implantate.
- Angelika Maschke für die Zusammenarbeit während des „FAH-Projektes“ und die Partikelgrößenbestimmungen.
- Allison Dennis für die exakte und schnelle Durchsicht vieler englischer Texte einschließlich dieser Arbeit.
- Miriam Breunig und Renate Liebl für die Hilfe am Konfokalen Mikroskop.

- Axel Ehmer für die sehr nette gemeinsame Zeit im Labor.
- Dem gesamten Bits&Bytes-Team für die nette, schnelle und kompetente Hilfe bei Computerproblemen.
- Albert Weingart für seine technischen Hilfestellungen und die gute „Labor-Nachbarschaft“.
- Lydia Frommer, Liane Öttl, Christine Niel, Andrea Blaimer, Milada Strnadova und Stefan Kolb für vielerlei technische und organisatorische Hilfe.
- Dr. Michael Hacker, Christian Becker, Angelika Berié und Edith Schindler für die Unterstützung bei der Elektronenmikroskopie.
- Silvia Tonoli für die Beteiligung an Arbeiten des Kapitels 4.
- Barbara Weiser für die Unterstützung bei statistischen Auswertungen.
- My national and international collegues within the project of the European Union for many helpful Discussions and a nice time during the international Meetings.
- Allen, die sich um die Ausrichtung der Lehrstuhl-Schafkopfturniere gekümmert haben und allen Mitspielern.
- Dr. Markus Neubauer und Robert Knerr für die Mühe mit den Fussball-Tipps.
- Allen Mitstreitern bei den „Jedermann-Zehnkämpfen“.
- Meiner „pivaten“ Schafkopfrunde Sigrid Drotleff, Dr. Martina Hubensack und Dr. Erich Schneider für viele schöne Abende und für die gute Freundschaft.

… und allen meinen Freunden, die mich auf meinem Weg begleitet und unterstützt haben.

Meinen Schwiegereltern Ulrike Geltinger und Dr. Rudolf Geltinger bin ich unendlich dankbar dafür, dass sie mir ihre Tochter zur Frau gaben. Allen anderen Angehörigen dieser Familie danke ich sehr für die herzliche Aufnahme in Ihren Kreis.

Abschließend gilt mein innigster Dank meiner Frau Eva, meinen Eltern Rosemarie und Richard Guse und meiner Schwester Tanja Guse, sowie meinem Freund Dr. Reinhard Pröls und meinem Trauzeugen Stefan Zeitler für ihre Liebe und Freundschaft, die mein Leben zu etwas Besonderem machen! Vielen Dank, Eva, dafür, dass Du mich liebst und Dein Leben mit mir verbringen möchtest!

HERZLICHEN DANK!!!